Exploring the 4D scales of eco-geomorphic interactions along a river corridor using repeat UAV Laser Scanning (UAV-LS), multispectral imagery, and a functional traits framework.

Christopher Tomsett[1], Julian Leyland[1]

[1]School of Geography and Environmental Science, University of Southampton, Highfield, Southampton, SO17 1BJ, UK.

Correspondence to: Christopher Tomsett (C.G.Tomsett@soton.ac.uk)

Abstract. Vegetation plays a critical role in the modulation of fluvial process and morphological evolution. However, adequately capturing the spatial and temporal variability and complexity of vegetation characteristics remains a challenge. Currently, most of the research seeking to address these issues takes place at either the individual plant scale or via larger scale bulk roughness classifications, with the former seeking to characterise vegetation-flow interactions and the latter identifying spatial variation in vegetation types. Herein, we devise a method which extracts functional vegetation traits using UAV laser scanning and multispectral imagery, and upscale these to reach scale ~~guild~~functional group classifications. Simultaneous monitoring of morphological change is undertaken to identify eco-geomorphic links between different ~~guilds~~functional groups and the geomorphic response of the system ~~in the context of long-term decadal changes.~~. Identification of four ~~guilds~~groups from quantitative structural modelling ~~based on analysis of terrestrial and UAV-based laser scanning and~~ and two further ~~guilds~~groups from image analysis was achieved~~. These~~ and were upscaled to reach-scale ~~guild~~group classifications with an overall accuracy of 80~~%~~%. Plant structure was then used to assess seasonal changes in excess vegetative drag and ~~links~~relate these to ~~magnitudes of~~ geomorphic ~~activity explored. We show that different vegetation guilds have a role in influencing morphological~~ change ~~through the stabilisation of banks, but that limits on this influence are evident in the prior long-term analysis~~across the study site. This research reveals that remote sensing offers a solution to the difficulty of scaling traits-based approaches for eco-geomorphic research, and that future work should investigate how these methods may be applied to larger areas using airborne laser scanning and satellite imagery datasets.

1. Introduction

Fluvial eco-geomorphic interactions are co-dependent, complex, and variable across space and time, representing a continued area of interest within river research (Thoms and Parsons, 2002). The diversity of eco-geomorphology in river corridors can be attributed to surrounding land use, existing morphology, and flood regimes (Naiman et al., 1993), whilst this same diversity simultaneously influences the flow of water and sediment, ultimately affecting morphology ~~(Diehl et al., 2017)~~(Diehl et al., 2017a) and floodplain conveyance (Nepf and Vivoni, 2000). The role of vegetation within the river corridor is well established, benefiting the local ecology (Harvey and Gooseff, 2015; Sweeney et al., 2004) alongside playing a role in natural flood

management schemes and reconnecting channels and floodplains (Lane, 2017; Wilkinson et al., 2019), especially for small catchments where land cover is more influential for flooding (Blöschl et al., 2007). This is important when considered against a backdrop of a rapidly changing climate where flow extremes are more varied, flooding more likely ~~(Unisdr and Cred, 2015)~~(Unisdr and Cred, 2015), and riparian vegetation is likely to undergo shifts in composition (Rivaes et al., 2014; Palmer et al., 2009). Consequently, adequately measuring and monitoring vegetation with the fluvial domain is critical to understanding how these systems will respond to varying climatic and ~~hydrological~~hydraulic conditions.

The characterisation of riparian vegetation distribution over larger (>1 km) scales has typically relied upon the use of coarse classifications such as those identified in the Water Framework Directive (e.g. Gilvear et al., 2004), using techniques such ~~are~~as aerial imagery and satellite remote sensing (see Tomsett and Leyland, 2019). Any characterisation must be scalable and geographically transferable to cover the vast range of different fluvial landscapes, whilst still accounting for the complexity presented within river corridors. Over-simplified, coarse classifications may altogether miss the vegetation complexity that exists, whilst conversely, highly detailed models tend to be necessarily localised and less transferable to alternate systems and scenarios.

Traits-based classifications, developed and used within ecology, offer a scalable and transferable approach which can be applicable to the fluvial domain ~~(Diehl et al., 2017). They~~(Diehl et al., 2017a), and have been shown to be useful for modelling topographic response to changing vegetation, sediment, and flow conditions (Diehl et al., 2018; Butterfield et al., 2020). ~~However, challenges remain in broad application of this approach, with the characterisation of vegetation in the highly detailed manner required to extract traits metrics being challenging over larger (e.g. >1 km) scales.~~However, the application of traits-based classifications over larger reaches has yet to be fully realised, due to the challenges in collecting appropriately high resolution data at these scales (e.g. >1 km). If such challenges can be overcome, it offers an opportunity for those analysing vegetation both within the river corridor and elsewhere in the landscape to obtain spatially explicit data on vegetation that was previously unattainable.

To address these gaps, herein we examine the scales over which different traits can be collected from remote sensing methods and assess how well these traits can be used to establish eco-geomorphic relationships. We use a UK based temperate river as an ~~exemplar~~example site to demonstrate the effectiveness of novel remote sensing techniques for characterising vegetation~~.~~ through time. We investigate the limits of trait detection and the scales at which they are most appropriately used to enhance eco-geomorphic understanding, enabling us to establish the applicability of these methods to a variety of river corridor environments. Below we introduce the concepts of plant functional traits and hydraulically relevant traits before establishing the aims of this research.

1.1. The Importance of Vegetation

It is well understood that vegetation plays a key role within the river corridor and that how vegetation is ~~modelled~~represented in models (e.g. constant and varying roughness values, rigid cylinders etc.) can affect the outcomes of hydrodynamic simulations. Channels with in-stream vegetation may experience roughness values an order of magnitude higher than non-vegetated channels (De Doncker et al., 2009), capable of reducing velocities by up to 90% (Sand-Jensen and Pedersen, 1999). ~~However, foliage type and how vegetation is modelled affect the influence that the vegetation has on~~, with stem shape, the amount of foliage, and deformation at various flow stages, all influencing river flow (James et al., 2008). The challenges posed by quantifying in-stream vegetation means that it is often difficult to make estimations of in-stream roughness ~~(O'hare et al., 2011). Conversely, above water vegetation~~(O'Hare et al., 2011). Conversely, terrestrial vegetation that influences flow during periods of flooding is easier to measure and monitor depending on the scales of analysis. Banks are typically eroded via mechanisms of mass ~~failures~~failure or entrainment (Hughes, 2016) ~~and so~~, therefore any stabilising effects of vegetation ~~must~~will influence these processes. Vegetation can reduce stream power, increase soil cohesion, and influence soil moisture levels, all of which can help to ~~reduce~~limit bank erosion (Simon et al., 2000; Fox et al., 2007; Kang, 2012). Bank collapse is influenced by three dominant factors, the extra mass of the vegetation, the shear strength provided by root reinforcement, and changes to bank pore water pressure (Wiel and Darby, 2007), with above ground biomass therefore directly influencing the mechanical and hydraulic properties of the substrate (Gurnell, 2014). The above ground biomass also has a direct influence on river flow and sediment transport when submerged (Gurnell, 2014), acting as a sediment trap and stabilising bars (Hortobágyi et al., 2018; Sharpe and James, 2006), although this is stage dependent and depends on plant volume and structure.

The below ground biomass is of equal importance, with root networks decreasing the erodibility of beds and banks by increasing the critical shear stress required for erosion to take place (Millar and Quick, 1998; Wiel and Darby, 2007). The presence of grass compared to bare sediment can increase the stability of soil by a factor is 1.97 (Julian and Torres, 2006) and that comparisons between trees and grass can lead to similar increases in stability again (Millar and Quick, 1998; Huang and Nanson, 1998). Furthermore, the below ground portion of vegetation is highly influential in vegetation removal during peak flow events (Caponi et al., 2020; Bankhead et al., 2017; Francalanci et al., 2020), a critical phase in the feedback loops between vegetation, flow, and morphology. Yet the difficulties in obtaining below ground data is well noted when compared to above ground data, and continues to remain a challenge for remote sensing studies.

1.2. Plant Functional Traits

~~Functional traits originate from ecological research, whereby criticism of using functional types led to a need for a more robust system of classification for ecological studies. Functional types represent vegetation based on its morphology and physiology, amongst other factors (Box, 1981; Box, 1996), but these attributes can exhibit greater variation within functional types as opposed to between them (Reich et al., 2007; Wright et al., 2005), as well as not varying between different types at all (Van~~

~~Bodegom et al., 2012). Assessment of plants based on their functional traits has been seen as a method to overcome the shortcomings of the classic typological approach (Quétier et al., 2007).~~

~~Much like the attributes of a plant type, plant functional traits are morphological, physiological, or phenological attributes that are measurable at the individual plant level (Violle et al., 2007; Kattge et al., 2011; Savage et al., 2007). These measures can either be direct measures of a function such as photosynthesis or be a surrogate measure for a function such as leaf area. To be classed as 'functional' for ecology, traits must affect either plant growth, reproduction, or survival (Violle et al., 2007). Traits can either be effect or response based, depending on whether they have an influence on or are influenced by their wider environment (Violle et al., 2007). The benefit of traits based methods is the applicability between different sites without needing species specific data (Mcgill et al., 2006). Therefore, the findings of community response to factors such as land use or climatic gradients (e.g. De Bello et al., 2006; Garnier et al., 2006) can be applied to a different location with similar trait composition. This is possible through the creation of guilds which describe plant groups with similar traits (Lytle et al., 2017) providing a scalable framework for eco-geomorphic research.~~

Functional traits originate from ecological research, and are morphological, physiological, and phenological attributes that can be measured at the individual plant level (Violle et al., 2007; Kattge et al., 2011; Savage et al., 2007). These can either be direct measurements of a function, such as photosynthesis, or a surrogate measure for that function, such as leaf area, but to be classed as functional in ecology these must either affect plant growth, reproduction, or survival (Violle et al., 2007; Quétier et al., 2007). These measured traits can either be an effect or response trait, whereby they either have an influence on or are influenced by their surrounding environment respectively (Violle et al., 2007; Kattge et al., 2020).

One of the benefits of collecting traits-based data, is the ability to group plants that display similar functional traits into functional groups (Blondel, 2003). Herein we specifically use the term 'functional group' (*sensu* Blondel, 2003) because we explore how aggregated ecosystem processes ultimately affect geomorphological response. This approach provides a scalable framework for eco-geomorphic research, increasing the applicability of research at one site to another without the requirement to contain the same species, rather only the need for those species to have similar traits (Mcgill et al., 2006). Therefore, the findings of a community response to factors such as land use change or climate change in one location can be applied to different locations with similar trait compositions (De Bello et al., 2006; Garnier et al., 2006). This is supported in findings by Tabacchi et al. (2019) into bio-geomorphological succession, whereby taxonomic approaches worked well but traits-based methods accounted for variation in local and regional conditions better, which is essential for scalability.

Traits-based approaches are well suited for eco-geomorphic research due to the strong environmental gradients within fluvial systems (Naiman et al., 2005). ~~Vegetation responds to hydrological variables, such as water availability and disturbance events (Hupp and Osterkamp, 1996)~~Vegetation responds to hydrological variables, such as water availability and disturbance events (Hupp and Osterkamp, 1996) whilst also influencing flow, sediment transport, and morphological stability (Gurnell, 2014),

meaning that the bi-directional nature of this relationship maps well onto a traits-based framework. ~~O'hare et al. (2016)~~O'Hare et al. (2016) have assessed the traits of nearly 500 species that influence river processes, revealing evidence of a broad link between plant form, distribution, and stream power within the UK ~~(O'hare et al., 2011)~~(O'Hare et al., 2011). Moreover, traits-based approaches allow for a more comprehensive view on eco-geomorphic interactions than a purely taxonomic approach due to the environmental conditions having a larger influence on trait compositions than species compositions (Göthe et al., 2017; Corenblit et al., 2015).

To date, ~~the majority of~~most traits-based research has focussed on ecological responses to ~~hydrological~~environmental conditions. For example, greater inundation likelihood has been shown to increase the presence of plants with longer and younger leaves (Stromberg and Merritt, 2016; Mccoy-Sulentic et al., 2017) whilst also being less woody (Kyle and Leishman, 2009; Stromberg and Merritt, 2016)~~, with frequent inundation and higher stress environment necessitating greater flexibility.~~. Conversely, plants in lower stress environments tend to be taller with longer life cycles (Kyle and Leishman, 2009; Stromberg and Merritt, 2016; Mccoy-Sulentic et al., 2017). Factors such as nutrient loading (Baattrup-Pedersen et al., 2016; Lukacs et al., 2019), light conditions (Baattrup-Pedersen et al., 2015), carbon availability (Lukacs et al., 2019), and anthropogenic interference (Baattrup-Pedersen et al., 2002; ~~O'briain~~O'Briain et al., 2017)~~ are all key controllers of trait composition, with the environmental conditions better related to trait, rather than species, composition (Göthe et al., 2017).~~ are all key controllers of trait composition. Furthermore, individual species have been shown to demonstrate differing traits depending on external stresses. *Populus nigra* trees were found to be smaller, have greater flexibility, and had a higher number of structural roots at a bar head when compared to a bar tail ~~(Hortobágyi et al., 2017).~~(Hortobágyi et al., 2017). Further work demonstrated that the ~~smaller species~~trees located at the bar head were ~~incapable of~~less effective at trapping sediment when compared to those at the bar tail (Hortobágyi et al., 2018)~~, highlighting the importance of traits rather than taxonomic approaches.~~. This highlights that in certain examples, the morphological response to a vegetation may be harder to identify from taxonomic approaches alone, with traits-based data helping to unpick the processes that are occurring.

~~Hydrological variability can also influence trait assemblages. For example, mean flood frequency across 15 sites was found not to be related to trait diversity, whereas the magnitude of a 20 year flood and the variability in flood frequency were both related (Lawson et al., 2015). Controlled field experiments with artificial flooding and drought showed a decrease in species richness in both scenarios, although trait diversity was more tolerant to drought conditions (Baattrup-Pedersen et al., 2018). Rivers with more variable flows tend to encourage pioneer species and those with prolonged drought seeing an increased abundance of water tolerant species (Aguiar et al., 2018). As a result, these responses mean successful river restoration projects should focus on the type of restoration more than the extent (Göthe et al., 2016). Taxonomic approaches can still perform equally well for fluvial studies, but traits based approaches tend to account for local and regional conditions better (Tabacchi et al., 2019), which is necessary for scalability.~~

~~Research into effect traits and their geomorphic influence has received less attention as traits concepts have only recently started to be explored in hydrological research. However, as noted by Corenblit et al. (2015), the interactions between plant traits and fluvial systems are linked, with hydrological conditions affecting plant establishment and survival and plant morphological traits affecting morphology and subsequent establishment. There is evidence that changing traits can alter the morphological evolution of channels, with invasive species that have higher branching densities and less flexibility increasing aggradation through reductions in near bed velocities (Manners et al., 2015). Guild location impacts the morphological response, with analysis of bars showing different responses downstream and also laterally based on the traits of the dominant species in these directions (Hortobágyi et al., 2018). This is supported by Butterfield et al. (2020) who when examining changes in multi annual elevation found that guilds at different locations, experiencing different hydraulic conditions, had differing impacts, but also that guilds could not explain all the variation in morphological response. It was found that differing canopy architectures that interacted with flow were likely to be the prominent driver of topographic response, supporting the research of Manners et al. (2015). However, trait diversity can impact morphological response as much as the individual traits, with combinations of guilds interacting to alter responses (Hortobágyi et al., 2018), from which spatially averaging to areas of dominant guilds may oversimplify the complexity of interactions.~~

~~Hydrologically~~Research into effect traits and their geomorphic influence has received relatively less attention as traits concepts have only recently started to be explored in fluvial research. However, as noted by Corenblit et al. (2015), the interactions between plant traits and fluvial systems are linked, with hydraulic conditions affecting plant establishment and survival, and with plant traits affecting flow and subsequent morphology. Temporally, changes in the dominant traits can lead to changing morphology (Manners et al., 2015), whilst spatially the location of dominant traits has been shown to alter morphological response, with combinations of different functional groups adding to the complexity (Hortobágyi et al., 2018). However, functional groups alone cannot explain all the variation in topographic response, with different groups, in different locations, under different hydraulic conditions, exhibiting different topographic responses (Butterfield et al., 2020).

1.3. Hydraulically Relevant ~~Functional~~ Traits

Not all vegetation ~~functional~~ traits are equally relevant when considering direct relationships between vegetation, ~~hydrology~~river flow, and morphology. Moreover, not all traits can be obtained from remote sensing techniques, a necessary requirement when upscaling to larger domains. Below we ~~identify the~~briefly summarise vegetation traits that are ~~directly~~ relevant to ~~river systems~~fluvial environments and which ~~can potentially~~have the potential to be captured via remote sensing techniques, thereby allowing the upscaling of any developed methods of characterisation. These are based off Table 2 in Diehl et al. (2017a) which highlights the morphological effect of vegetation traits on geomorphic form.

~~Existing studies that have considered vegetation–flow interactions have focused on plant height and frontal area as key metrics which explain momentum exchanges in river flows. The height of the plant affects the amount of interaction (Nepf and Vivoni,~~

2000), with varying flow depth determining the proportion of the plant frontal area which is submerged. Frontal area is an often used proxy for the scale of obstruction and is a component of the drag formulation which can have a larger impact on flow conditions than the selection of a drag coefficient (Järvelä, 2004; Wilson et al., 2006). However, the limitations of 2D metrics to describe the complex nature of plants has been highlighted, with the use of 3D data and plant volume offered as improved methodsBoth plant height and frontal area are key traits which influence momentum exchange in river flows. The height of a plant will alter the extent of interaction it has with flow at various stages, whilst the frontal area of the submerged plant structure will impact the drag exerted on the water column (Nepf and Vivoni, 2000; Järvelä, 2004; Wilson et al., 2006). Using 2D frontal area to describe the complex structure of plants is not without limitations, and the possibility of using 3D data has offered improvements in this regard (Whittaker et al., 2013; Vasilopoulos, 2017).

Under various flow conditions, the The frontal area of a plant may change due to flexing and reshaping, with studies showing that notwill vary under different hydraulic conditions, making flexibility an important trait when investigating morphological response. Not accounting for thisflexibility can limit the applicability of study results of drag models (Sand-Jensen, 2008; Whittaker et al., 2013). A higher leaf area increases the momentum absorbing area of plants with de-leafed vegetation not bending until a higher threshold velocity is reached (Wilson et al., 2003; Järvelä, 2002a). Drag has been calculated using leaf area, although not a 1:1 relationship it was shown to be suitable for estimating vegetative resistance (Jalonen et al., 2012). The contribution of foliage to resistance decreases with flow speed, Whittaker et al. (2013) noting a drop in the drag contribution of foliage from 75% to 20–50% at speeds under and over 0.5 ms^{-1} respectively. This is due to the reshaping of plant structure during higher flows leading to reductions in drag (Armanini et al., 2005), with the rate at which this reduction happens being plant dependent (Järvelä, 2002b; James et al., 2008; Boothroyd et al., 2017). The vertical distribution of plants also has a significant impact on flow, with different vertical distributions such as step changes or continuous variations, impacting flow differently and being more important than multi-plant arrangement, with differences in foliated and non-foliated vegetation deforming at different threshold velocities (Wilson et al., 2003; Järvelä, 2002a). Likewise, differences in woody and non-woody stems for plants of similar shape will influence their flexibility, with woody stems requiring a higher flow rate for deformation to occur (O'Hare et al., 2016; Sand-Jensen, 2003). However, the ability to obtain vegetation stem flexure directly from remote sensing is currently not possible, yet leaf area from remote sensing does show potential and taxonomic approaches may better identify the 'woodiness' of a species. Likewise, the vertical distribution of vegetation is important in determining the interaction between foliage and flow stage (Lightbody and Nepf, 2006; Jalonen et al., 2012)., which can be obtained from remotely sensed data.

The arrangement of plants is still important in determining bulk drag, with drag coefficient values for a single foliated stem not representative of stems occurring in bulk vegetation. At patch scales, the density and configuration of plants can impact the resultant drag effects. Although this is an extension of the individual plant-based methods within ecological research, including density and configuration allows for the impact of multiple plants on drag to be accounted for. The non-equivalence between

the drag induced by individual plants and stems and those in bulk vegetation requires the inclusion of bulk factors into vegetation analysis (James et al., 2008). Higher ~~plant~~ densities ~~within a channel~~of plants will lead to an increase in drag ~~coefficients, however~~, with differences in the arrangement ~~of vegetation within~~and density of patches causing variation in the ~~channel has a negligible impact~~resultant reduction in water velocities (Järvelä, 2002b; Kim and Stoesser, 2011; Sand-Jensen, 2008). ~~Sand-Jensen (2008) identified that there was a difference in downstream flow between evenly distributed plants and the same biomass distributed into high density clumps, with the former providing the larger increase in drag and impeding flow the most. Therefore, spatial variation in plant distribution may be more important than the density of the patches themselves. A higher stem density does result in more scour around stems and deposition to be further from the scour sites, however overall deposition does not increase with increased stem density (Follett and Nepf, 2012).~~

~~Whilst both vegetation structure and distribution of individual plants directly impact flow, many other vegetation traits can impact sediment transport processes, for example through playing a role in altering the erodibility of periodically submerged banks or bar surfaces, or through increased resistance from root structures. Although vegetation height, frontal area, and leaf area are all key effect traits which can be measured directly, accounting for secondary impacts of vegetation related to below ground biomass for example, and how all traits vary spatially and temporally remains the challenge for advancing our understanding of eco-geomorphic interactions.~~

~~1.4. Remote Sensing of River Corridor Vegetation~~

. The resultant changes in flow patterns through patches of higher density vegetation can subsequently increase scour around individual stems (Follett and Nepf, 2012), highlighting the need to account for plant spacing when examining changes in morphology, which remote sensing is capable of achieving. At the reach scale, functional groups have an aggregated response in modulating scour or deposition, and resultant planform morphology. Vegetation dynamics have been described using traits-based frameworks previously in fluvial systems (Diehl et al., 2017a; Diehl et al., 2018; Butterfield et al., 2020), with a wealth of studies showing the wider impact that vegetation has on planform morphology and erosion in flumes (Van Dijk et al., 2013; Coulthard, 2005; Bertoldi et al., 2015), modelling studies (Oorschot et al., 2016; Crosato and Saleh, 2011), and field based research (Bywater-Reyes et al., 2017; Diehl et al., 2017b).

Whilst we have focused on hydraulically relevant traits that can be measured using remote sensing techniques, Diehl et al. (2017a), present others which cannot be easily obtained from the remote sensing techniques outlined below. Factors such as plant biomass, buoyancy, and root architecture are all outlined as having a role in affecting subsequent morphology (Sand-Jensen, 2008; Abernethy and Rutherfurd, 2001; De Baets et al., 2007). This highlights the potential role of taxonomic approaches alongside the measurement of structural data to both capture the variability where possible and enhance this with wider datasets on traits that cannot be remotely sensed but are still relevant to morphology.

1.4. Trait Data Collection

Although many of these traits are inherently measurable in the field, many of them are not obtainable from current remote sensing methods. Direct trait extraction for riparian vegetation from airborne (i.e. large scale) remote sensing has not yet been utilised to enhance eco-geomorphic studies. Currently, the collection of trait data relies on ~~direct~~ ground~~-~~-based field surveys and lab analysis, or species ~~are~~being identified in the field and traits ~~taken~~inferred from ~~databases (e.g.~~lookup tables; such as the TRY database (Kattge et al., 2020)~~).~~. Methods are often dependent on site access, species richness, and variation within the study area (Palmquist et al., 2019), utilising methods such as quadrat surveying or transect sampling. This technique is effective for establishing traits but is limited by the spatial extent of ground coverage. Some variables inevitably require the use of databases to avoid substantial disturbance, such as the estimation of root characteristics (e.g. Stromberg and Merritt, 2016; Aguiar et al., 2018; Baattrup-Pedersen et al., 2018)~~, although databases should be used with caution; for example, maximum plant height~~. However, it is ~~not related to the plant submergence height at the time of a particular flow event, and great variation~~ known that a single species can ~~be seen in both effect and response~~display different traits ~~for a singular species~~depending on their position relative to the channel (Hortobágyi et al., 2017; Hortobágyi et al., 2018). Therefore, ~~accounting for temporal and spatial variation in~~ knowledge of a plant location, which can be obtained from remote sensing data, alongside using plant traits databases is important ~~and highlights the need for temporally and spatially relevant data collection.~~for successfully utilising such traits-based analysis in the fluvial domain. Although efforts have been made to utilise remote sensing methods to infer traits in other fields (e.g. Anderson et al., 2018; Valbuena et al., 2020; Zhao et al., 2022), these typically relate only to vegetation height and volume.

~~For~~In fluvial research, multispectral imagery can be used to determine species ~~using~~, which can then be used to identify dominant traits, via supervised and unsupervised classifications ~~with good accuracy~~ (Butterfield et al., 2020). Outside of fluvial research there is an increasing awareness of the potential of remote sensing methods to help drive the scalability of functional traits as an analysis framework, especially in relation to physical traits such as plant height, leaf area index, phenology, and biomass (Abelleira Martínez et al., 2016; Aguirre-Gutiérrez et al., 2021), yet considerable limitations remain due to the uncertainty in relating spectral and physical properties to functional traits (Houborg et al., 2015). Upscaling localised high resolution data is possible however, for example from TLS (Terrestrial Laser Scanning) to large scale ALS (Airborne Laser Scanning) data ~~(Manners et al. (2013)~~(Manners et al., 2013).

Advances in UAV (Uncrewed Aerial Vehicle) remote sensing can ~~create an important link between these two~~offer a way of bridging the scales ~~of data collection~~from ground surveys to larger extents. UAV data collection allows high resolution imagery and active remote sensing methods such as laser scanning to be conducted on large reaches relatively easily (Tomsett and Leyland, 2019), increasing coverage and providing a middle ground for relating local to large scale data. Multispectral cameras have already helped to improve the classification of vegetation from UAVs (Al-Ali et al., 2020), and active UAV-LS (UAV

Laser Scanning) has ~~also~~ been shown to be comparable in estimating tree structures to TLS methods (Brede et al., 2019). Such methods ~~therefore~~ present an opportunity to not only classify vegetation by types and assign them to ~~guilds~~functional groups, but also to define ~~guilds~~these very groups based on characteristics acquired from remote sensing directly, before upscaling ~~this~~them to reach scale classifications. Moreover, a key advance in using UAV based methods for collecting vegetation data is the spatial resolution at which functional groups can be discretised and the temporal resolution which can be achieved by undertaking multiple repeat surveys. The potential to capture evolving 3D data through time (which we refer to as the 4th dimension herein) provides arguably the biggest advantage of using UAV based methods to collect data, avoiding the need to make assumptions about variability through phenological cycles by collecting this information directly.

1.5. Aims

The aim of this research is to ~~develop a set of scalable~~use UAV derived and terrestrial 3D datasets to extract relevant plant traits ~~based 3D vegetation metrics~~ which can be used to assess the spatial and temporal (i.e. 4D) variation and importance of eco-geomorphic interactions on ~~an exemplar~~a UK river system. This is achieved using the following specific objectives:

1. ~~Undertake an assessment of the longer term (multi-decadal) eco-geomorphic evolution of the channel using satellite remote sensing, to compare planform evolution within vegetated and non-vegetated channel sections.~~
2. ~~2.~~1. Identify and select ~~hydrologically~~hydraulically relevant traits which can be extracted from high resolution remote sensing data.
3. ~~3.~~2. Establish the presence of ~~vegetation guilds~~functional groups (those with similar traits) for the river reach~~, based on~~ using exploratory analysis and ~~object orientated random forest classifications.~~machine learning.
4. ~~4.~~3. ~~Compare~~Establish links between the spatial ~~extent of these guilds to~~variation in functional groups and morphological change ~~over the study~~ across a two year period to ~~establish~~identify eco-geomorphic feedbacks~~.~~ that may be present.
4. Utilise the structural data to identify how roughness across functional groups may change seasonally across summer and winter conditions throughout the study area, how interactions between water and vegetation vary across different flow depths, and the impact these both have on erosion and deposition.

2. Study Site

The ~~exemplar~~study site is located on the upper course of the River Teme on the English-Welsh border in the UK (Figure 1A). The study area consists of two ~~broader regions; the~~distinct reaches; an upstream section consisting of open grassland with patches of heterogeneous vegetation, and ~~the~~a downstream section which flows through denser vegetation and woodland. The River Teme is a highly mobile, gravel bed river within an alluvial floodplain which exhibits numerous avulsions~~.~~, typical of many UK rivers. There is active lateral erosion of the channel, depositional gravel bar features, and woody debris dams across

the study site (Figure ~~1A~~1B). The reach has typically low flows (Figure ~~1B~~1C), with an average depth of 0.69 m (+/- 0.15 m) throughout the year with slightly higher average flow depths in the winter months (November – February, 0.79 m +/- 0.15 m). 95% of river depth has been below 0.99 m and 99~~.9~~% of the flow depth has been below 1.48 m. The largest recorded river depth was 2.85 m on the 16th February 2020 during Strom Dennis. ~~Figures are obtained from a gauge station 3 km downstream of the study site, starting from the earliest gauge record.~~

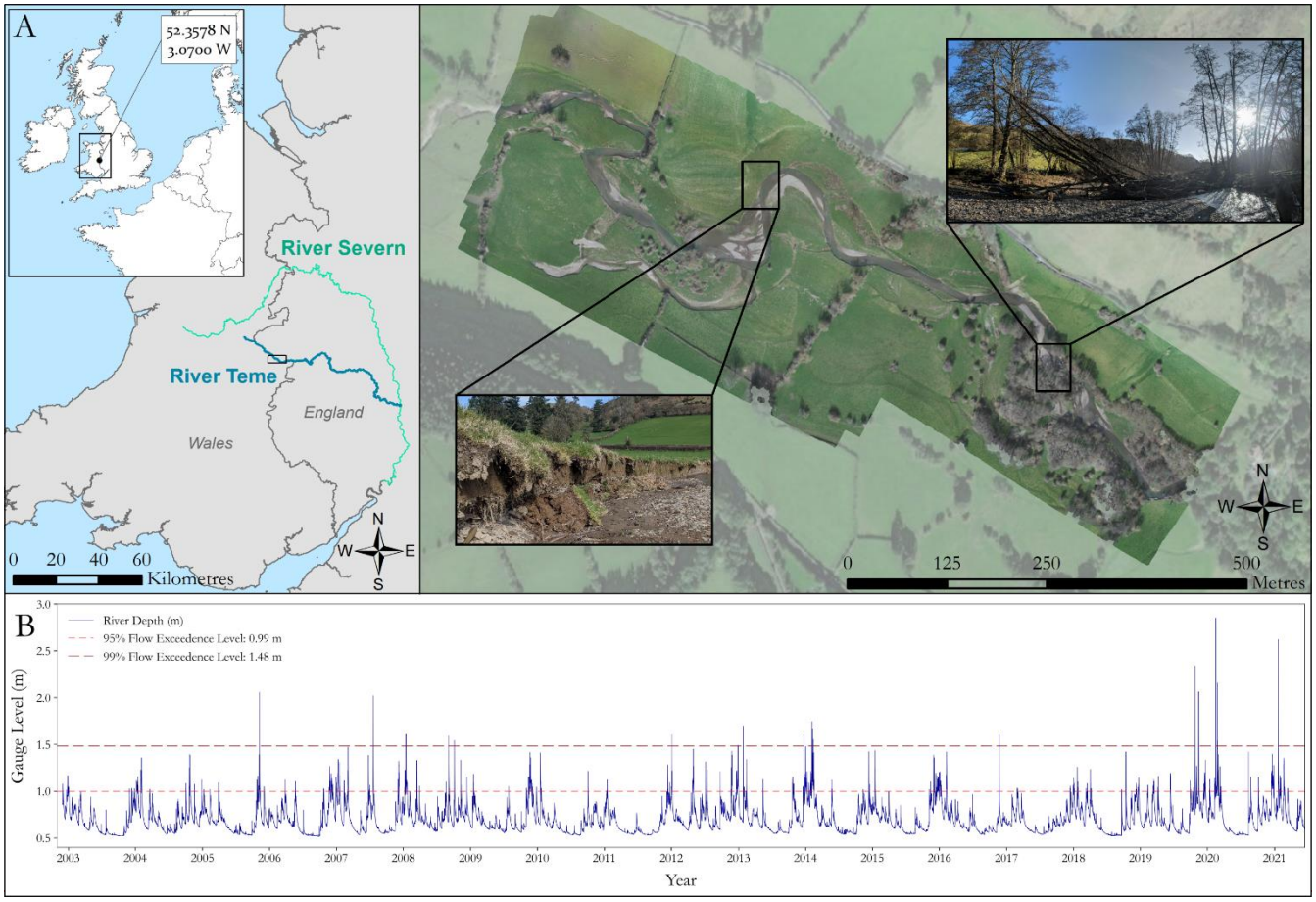

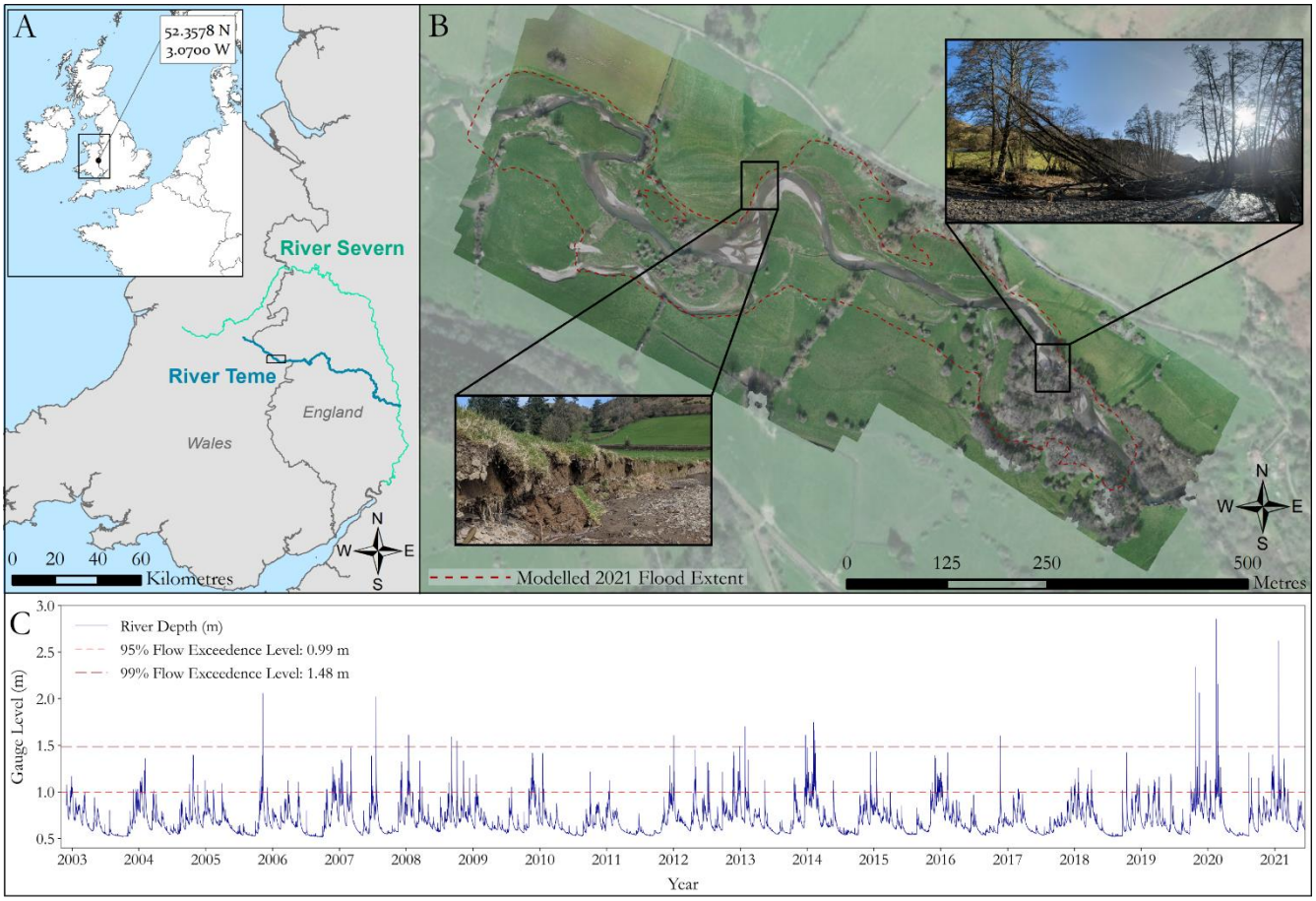

Figure 1 ~~Study Site of the River Teme and the long term water level at the Knighton gauge station 3km downstream.~~ **A) Study Site Location on the River Teme, UK.** ~~Inset~~**B) Plan view of the reach with inset images** ~~show~~**showing active bank erosion and a large debris dam caused by falling trees. The red dashed outline indicates the flood extent modelled in section 3.4. Orthoimagery collected February 2020 and background imagery provided by ESRI (2021).** ~~B~~**C) River** ~~Gauge Level~~**gauge level at the Knighton monitoring station ~**~~1~~**2 km downstream from study reach (data available from 2002 – present, operated by the UK Environment Agency).**

3. Methods

~~3.1. Long Term (Decadal) Analysis~~

~~To assess the longer term context of eco geomorphic interactions within the study reach, historical satellite imagery was analysed to identify channel mobility in relation to riparian vegetation. Channel mobility was assessed by digitising bank edges across multiple years. This method is well established and has been used previously to study the evolution of a large river confluence (Dixon et al., 2018) and for multi decadal analysis of a single river (Yao et al., 2013; Gupta et al., 2013), to identify the drivers of morphological change. These have typically been restricted to coarse (e.g. 30 m ground resolution) satellite datasets, with planform change only detectable if it is greater in magnitude than the image resolution. This can result in mixed~~

pixels; where multiple land cover and vegetation types are misidentified into one category (Henshaw et al., 2013). Here we make use of high spatial resolution imagery from Google Earth (0.5 – 2 m, source dependent (Google Earth Pro, 2021)) and Pleiades (0.5 m) to identify historical changes in channel location and vegetation cover. Google Earth historical imagery for the years 2000, 2006, 2008, and 2009 and Pleiades data from 2013, 2015, 2016, 2018, and 2020 were used from which bank lines were digitised, resulting in 20 years of channel evolution. Banks under tree cover were identified where possible using a mix of spectral bands (Pleiades data only) to highlight channel position. To account for the images being taken at various time periods throughout the years and subsequently having different flow regimes, bank tops were digitised as opposed to water edges to reduce uncertainty resulting from variable flow stage. The exception to this was where no clear bank top was present, for example on the large bars, where evidence of usual high flows from colour changes and trash lines in the imagery were used to guide digitisation of bankfull channel width.

All analysis of bank movement was performed in ArcGIS using the Digital Shoreline Analysis System (DSAS, (Himmelstoss et al., 2018)) with a 1.5 km long baseline created for both left and right banks based on the dominant river planform trend. Transects were cast every 5 m and manually edited where necessary in order to intersect the outermost bank, especially on tight meander bends. The Shoreline Change Envelope (SCE), the distance between the nearest and furthest bank from the baseline, is used to infer total channel mobility throughout the reach.

To assess the impact of vegetation, the channel was classified into two classes: those containing structurally large vegetation and those that did not. Areas classed as containing structurally large vegetation could either include a small number of trees clumped around the channel, a linear section of vegetation on one bank, or larger areas of vegetation such as woodland. These regions were user defined based on all of the image sets available and were used to group transects within regions containing large vegetation and those that did not, for comparison of the SCE statistics. As vegetation may have an influence on both the local scale and broader reach scale morphology, the analysis was repeated for changes excluding the reoccupation of new or former channels (classed as avulsions). To achieve this, DSAS transects that spanned across two separate channels from different years were removed. Each individual channel was then reanalysed using separate baselines, consequently the impact on the results from channel switching can be isolated and removed.

Statistical comparison was undertaken of the SCE values for sections containing large vegetation and sections that did not. These could be used to identify any differences in the SCE values and therefore inferred mobility of these sections, and the influence vegetation may have on planform evolution. To investigate the morphological process of avulsions, the development of new channels between satellite images was also tracked. New and developing channels which were visible in satellite imagery were digitised for each set of images. These were compared to UAV flood extent imagery from February 2020 alongside historical LiDAR data from 2007 of the river corridor and qualitatively assessed in relation to how topography and flood events influence planform, and the processes by which channel switching occurs.

~~3.2.~~3.1. Field Collection of High Resolution 4D data

~~High~~A series of six high resolution UAV-LS (UAV Laser Scanning) and UAV-MS (UAV Multispectral ~~Imagery)~~) surveys were collected over the entire reach ~~through~~shown in Figure 1 from February 2020 until June 2021, capturing all seasonality. To complement these flights, a Terrestrial Laser Scanning (TLS) ~~surveys~~ survey using a Leica P20 was undertaken of vegetated and bar sections ~~were undertaken~~ to gain a benchmark ultra-high-resolution dataset for ~~comparison to the UAV-LS and for~~ characterising small herbaceous vegetation~~. A~~, co-registered to an accuracy of +/- 0.007 m with georeferenced scan targets. UAV-RGB (Red, Green, Blue) ~~survey was~~surveys were also undertaken during overbank flow ~~on the falling limb of~~from Storm Dennis in February 2020~~,~~ to identify the flood extent~~.~~, and September 2020 for classification validation. Table 1 summarises the survey dates, extents, ~~and~~ data collection methods, and point density for UAV-LS and GSD (Ground Sampling Distance) for UAV-MS. A detailed outline of the UAV based sensor set up, processing routine and accuracy assessment can be found in Tomsett and Leyland (2021). All data was processed in the WGS UTM Zone 30N coordinate system.

Table 1 Data collection methods, extent and point density for each survey date. TLS point density is based on the resultant point cloud after registration. UAV-LS point density is determined after cleaning of the raw clouds has taken place. Ground Sampling Distance (GSD) is the resolution of the resultant orthomosaics. ~~UAV-LS point density is taken once cleaning of the raw clouds has taken place.~~

Date	Survey	Sensor	Point Density/GSD
06/02/2020 (Winter)	Whole Reach	UAV-LS	778 m^{-2}
		UAV-MS	0.04 m GSD
18/02/2020 (Winter)	Whole Reach	UAV-RGB	0.02 m GSD
16/07/2020 (Summer)	Subsection	UAV-LS	810 m^{-2}
		UAV-MS	0.04 m GSD
		TLS	16,000 m^{-2}
14/09/2020 (Autumn)	Whole Reach	UAV-LS	762 m^{-2}
		UAV-MS	0.04 m GSD
		~~TLS~~	~~16,000 m^{-2}~~
~~14/09/2020 (Autumn)~~	~~Whole Reach~~	~~UAV-LS~~	~~762 m^{-2}~~
		UAV-~~MS~~RGB	0.~~04~~02 m GSD
14/04/2021 (Spring)	Whole Reach	UAV-LS	791 m^{-2}
		UAV-MS	0.04 m GSD
03/06/2021 (Summer)	Whole Reach	UAV-LS	804 m^{-2}
		UAV-MS	0.04 m GSD

~~A detailed outline of the UAV based sensor set up, processing routine and accuracy assessment can be found in Tomsett and Leyland (2021), with a short overview of the system provided below. UAV-LS and UAV-MS were collected using a DJI Matrice 600 Pro multirotor aircraft, capable of flying for 20 minutes per flight. Two sets of batteries allow for the spatially complex 1 km reach of the River Teme to be captured with some redundancy. Multispectral imagery was obtained from a MicaSense RedEdge-MX camera, collecting imagery with a ground resolution of ~0.035 m across five spectral bands, consisting of blue (475 nm), green (560 nm), red (668 nm), red edge (717 nm), and near infra-red (842 nm) wavelengths (Micasense, 2021). The laser scanner is a Velodyne VLP-16 Puck Lite, firing 16 laser-detector pairs at approximately 300,000 points per second, with a 360° horizontal and 30° vertical field of view. The sensor has a range of up to 100 m and a typical ranging accuracy of +/- 0.03 m (Velodyne Lidar, 2016). Both sensors use direct georeferencing from an Applanix APX-15, which utilises multi-frequency GNSS and MEMS (Micro-Electro-Mechanical System) inertial motion unit to provide post processed positional and orientation accuracies up to 0.02 m and 0.025° respectively (Applanix, 2016). This removes the need for extensive GCP placement throughout the reach. Georeferenced point clouds from the laser scanner and Structure from Motion based point clouds and orthomosaics from the multispectral imagery were produced, both with vertical accuracy under 0.1 m. UAV-RGB imagery was collected from a DJI Inspire 2 with a Zenmuse X4S camera, resulting in a ground resolution of 0.017 m from a flight height of 60 m. An on-board EMLID REACH M2 provides positioning accuracy of up to 0.015 m when post-processed (Emlid, 2021), with a connection to the on-board camera to allow image captures to be timestamped to assist with the SfM processing. TLS data was captured in July 2020 using a Leica P20 Scanstation, collecting high resolution (0.0031 m point spacing at 10 m distance from scanner, resulting in a mean point density of 16,000 points per m^2 within the area of interest) scans of two locations. The first, an area of channel containing large vegetation at the inlet of the study site (two convergent TLS scans), and the second, part of a large meander bend in the centre of the study area (four convergent TLS scans) where large vegetation was absent. Targets were used to register scans together, acquired using a Lecia TS06 total station, with a resultant scan registration accuracy of +/- 0.007 m.~~

~~3.3.~~3.2. Vegetation Functional Trait Extraction

The workflow developed to extract plant functional traits consisted of five steps: (1) Separation of individual plant point clouds ~~that could be used for analysis~~from the UAV-LS and TLS data, (2) Analysis of these individual clouds to extract metrics related to their traits, (3) Separation of plants into ~~guilds~~functional groups adapted from ~~Diehl et al. (2017) based on similar traits, (4) Identification of guild properties extractable from temporal~~Diehl et al. (2017a), based on similar traits, (4) Identification of functional group properties from UAV-LS and UAV-MS datasets for reach scale classification inputs, and (5) Use of an object-based random forest classifier to determine the spatial discretisation of ~~guilds~~these functional groups. These steps are outlined in the following sections.

~~3.3.1.~~3.2.1. Point Cloud Segmentation

A number of automatic methods exist to classify very dense point cloud scenes into different groups (e.g. Brodu and Lague, 2012; Zhong et al., 2016). However, the majority of these are designed for very high-resolution TLS datasets and so here a semi-automated approach was employed. Smaller vegetation, whose structural composition cannot be fully resolved from UAV-LS data, were analysed from the summer TLS survey. Automatic classification of ground/non-ground points was performed using the progressive morphological filter in the LidR package ~~(Roussel et al., 2020)~~(Roussel et al., 2020) before manually segmenting in CloudCompare (https://www.danielgm.net/cc/) to create individual plant models (Figure 2, *Raw Point Cloud*).

For the herbaceous plants in the TLS data, leaves and flowering parts were manually removed from the clouds so as not to ~~interfere~~influence with the quantitative structural modelling (QSM~~).~~.; see 3.2.2). This was done based on field images and the structural appearance of the clouds to leave just the structural components. Although foliage ~~is~~ has been shown to be important, for the methods used herein ~~they~~it could not be ~~accounted for~~ fully resolved due to insufficient point densities. Any statistical outliers were then detected~~, removing~~ and removed from the dataset, identifying points ≥2.5 standard deviations ~~and~~ above the mean separation distance between points within the segmented cloud. This process was repeated for plants in both TLS scan locations, resulting in a sample dataset consisting of 37 herbaceous plants. Plants were selected in the main TLS point cloud that represented complete vertical profiles to minimise the effect of shadowing from different scan angles.

Tree segmentation also used a combination of manual and automatic classification, based on surveys undertaken in leaf-off conditions, exposing the full ~~internal~~ tree structure. 24 trees were selected from across the reach representing a range of structures and sizes from which complete models could be created. ~~As above, initial~~Initial separation of ground and vegetation points was performed using a progressive morphological filter. ~~Whilst automatic classification methods such as CANUPO exist (Brodu and Lague, 2012), the UAV-LS point densities necessitated the manual extraction of individual trees, prior to interactive filtering using a number of statistical measures. Local~~Trees were then manually extracted prior to interactive filtering using a number of statistical measures; local volume density helped to separate points distinct from the main tree woody structure, whilst linearity metric filters (how aligned points are within a set radius) ~~remove~~removes points that are highly complex or not part of the main tree structure. The statistical outlier removal tool and a final manual check can then be used to remove any remaining ~~erroneous~~ points which are not part of the main tree structure. This resulted in a point cloud of predominantly large branches, with a clearer structural profile as can be seen in Figure 2 (*Filtered Point Cloud*). The thresholds for separating individual trees are size, structure, and point density dependent, hence the need for interactive selection.

~~This~~ Although this adds an element of user bias as to what is deemed a 'main' branch, ~~but~~ the lower density of UAV-LS scans makes ~~this a~~user input necessary ~~method~~ before reconstructing vegetation models (Brede et al., 2019). Shrubs and grasses

whose structure could not be fully resolved from the UAV-LS or TLS data were not analysed for traits extraction. ~~Aside from requiring many TLS scans to capture the extensive and complex branching networks of these plants, in eco-geomorphic terms a traits-based rather than bulk roughness approach is likely to be limited~~Grasses are typically too short to remotely sense with high degrees of confidence, and the complex and extensive nature of the branching network of shrubs would require several TLS scans per plant, with numerous plants needing to be surveyed to get a reliable trait description. As a result, point clouds for shrub classes were only used for classification training, frontal area, and density calculations.

~~3.3.2.~~3.2.2. Trait Metric Extraction

~~For the reconstruction of vegetation stems into cylindrical models, the open source TreeQSM method was applied to the partitioned UAV-LS and TLS derived vegetation data (Brede et al., 2019).~~The hydraulically relevant traits collected were based on those noted within Diehl et al. (2017a) that could be measured using the remote sensing methods within this study. These were; plant height, number of branches, maximum branching order, stem diameter, plant volume, frontal area, and plant density. For the reconstruction of vegetation stems into cylindrical models, the open source TreeQSM method (Raumonen et al., 2013) was applied to the partitioned UAV-LS and TLS derived vegetation data. TreeQSM utilises 'patches' to determine connected points in the vegetation cloud, before growing the tree structure by joining patches together to form a complete model (Raumonen et al., 2013). These are created using user defined initial patch sizes to adjoin points, before refining the patch sizes using minimum and maximum ~~sizes~~limits to create a complete model. This allows the coarse branch structure of the tree to be identified (Figure 2, *Segmented Point Cloud*). Sections are then generalised as cylinders, both for computational efficiency and ~~as~~because they provide a robust representation of trees (Raumonen et al., 2013). ~~These~~The cylinders ~~can~~are then ~~be~~ used to describe the overall structure and properties of the individual plant (Figure 2, *QSM Cylinder Model*). A full method description can be found in Raumonen et al. (2013). QSM methods have been noted to overstate the volume of smaller branches and are sensitive to noise in the data alongside variable point density (Fang and Strimbu, 2019; Hackenberg et al., 2015). However, QSM reconstructs tree structures in a manner which resolve many of the hydraulically relevant vegetation traits.

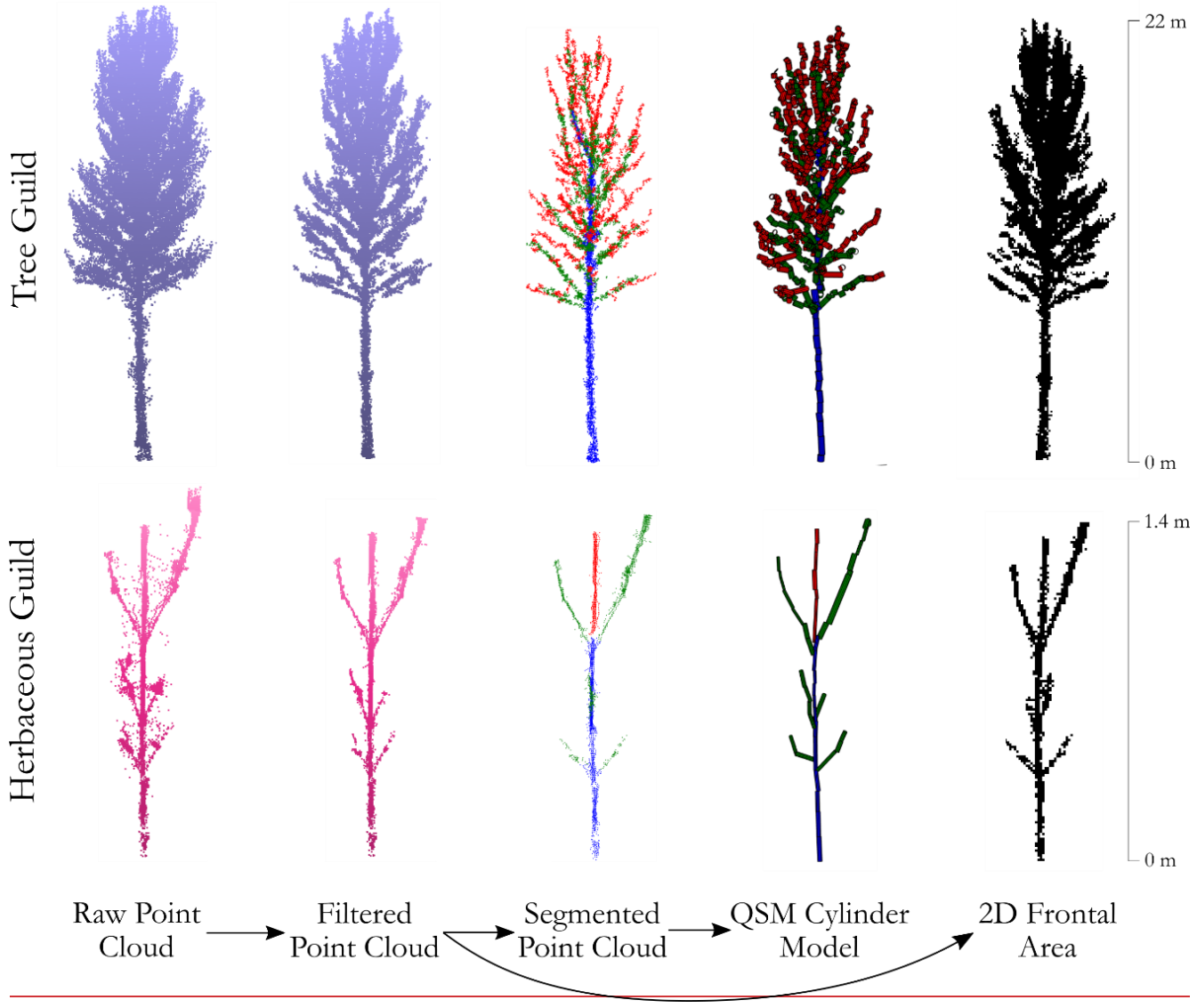
Tree Guild
22 m
0 m
Herbaceous Guild
1.4 m
0 m
Raw Point Cloud
Filtered Point Cloud
Segmented Point Cloud
QSM Cylinder Model
2D Frontal Area

485

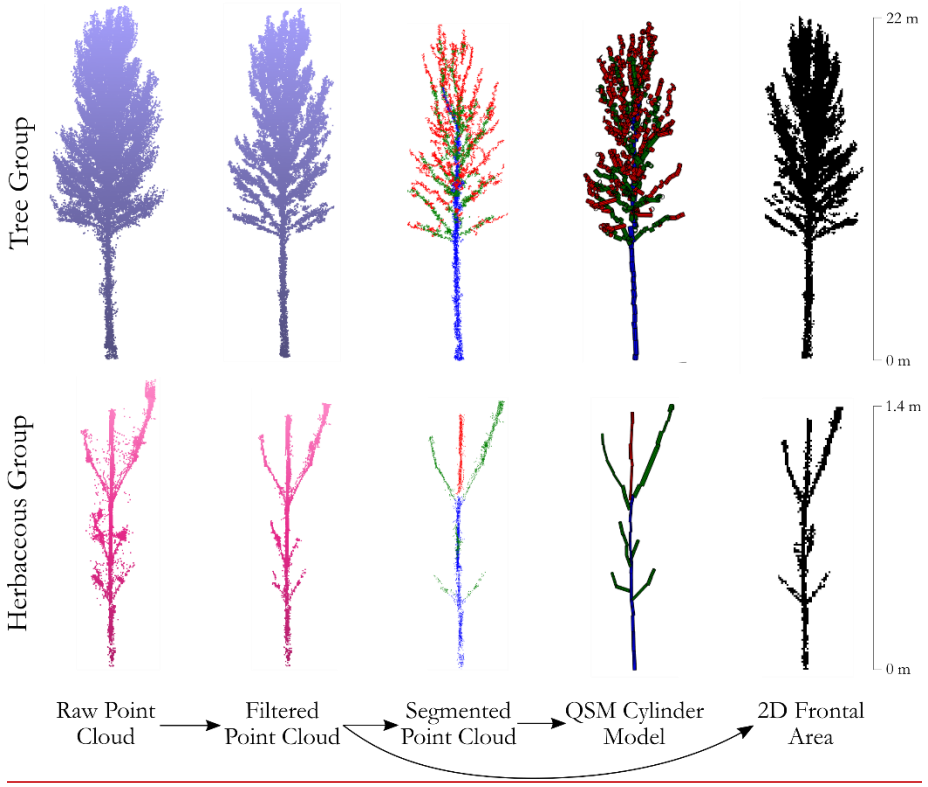

Figure 2 Vegetation trait extraction, from an individual raw point cloud to a cylindrical model and frontal area. The process is demonstrated for two extracted vegetation point clouds, a large tree within the study reach collected from UAV-LS data, and a ~~small~~ perennial on the central bar collected from TLS, note the difference in scales. The segmented point cloud is coloured by branching order from blue to green to red, with the cylinders coloured in the same manner. The 2D frontal areas are based on the filtered point clouds rather than the segmented point clouds or QSM cylinder models, and as such these steps are not required to compute the frontal area data.

Patch diameters (which are used to determine adjacent points within the same tree) were chosen following a parameter sensitivity exercise, with the range of values initially based around those of Raumonen et al. (2013) and Brede et al. (2019) for TLS and UAV-LS approaches respectively. A visual assessment was performed to identify parameters that created models similar to the observed vegetation structure in the point cloud ~~structure,~~ due to the lack of reference data. After testing for the optimum patch sizes for reconstruction, the TLS scans of herbaceous vegetation initial patch diameter was set at a size of 0.005 m, with the second patch diameter minimum and maximum sizes of 0.002 and 0.01 m. The minimum cylinder radius was set to 0.005 m, prescribing the smallest detectable branch structure of the extracted herbaceous plants. For the UAV-LS derived tree data, the initial patch diameter was 0.2 m, with the second patch dimeter minimum and maximum sizes of 0.1 and 0.5 m. The minimum cylinder radius was 0.1 m, based on manual measurements of tree branches within the point cloud that were detectable. For each individual plant model the cylinder reconstruction and variable extraction was repeated ten times. As the modelling begins at a random location each time the start point can affect the results, and so multiple averaged simulations

~~provides~~provide a more ~~accurate~~representative solution. The modelling produces a number of metrics, but for this study hydraulically relevant traits of plant height, number of branches, stem diameter ~~at breast height~~, volume, and maximum branching order, were collected. For each metric of interest, the average value and standard deviation of these values are taken from the ten runs.

The frontal areas of all segregated vegetation clouds were extracted alongside the construction of the cylinder models, based on the 2D methods described by Vasilopoulos (2017). For each discretised filtered plant point cloud~~,~~ (Figure 2, *Filtered Point Cloud*), the data was flattened from 3D to 2D by collapsing the data along a single horizontal dimension on a regular grid (Figure 2, *2D Frontal Area*). The grid resolution was set at half the width of the minimal detectable feature resolved by the QSM modelling; 0.~~005~~0025 m for the TLS derived herbaceous plants and UAV-LS 0.05 m for UAV-LS derived trees. Each plant was flattened along the X and Y axis respectively, with an average frontal area taken.

3.3.3 ~~Guild~~ Identification of Functional Groups

~~Based on the separated points clouds, each were assigned to a guild based loosely on hydrologically relevant traits outlined in O'hare et al. (2016) and Diehl et al. (2017). As outlined above, a decision was made to discretise grasses and shrubs using bulk roughness metrics due to their relative homogeneity and the need for ultra high resolution data. Short branching herbs and taller single stemmed herbs were identified, with discrepancies in flexibility, branching, and height, likely to influence hydrology differently. Woody vegetation was further split in to two guilds, those with high diameter at breast heights (DBH) that had low density of trunks and those with lower DBH that had a higher trunk density. The analysis was preformed separately for woody and herbaceous vegetation. As the aim was to identify characteristics that would separate out the guilds from remotely sensed data, there was little need to compare woody and herbaceous species directly as height would be a dominant component.~~

~~In order to~~For the separated individual plant point clouds, each were assigned to a functional group adapted from those outlined in O'Hare et al. (2016) and Diehl et al. (2017a). These groups were grasses, short branching herbs, tall single stemmed herbs, shrubs and bushes, low DBH trees, and high DBH trees. As discussed previously, shrubs and grasses were not identified using trait extraction. Short branching herbs and taller single stemmed herbs were separated due to the likely discrepancies in flexibility, branching architecture, and height, all of which interact differently with flow. Large woody vegetation was split into two functional groups, those with high diameter at breast height (DBH) that had low density of trunks, and those with lower DBH that had a higher trunk density, to account for the different interactions with overbank flow.

To assess whether remotely sensed data could separate out plants into their ~~guilds~~functional groups in a statistically robust way, a Principal Components Analysis (PCA) was undertaken to identify the variables which explained the most variation within ~~their~~the derived trait metrics. The metrics used for the PCA ~~analysis~~ were those obtained from the QSM and frontal

area calculations outlined previously, which were normalised to remove the influence of different scales (Alaibakhsh et al., 2017). The principal components identified were used to inform the classification of reach scale ~~guilds~~functional groups, identifying those variables that most explained the variation between ~~guilds.~~groups. The PCA was performed separately on the two herb groups and the two woody groups, as although height would be an obvious dominant variable between these two groups, it would not necessarily be one within the groups. All of the herbaceous point clouds from the TLS survey were used in the herbs group PCA, and all the high and low DBH trees from the UAV-LS data were included in the woody group PCA.

3.2.4. ~~Linking~~ Traits ~~to~~and Land Cover Metrics at the Reach Scale ~~Metrics~~

To scale the analysis from individual plants to the entire reach level, a method of linking plant scale traits to broader scale data is required. Convex hulls representing the spatial extent for each vegetation point cloud extracted and analysed above were used to define the regions from which UAV-LS and UAV-MS data were extracted. For small herbaceous vegetation, this was buffered by 0.25 m to account for any misalignment between TLS and UAV-LS clouds. For tree vegetation polygons this buffer was increased to 1 m to incorporate peripheral branches and leaves removed during point cloud filtering. ~~Polygons~~11 polygons for ~~small branching trees and large~~ shrubs and bushes were created based on field ~~observations~~notes from various surveys and photographs from the summer surveys, their outlines in the UAV-LS point clouds, and UAV-MS imagery. ~~A total of~~Similarly, 11 polygons were ~~created for this combined guild category, with 11 made~~defined for grasses. In addition to these vegetation functional groups, 8 polygons for water classes, and 5 for a combined gravel bars and bare earth~~.~~ class were also created using the same technique to classify the remaining land cover. Within these polygons, multiple seasonal variables were extracted for scaling local ~~guild~~functional group identification to reach scale classification. The structural characteristics of the point cloud were extracted through TopCAT (Brasington et al., 2012), obtaining the standard deviation, skewness, and kurtosis over a ~~decimated~~sampled grid at ~~both~~ 1 and 4 m resolutions, the latter to account for larger vegetation footprints. The 4 m resolution ~~decimated~~ grid only considered points classified as vegetation in the initial 'ground/other' point clouds to remove ground points from further analysis. To extract a Canopy Height Model (CHM), a bare earth digital terrain model (1 m resolution) was subtracted from a 0.25 m resolution digital surface model incorporating the vegetation points. The Normalised Difference Vegetation Index (NDVI) across the reach was calculated using the red band along with both the red-edge and near infrared bands of the MicaSense orthomosaic images to produce two separate NDVI layers. As the red-edge can be used to separate out vegetation signatures, using a combination of both was expected to help differentiate plants with similar structural but different spectral properties~~. Analysis of structural and spectral data was performed for each of the four seasons~~ (Schuster et al., 2012). Analysis of structural and spectral data was performed for each of the surveys to gain an insight in to how these properties vary temporally. For each of the vegetation polygons, the attributes of each of these layers for each season were extracted using zonal statistics. The mean and standard deviation for each attribute for each ~~season~~survey were then calculated across the different ~~guilds~~functional groups for use in the classification model.

3.2.5. Reach Scale ~~Guild~~Functional Group and Land Cover Classification

To scale from ~~guilds~~groups created from individual UAV-LS and TLS derived plants, to the entire reach, an object~~-~~-based random forest classification was undertaken. Object~~-~~-based approaches overcome some of the issues of variation and complexity in high resolution images (Myint et al., 2011), improving continuity in the results (Duro et al., 2012; Wang et al., 2018). The RGB bands from the multispectral camera and the CHM were combined to create a 4-layer image from which to ~~classify~~identify distinct objects in summer imagery for 2020 and 2021. The Felzenszwalb Algorithm was applied which uses graph based image analysis to segment an image into its component parts based on the pixel properties (Felzenszwalb and Huttenlocher, 2004). This results in regions within the image being grouped base on them having similar properties according to the input layers, avoiding the salt and pepper effect found in traditional pixel by pixel classification approaches (Wang et al., 2018).

Table 2 Description of ~~guilds~~functional groups and land cover classes used for training the random forest classifier, showing the number of training objects from the image segmentation for 2020 imagery, and the training area size.

~~Guild~~Functional group/Land cover	No. of Training Objects	Training Area Size (m^2)
Grasses	93	321
Branching Herbs	15	25
Single Stemmed Herbs	16	29
Branching Shrubs	135	388
Low DBH Trees	158	876
High DBH Trees	62	238
Gravel Bars and Bare Earth	122	641
Water	41	157

In total, 644 training objects were identified ~~using~~ for the 2020 summer imagery, with the previously discretised vegetation convex ~~hull regions, with~~ hulls having multiple training objects present within each ~~training~~ sample (Table 2). A random forest classifier was then trained ~~based on the layers that were deemed to distinguish between the different guilds~~using this 2020 data, having proved an effective machine learning technique (Adelabu and Dube, 2015; Chan and Paelinckx, 2008; Adam and Mutanga, 2009)~~, with a water mask included to reduce errors associated with varying flow stage.~~. The layers that were deemed to distinguish between the different vegetation functional groups, gravel bars, and water in 3.2.4 being used as the input, and a water mask included to reduce errors associated with varying flow stage. As the distinguishing features of each functional group required the inclusion of both summer and winter data, an annual classification as opposed to a seasonal one, is undertaken. This helps to improve confidence in the classification where variation in reach scale metrics happen both between

groups and between seasons. An analysis of model accuracy vs number of forests showed a convergence of accuracy above 100 forests and a reduction in band importance variability above 300 forests (Figure 3). Higher variation in band importance suggested that the number of trees was influencing the likelihood of an optimal solution. This random forest classification was then applied to the remaining objects within the reach for 2020, and also for all objects detected in the 2021 data.

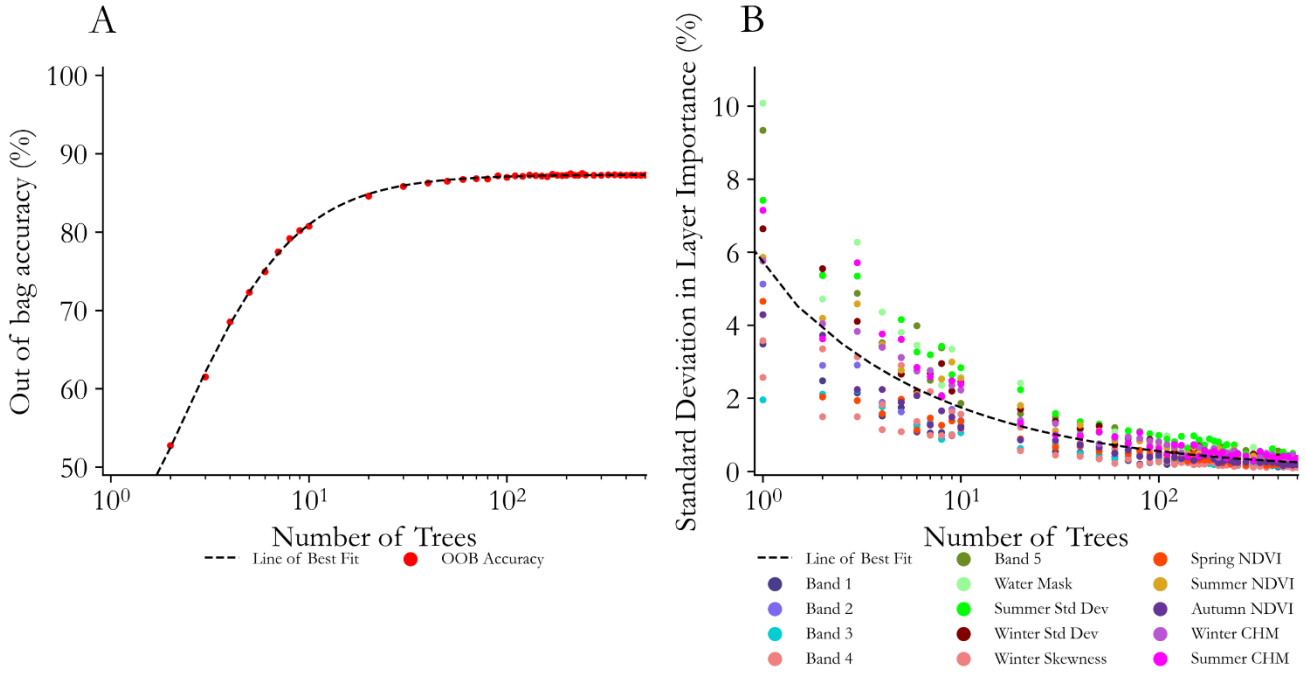

Figure 3. Random forest classifier out of bag accuracy and variations in band importance for functional group classification. A) Out of bag accuracy scores for different numbers of trees used within the random forest classification, showing a distinct levelling off in accuracy after ~100 trees are used. B) The standard deviation in individual band importance across 10 sample runs to identify at what number of trees band importance becomes consistent across all runs, in this instance around 300 trees.

Due to the limited number of extracted samples ~~being used~~from the point clouds, there were not enough ~~training samples~~ to split into a training and test dataset. The multi-tree approach of random forests is constructed on a sample of the dataset and as such can be tested against itself to determine an out of bag accuracy score. It also successively adds and removes bands to determine the band importance in the classification (Adelabu and Dube, 2015). Alongside this self-assessment, for the final ~~guilds~~functional group classes a total of 80 random points were generated across the study site with an equal number in each outputted ~~guild~~group. These were manually classified using high resolution ortho-imagery from a UAV-RGB (0.02 m resolution) survey from September 2020, in field photographs, and study site knowledge. The output classification ~~was~~could not ~~visible~~be seen when undertaking this accuracy assessment and the order of the control points shuffled to remove user bias.

The classified ~~guilds~~functional groups map for 2020 was then used to extract the predicted ~~guilds~~functional groups of these points before a confusion matrix was utilised to assess the accuracy of the classification.

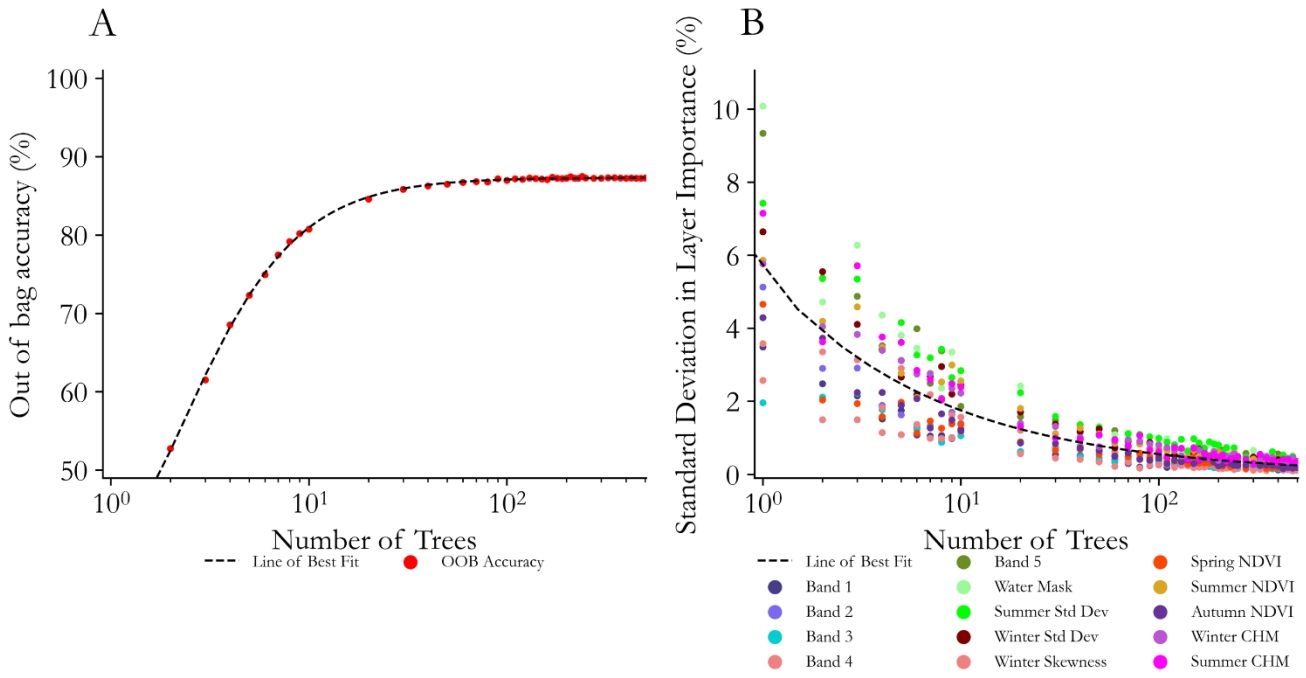

~~**Figure 3 Random forest classifier out-of-bag accuracy and variations in band importance for guild classification. A) Out-of-bag accuracy scores for different numbers of trees used within the random forest classification, showing a distinct levelling off in accuracy after ~100 trees are used. B) The standard deviation in individual band importance across 10 sample runs to identify at what number of trees band importance becomes consistent across all runs, in this instance around 300 trees.**~~

3.3. Morphological Change

The M3C2 algorithm (Lague et al., 2013) was employed to calculate morphological change, whereby the surface normals from a subsampled cloud of core points (here at 0.1 m resolution) are calculated, and change along the normal direction is identified with the calculation of a local confidence interval. This overcomes some of the limitations of traditional elevation model differencing which ~~can't~~cannot account for the direction of change~~.~~, a problem that is pronounced for example on the vertical faces of river banks (Leyland et al., 2017). The benefits of using both SfM and UAV-LS data allows their respective drawbacks to be overcome through combining both datasets. SfM has been shown to perform poorly in vegetated reaches~~, whereas~~ where UAV-LS maintains good ground point densities, ~~whereas~~yet SfM provides good continuity and high point densities in unobstructed areas. Therefore, in order to obtain good surface normals for assessing change, both the ~~two~~UAV-LS and UAV-SfM clouds were merged for each survey date (see Tomsett and Leyland (2021) for error analysis) and their vegetation

removed through the use of the same progressive morphological filter used previously ~~to produce~~. These resultant clouds ~~which~~ were then differenced from their preceding survey date using the M3C2 algorithm.

3.4. Assessing Time Varying Eco-Geomorphic Interactions and Functional Group Hydraulic Roughness

To identify the presence of possible eco-geomorphic feedbacks and establish whether there were differences in directions or magnitudes of morphological change between the different functional groups, the classified functional group maps were compared to the morphological change detection datasets. Each pixel of the vegetation maps had the corresponding morphological change values extracted, with the vegetation maps for year one being used for both the February- July 2021 and July – September 2021 morphological change values, and the vegetation maps for year two being used for the September 2021 – April 2022 and April – June 2022 morphological change values. The distribution of these datasets as well as the grouped total net change was then compared between each time interval to reveal the annual patterns of erosion and corresponding functional groups.

To assess the potential seasonal influence of different functional groups on the conveyance of water through the reach a different approach was required because each of the full classification maps produced necessarily utilised data from both summer (leaf-on) and winter (leaf-off) conditions. To assess the changing nature of the functional groups through time, the point clouds used for extracting traits from the herbaceous and tree groups, along with ten individual shrub point clouds, were used to estimate the depth varying excess drag created for summer and winter vegetation states. The depth of flow used in the calculations was determined based off a large flood event that occurred in the winter of 2020/21 (see Figure 1), representing a maximum hypothetical flow depth from which to assess the interaction between vegetation and flow. The flood extent, flow velocities, and depth used to calculate drag was modelled using Delft3D (Deltares, 2021), set up using measured DEMs and SfM corrected bathymetry along with flow conditions constrained by the gauge data measured downstream of the reach.

For each of the functional groups derived, the frontal areas at depths of up to 0.1, 0.5, 1, 2, and 4 m were extracted, with these elevation bands representing natural breaks in different vegetation vertical structures. Each of these depth dependent frontal areas were then used to determine the excess drag component (F) of a single plant according to,

$$F = \frac{1}{2} C_D A_0 \rho U^2 \quad [1]$$

where C_D is the coefficient of drag, A_0 is the frontal area of the plant facing the flow, ρ is the fluid density, and U is the velocity of the fluid, estimated using Delft3D. The excess drag for an individual plant was then transformed into an excess drag per metre squared, being multiplied by the plant density. Plant density was calculated for each functional group by creating a raster

surface from extracted TLS and UAV-LS data of each relevant group (0.05 m resolution for herbaceous and 0.2 m for shrubs), using a local maximum filter to identify the top of individual plants, similar to the procedures used to delineate individual trees in dense canopies (Douss and Farah, 2022; Chen et al., 2020). The number of individual plants was calculated, and divided by the total patch area, to provide plant density. For trees, where the trunks could be reconstructed, the point cloud was inverted before running the local maximum model to identify the locations of tree trunks. A 0.2 m resolution raster surface was used for this and the number of trunks was counted to provide both sets of tree density data.

Drag coefficients were estimated using a combination of plant morphology and values from the wider literature. They were also adjusted seasonally, ranging from 0.55 to 1 (see supplementary material), with foliated plants being subject to a greater reconfiguration process during high flows (Sand-Jensen, 2008; Whittaker et al., 2013). The original frontal areas of each plant were also extracted from defoliated plants, and as such a comparison in the literature of foliated to non-foliated frontal area was used to adjust the frontal areas accordingly at each depth interval (Wilson et al., 2003; Järvelä, 2002a). As a result, four spatial distributions of hypothetical excess drag were calculated across the domain for the summer and winters of 2020 and 2021 (assuming the large flood inundation extent and flow) which could then be used to inform discussions of how the presence of different functional groups link to location on the floodplain and potential eco-geomorphic feedbacks.

4. Results

~~4.1. Decadal Scale Change~~

~~Analysis of planform shift from the year 2000 through to 2020 has identified that the channel is highly mobile, experiencing rapid change in places as well as more gradual evolution in others. From the 586 bank transects cast, the average SCE (extent of bank movement) was 38 m whilst the median change was 25 m. The smallest change was 1 m whereas the largest was 120 m. Comparison of sections with large vegetation present and absent suggests there is a greater average mobility in vegetation present sections (Table 3). This goes against the assumption that vegetation helps to reduce channel mobility. However, Figure 4 suggests that the areas where the channel has remained predominantly stable through time have some vegetation influence. Of the four areas of significant change, only one appears to follow the traditional meander development model of lateral erosion leading to a cut off, with the three remaining sections showing likely avulsion or previous channel reoccupation. Analysis of channel mobility excluding these avulsions indicates that reaches with large vegetation present have lower rates of lateral mobility, and that there is evidence of large vegetation reducing rates of planform shift.~~

~~Table 3 Transect statistics showing the difference between sections with large vegetation present and those where it is absent s, with and without channel reoccupations (avulsions). N refers to the number of transects within each category.~~

	~~SCE statistics for each scenario~~			
~~N~~	~~Mean~~	~~Median~~	~~Std. Deviation~~	~~Max.~~

Large Vegetation Present (Inc. Channel Reoccupation)	220	48	24	41	121
Large Vegetation Absent (Inc. Channel Reoccupation)	348	35	27	27	101
Large Vegetation Present (Exc. Channel Reoccupation)	290	10	8	7	47
Large Vegetation Absent (Exc. Channel Reoccupation)	339	22	16	18	72

Figure 4 (A) and (B) compares frequency of SCE values for sections with and without large vegetation being present, including and excluding avulsions. For reaches with large vegetation, removing the avulsions has a notable impact on the distribution, with many more transects falling within smaller SCE values. Although this shift is seen in the transects without large vegetation also, the change in distributions is less prominent and is supported by a smaller change in mean values, dropping from 35 m to 27 m for large vegetation absent reaches and from 48 m to 10 m for reaches with large vegetation present.

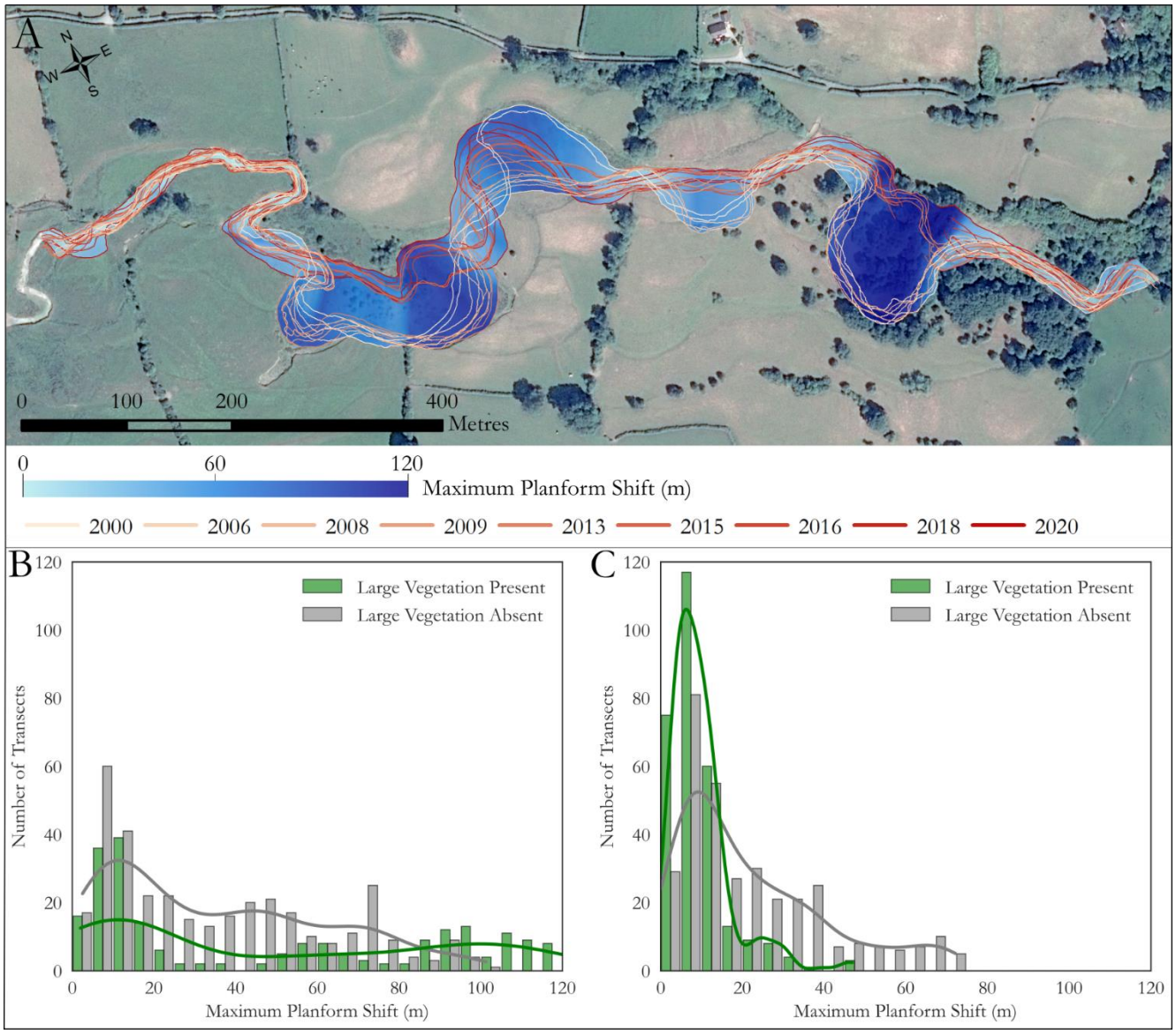

Figure 4 Results from the decadal DSAS analysis. A) DSAS results showing channel evolution from 2000 – 2020, with left- and right-hand banks digitised for each year. Spatial variability in maximum planform shift is shown in blue. Background imagery provided by ESRI (2021). B) shows the range of SCE values from both the left- and right-hand banks combined, for sections classed as containing large vegetation and those that do not. C) shows the SCE values when the effects of avulsion are removed from the data, for both large vegetation present and absent sections also.

This channel switching appears to involve reoccupation of former channels that have lower floodplain elevations during overbank flow events. The three erosion channels in Figure 5 show the stages of progression. Feature C demonstrates a completed channel neck cut off for a double meander bend. Both features A and B appear to be developing during flood events, with the orthomosaic insets showing the overbank flow captured during a flood event and the resulting channel position post

~~flood for feature B. This implies a consistent pattern in new channel development that occurs during successive overbank flow events.~~

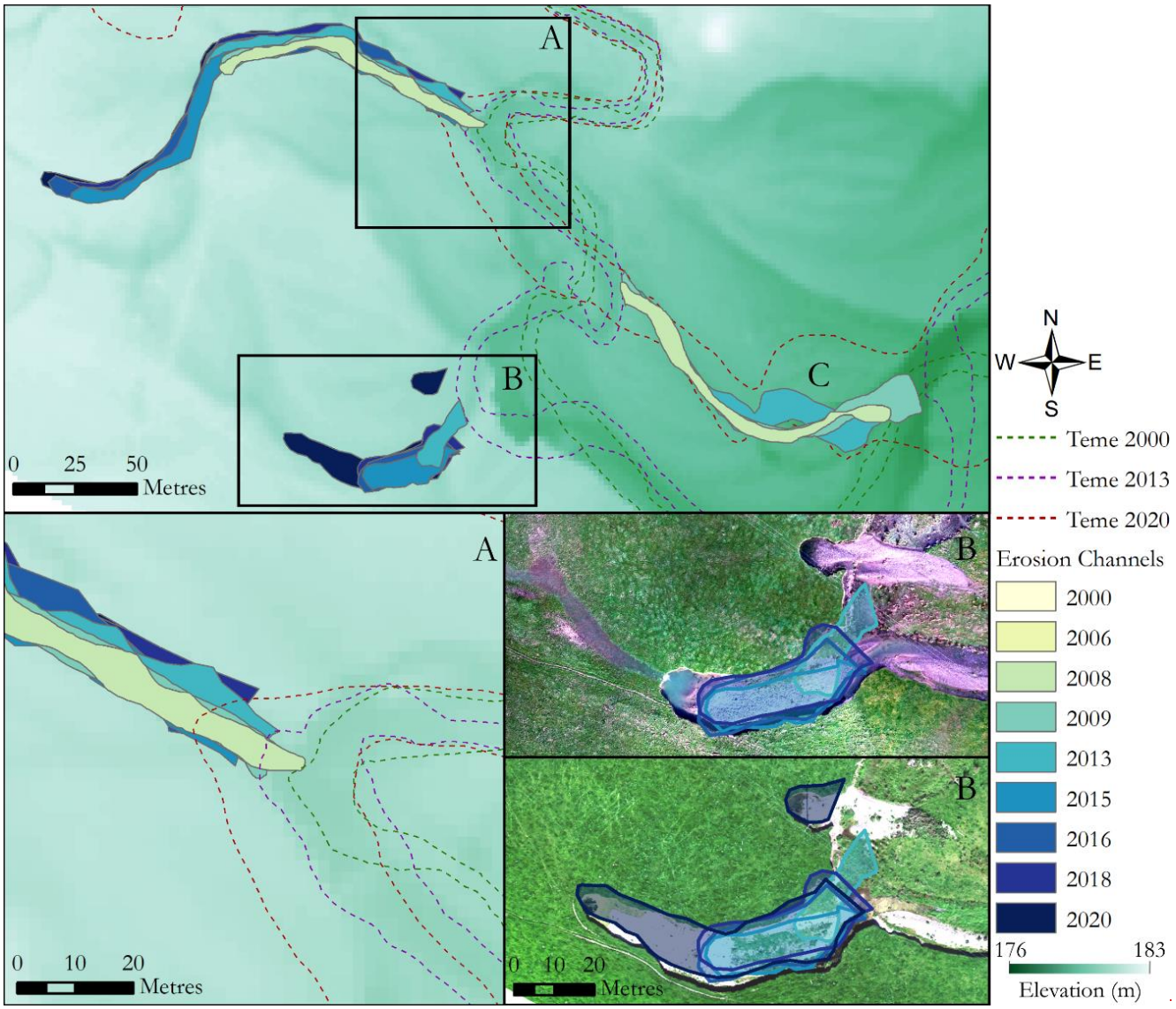

715 **~~Figure 5 Historical analysis of avulsion development across the floodplain. The top panel shows two developing channels (A and B) across the floodplain and one channel neck cut off (C). The bottom left panel (Channel A) shows how this development is influencing successive planform shift, and the bottom right panels (Channel B) demonstrates how this is linked to overbank flow.~~**

4.2. ~~Hydrologically~~Hydraulically Relevant Trait Analysis

4.2.1. Extraction and Analysis of Traits

The QSM analysis appears to output visually sensible results and produce models appropriate for the vegetation being ~~modelling (see Figure 2). Table 4 shows the standard deviation of a selection of QSM metrics as a percentage of the mean value. The repeat modelling was more consistent for larger vegetation, with lower relative standard deviations. However, for some metrics such as number of branches, herbaceous plants with few branches may be adversely affecting the results. For example, plants with 5 stems having errors of +/- 1 branch is a 20% difference, whereas for 20 stems this is only 5%. Overall, model repeats~~modelled (see Figure 2). The repeat modelling of the individual plants produced consistent trait results. The heights of herbaceous groups were consistent to within 4%, whilst tree groups were consistent to just over 1%. Repeat diameter calculations were within 16% (0.08 m) for tree groups and within 18% (0.002 m) for herbaceous groups, with higher discrepancies in the number of branches. For trees, the number of branches for each model repeat were within 9% of each other, equivalent to 12 branches, whereas for herbaceous functional groups this was 17%, which equates to under 1 branch. The complexity of the larger tree models makes this variation quite likely, especially when the resolution of branches approaches the resolution of the scan data, whereas for herbaceous groups the higher variation is a result of the low number of total branches, so an additional branch being identified has a larger impact on the results. Overall, model repeats of individual plants appear to have good agreement with one another, and provide a basis for separating out vegetation with similar ~~hydraulic~~ functional traits.

~~**Table 4 Standard deviations in trait values as a percentage of the mean values for herbaceous and tree guilds. Guilds aggregated to include all herbaceous and tree data. Expressed as a percentage of mean due to the varying scales of data between the two guilds.**~~

	~~Height~~	~~Number of Branches~~	~~DBH~~	~~Volume~~	~~MBO~~
~~Herbaceous Guilds~~	~~3.87~~	~~16.77~~	~~17.83~~	~~12.18~~	~~17.52~~
~~Tree Guilds~~	~~1.16~~	~~8.79~~	~~15.58~~	~~12.89~~	~~15.00~~

As no manual ecological field measurements were taken of plant structure, values extracted from the survey data were compared to those found in the wider literature and online databases. Within the tree functional groups, those with a low DBH had an average height of 18.2 m +/- 3.3 m, and a DBH of 0.39 m +/- 0.08 m. Field identification from photos taken on site identified a large number of these trees to be of the Poplar variety. Comparison with both the TRY databases (Kattge et al., 2020) and observations in the literature comparing height and DBH for these species (e.g. Burgess et al., 2019; Engindeniz and Olgun, 2003; Zhang et al., 2020) showed good agreement. The range of heights within the TRY database incorporated those measured from the trait extraction methods and aligned well with the comparison of tree heights and DBH identified by both Burgess et al. (2019) and Engindeniz and Olgun (2003),with the latter studying Poplars from Turkey as opposed to the

UK. Trees with a higher DBH were predominantly identified as a mix of Willow and Alder, with average heights of 14.9 m +/- 3.2 m with DBH values of 0.69 m +/- 0.11 m. This aligned well with the overall height ranges observed in the TRY database for Alder trees, and the only record with both height and DBH values for Alder showing a tree of 30 m having a DBH of 0.9 m. Southall et al. (2003) found diameters of up to 0.45 m for plants 8-9 m in height, with the trees in this study being both taller and larger in diameter suggesting a difference in maturity. Conversely, both Colbert et al. (2002) and Jurekova et al. (2008) both found DBH values within the observed range of diameters in this study for trees of similar height. This suggests that although the original QSM methods were tested on Fir, Spruce, Beech, and Oak trees, the methods are suitable for use on a wider variety of trees and produce results in line with those expected for the species being observed.

Field observations of the single stemmed herbaceous group identified a dominance of Marsh Thistle, with average heights of 1.14 m +/- 0.17 m and an average stem diameter of 0.013 m +/- 0.002 m. Height values align well with those found in the TRY database, with the majority of recorded heights between 0.8 – 2 m (Kattge et al., 2020). Van Leeuwen (1983) measured stem circumferences of between 0.026-0.070 m, equating to diameters of between 0.008 and 0.022 m, yet very little other literature or values on stem circumference or diameter are available. Nevertheless, both the observations of Marsh Thistle height and stem diameters suggests that the modelling has effectively reconstructed the vegetation. Likewise, comparison between the average height values of the branching herbaceous group, predominantly identified as Hedge Mustard, and those values in the TRY database indicate good agreement, with reconstructed values from the field having heights of 0.46 m +/- 0.12 m and values in the TRY database averaging 0.49 m, albeit with a much higher variation of +/- 0.25 m. As with the single stemmed herbaceous group, there is very little data to compare obtained values of stem diameter with. It would be expected that the branching herbs would have a lower diameter based on field images, and this is the case with an average of 0.011 m +/- 0.003 m. However, this is approaching the likely limit of detection of the TLS scans, whereby the stem diameter approaches the resolution of the scan data. Yet for both of the herbaceous functional groups, the methods deployed appear to have consistently modelled individual plants, and produced values in line with those in the wider literature. For both the herbaceous and tree groups, the extracted traits can be reliably used to examine which traits distinguish between different functional groups.

Figure ~~6~~4 shows the PCA plots of herbaceous vegetation metrics from the TLS scans ~~(A)~~ and woody vegetation metrics from the UAV-LS scans ~~(B).~~. It is clear that some separation of points through dominant metrics is possible, with both plots exhibiting two principal components capable of separating the defined ~~guilds. Panel A~~functional groups. Figure 4A shows the PCA plot for herbaceous vegetation. Height is identified as a clear component between each ~~guild~~functional group, as well as volume. Although the number of branches was not a key component for separating ~~guilds~~functional groups, branches per unit height explained some of the variability in the data. Taller plants may have a similar number of branches, and so accounting for plant height produces a density of branches independent of size to help explain plant structure. Of the four identified components, only ~~the~~ height is identifiable from the UAV-LS data for upscaling, however, point density and spectral properties may improve ~~guild~~group separation. ~~Panel B~~Figure 4B shows the PCA plot for woody vegetation. Height is less important in

distinguishing the two ~~guilds~~functional groups than for herbaceous vegetation, yet trees under or over certain heights are likely to be one ~~guild~~group or the other suggesting minimum and maximum threshold values. For separating ~~guilds~~functional groups, the most important components appear to be DBH and vertical skew which was expected as this was the basis for initial ~~guild~~functional group classes. DBH cannot always be easily extracted from UAV-LS data if it is incomplete, therefore as the vertical distribution acts in the same component direction, this can be used as a potential method for differentiating ~~guilds.~~functional groups. There is however considerable overlap in both of these PCA plots for woody and herbaceous vegetation. There are dominant trends such as the DBH and plant height for separation, but there is considerable variation within the ~~guilds~~functional groups for their QSM based metrics which may impact the final classification.

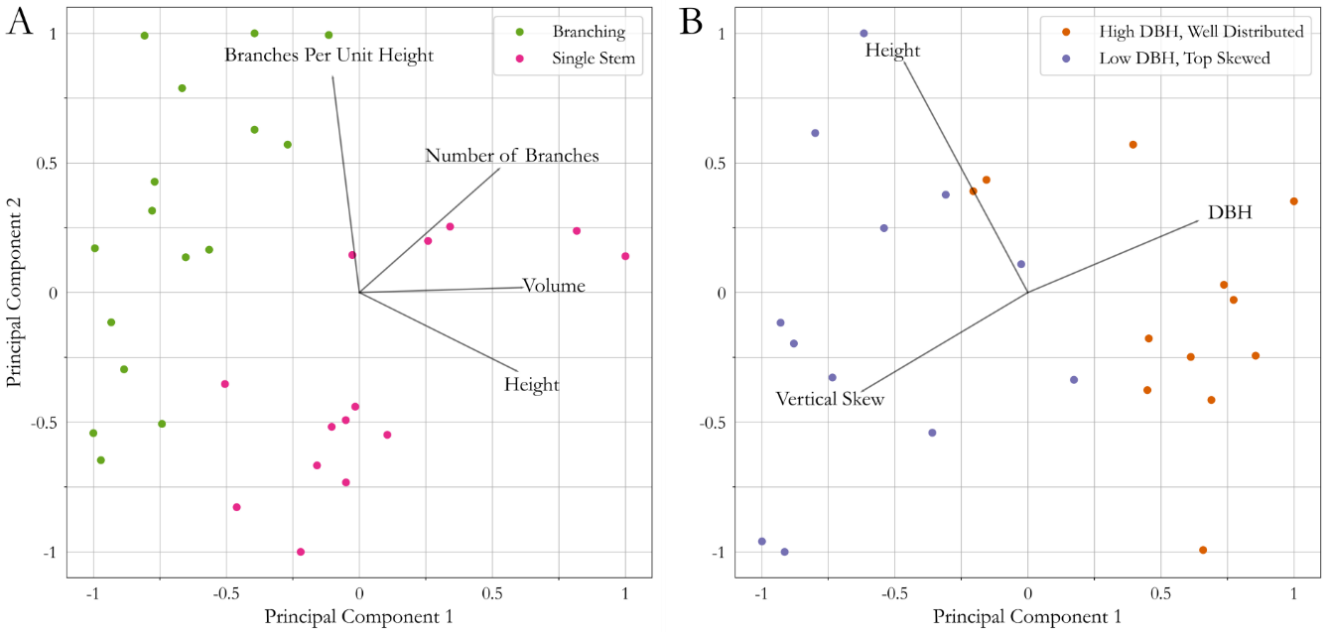

Figure ~~6~~4 PCA analysis of (A) herbaceous and (B) tree ~~guilds~~functional groups to investigate differences in trait characteristics. Lines indicate direction of each variable that explains variation in the data.

4.2.2. Linking PCA Clusters to Reach Scale UAV-LS Data

Figure ~~7~~5 shows the results of the seasonal analysis of different variables derived from UAV-LS and UAV-MS imagery for each of the ~~guild~~functional group classes. There are clear variables which can separate different ~~guilds~~functional groups with ease, for example the height of the canopy is a key indicator between woody, herbaceous, shrub, and grass ~~guilds.~~functional groups. Separating out similar ~~guilds~~functional groups does appear to be more nuanced. The High DBH and Low DBH woody ~~guilds~~functional groups both have very similar values and seasonal patterns of changes in NDVI values as well as in their height. This is unsurprising as the PCA analysis showed~~, with~~ height not being a dominant factor in explaining variation, with numerous samples showing crossover. Vertical skew did show ~~guild~~group separation, with the samples used for QSM analysis

collected in leaf-_off conditions. Figure ~~7 does suggest~~5 suggests that changes in winter skew are visible between the two ~~guilds~~tree functional groups, with a smaller amount of crossover as expected. Spring, summer, and autumn skewness is less informative, likely due to leaf-_on conditions ~~effecting~~affecting full tree reconstruction, with higher variability in results between the sample areas.

Separating out herbaceous ~~guilds~~functional groups is also a challenge. ~~Elevation~~CHM values for single stemmed herbs are more variable and cross over ~~in to~~into grasses and multi-branching herbs. However, the mean ~~elevation~~CHM values are higher, in line with the PCA analysis, and may enable herbaceous ~~guild~~group separation. Likewise, the average skew values help to differentiate between classes, but again the variability in the data suggests it is harder to separate by structural content alone. Conversely, spectral data shows great promise in differentiating between ~~guilds.~~functional groups. Both the absolute values between herbaceous ~~guilds~~functional groups show different as well as their seasonal patterns especially when utilising the red edge band for NDVI calculations.

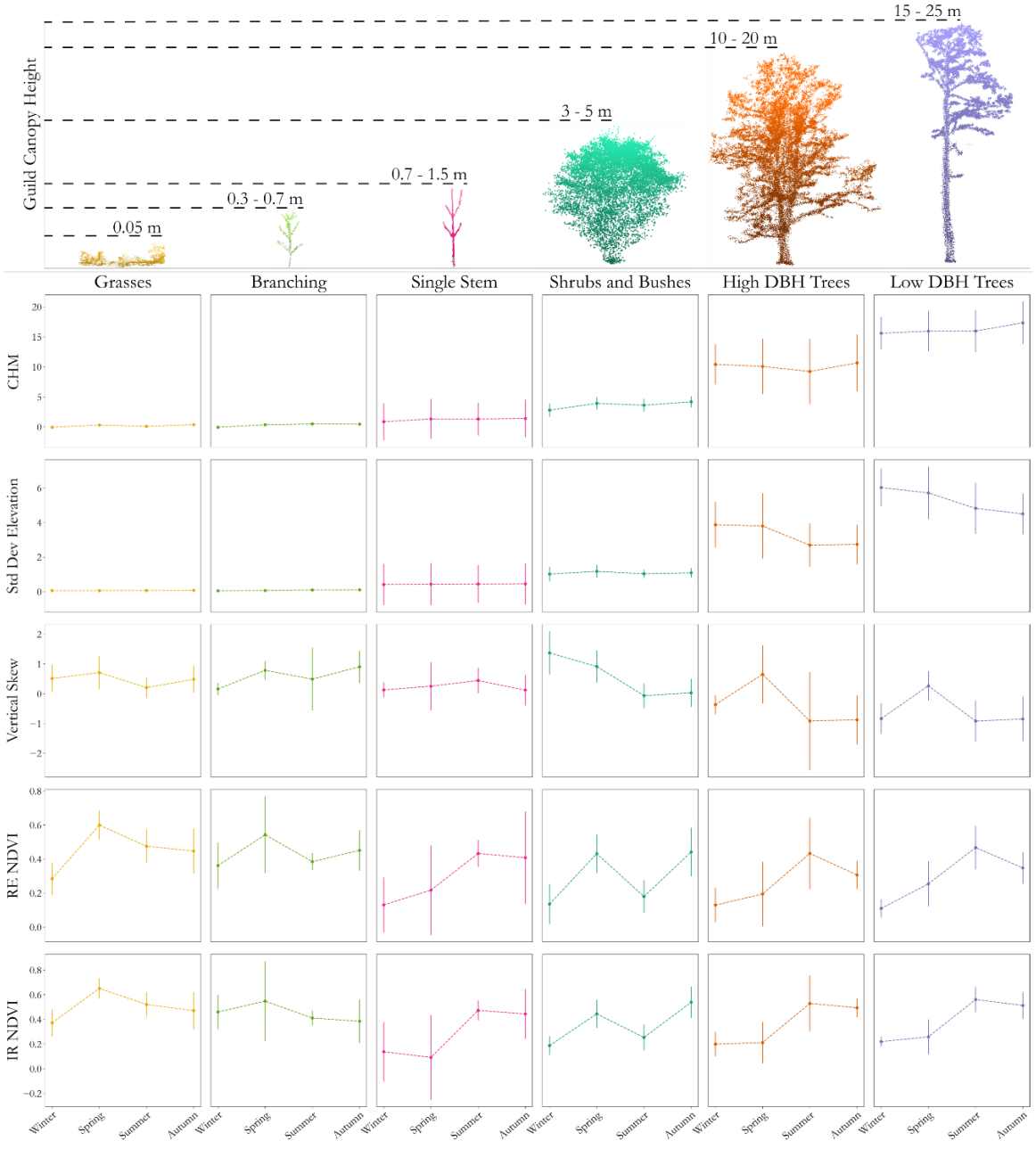
Guild Canopy Height
0.05 m
0.3 - 0.7 m
0.7 - 1.5 m
3 - 5 m
10 - 20 m
15 - 25 m
Grasses
Branching
Single Stem
Shrubs and Bushes
High DBH Trees
Low DBH Trees
CHM
Std Dev Elevation
Vertical Skew
RE NDVI
IR NDVI
Winter
Spring
Summer
Autumn

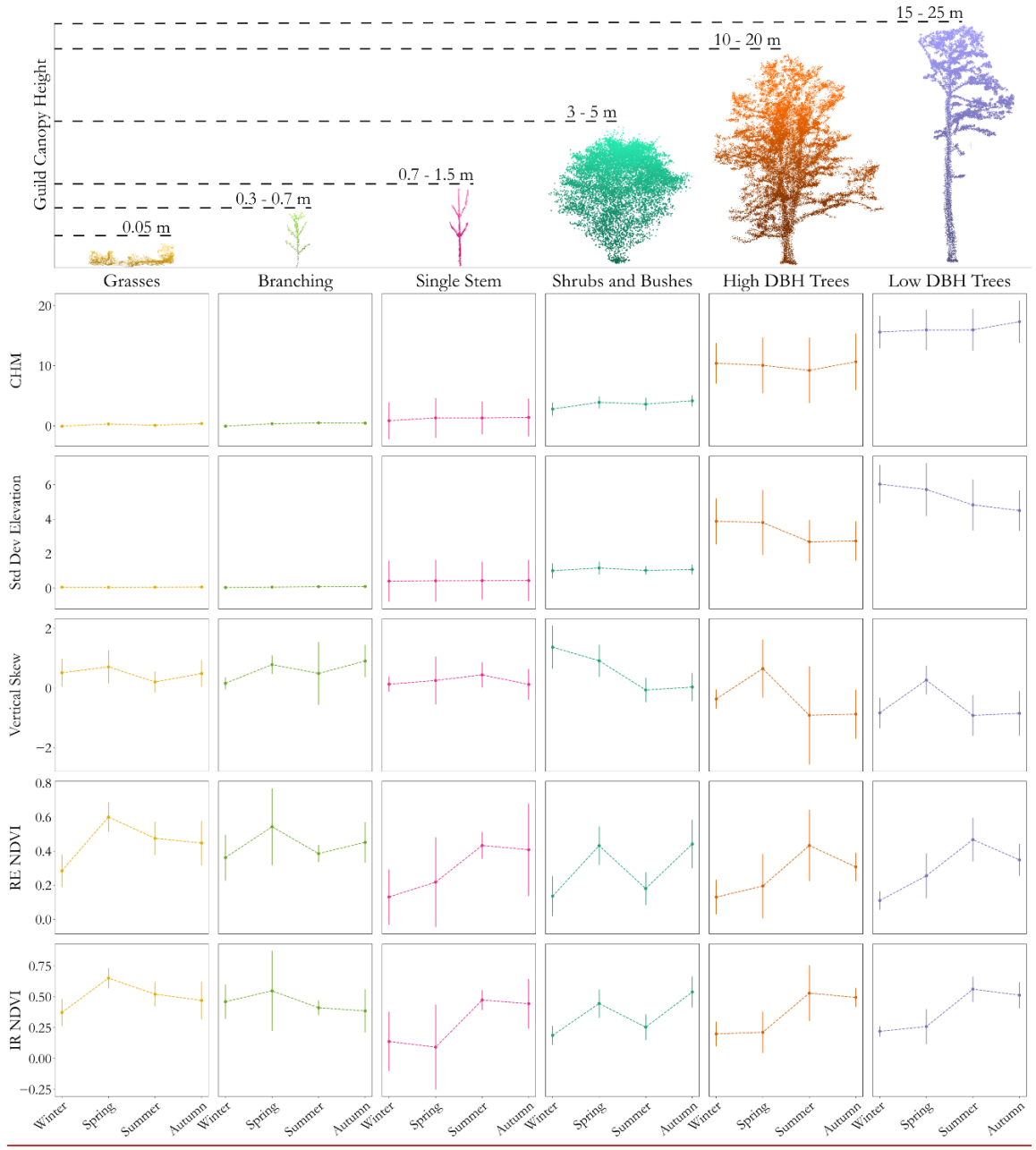

Figure ~~75~~ Results of seasonal analysis (X-axis within subplots) of different reach scale metrics (Y-axis) from UAV-LS and UAV-MS data for each identified ~~guild~~plant functional group. The point clouds at the top provide an example ~~point cloud~~ of vegetation in each ~~guild class~~functional group, with canopy height ranges acquired from trait extraction for the four analysed ~~guilds~~functional groups and from the reach scale analysis for the remaining grass and shrub ~~guilds~~functional groups. Error bars indicate one standard deviation around the mean, CHM (Canopy Height Model) is given in metres, IR refers to Infra-Red and RE to Red-Edge bands in the NDVI calculations.

4.2.3. Creation of Seasonal Reach Scale ~~Guilds~~Functional Group Maps

The ~~resultant classification from guild classification can be~~annualised reach scale classifications based on functional groups and land cover is shown in Figure ~~8 with many areas being classified as expected.~~6. There appears to be an over classification of ~~the branching~~ shrubs ~~class~~ based on initial comparisons with ortho-imagery, ~~whereby~~where the edges of larger vegetation and some predominantly grass regions appear to have been misclassified. This may be due to the large variation in structural and spectral characteristics of this ~~guild~~group which were less well accounted for. Herbaceous ~~guilds~~groups were predicted in areas that were to be expected~~, in~~; including mobile areas of the channel were larger vegetation would find it more challenging to establish. The out-of-bag accuracy score when training the random forest classifier with 300 trees was 87.2%. Figure ~~9 A~~7A shows the importance of each band in the classifier, with structural elements proving key in separating ~~guilds~~functional groups, especially using summer standard deviation

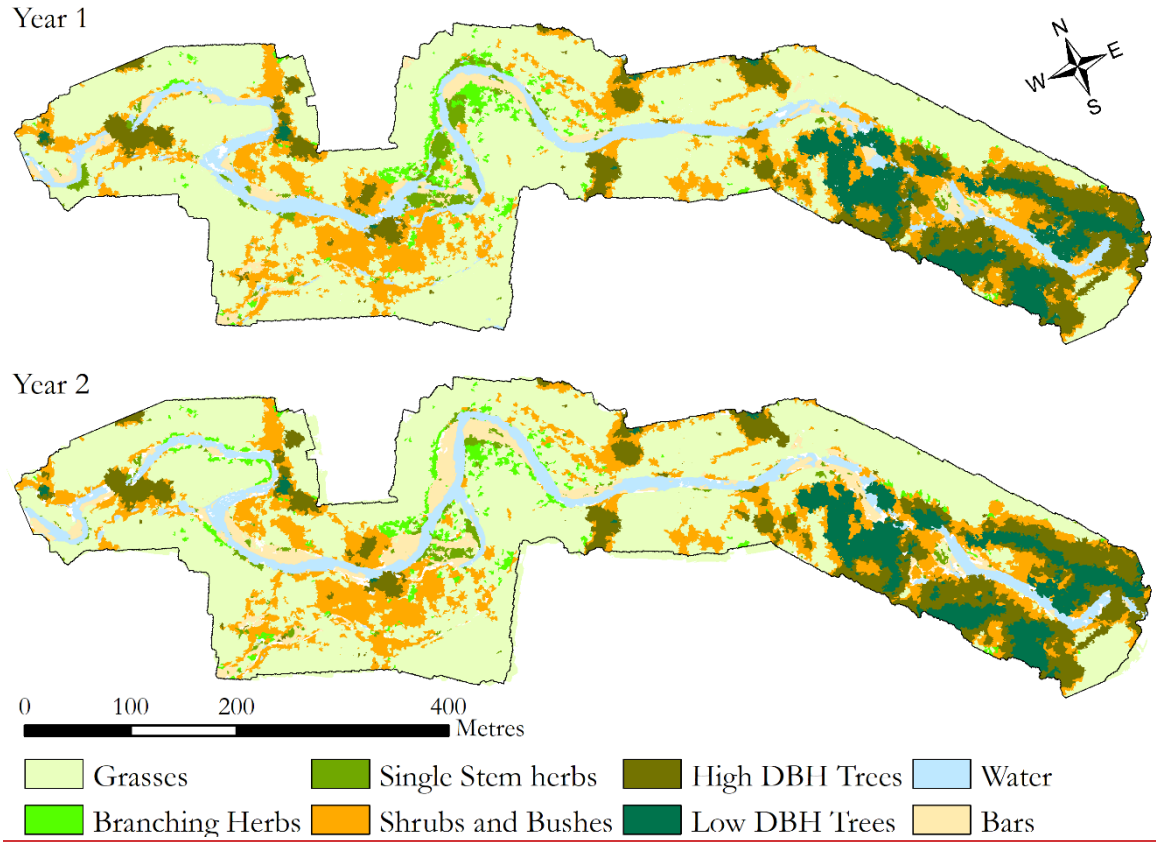

Figure 6 Resulting classification from reach scale analysis for the areas covered by both UAV-LS and UAV-MS data for year 1 and year 2 of the surveys. Note the over classification of shrubs and bushes, especially at the edge of larger wooded groups, and the changes in channel planform and functional groups through the central section of the reach.

of point ~~elevations~~heights. The near infra-red band and winter standard deviation are the next most important elements, with the remaining individual spectral bands providing a smaller contribution to the classification. The higher importance of the two NDVI layers implies that providing the classifier with analysed image data is more useful than individual bands alone. Likewise, the canopy models alone are less informative than the variation in ~~elevations~~plant height when detecting ~~guilds~~functional groups, supporting the use of manipulated rather than simple metrics to help improve classification.

The confusion matrix can be seen in Figure ~~9 B~~7B comparing the number of check points that are correctly and incorrectly predicted. The overall model accuracy is 80%, lower than the out-of-bag prediction. However, this is not surprising as training areas were delineated based on complete structural profiles for the QSM analysis and the total number of samples used for training was small relative to the possible variation across the reach. There was a general over classification of points ~~as~~within the grass ~~guild~~functional group, with only one grass control point incorrectly classed as branching herbs. Branching herbs which are more detectable from imagery and likely to return more laser scan points were classified reasonably well, only being misclassified as grass.

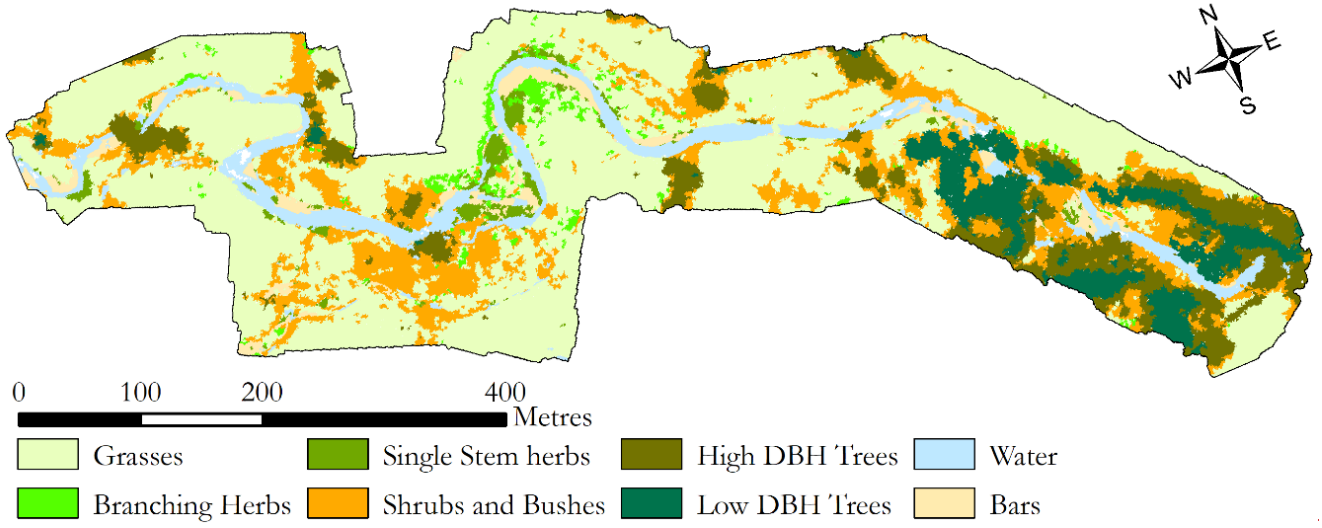

~~**Figure 8 Resulting classification from reach scale analysis for the areas covered by both UAV-LS and UAV-MS data. Note the over classification of shrubs and bushes, especially at the edge of larger wooded guilds.**~~

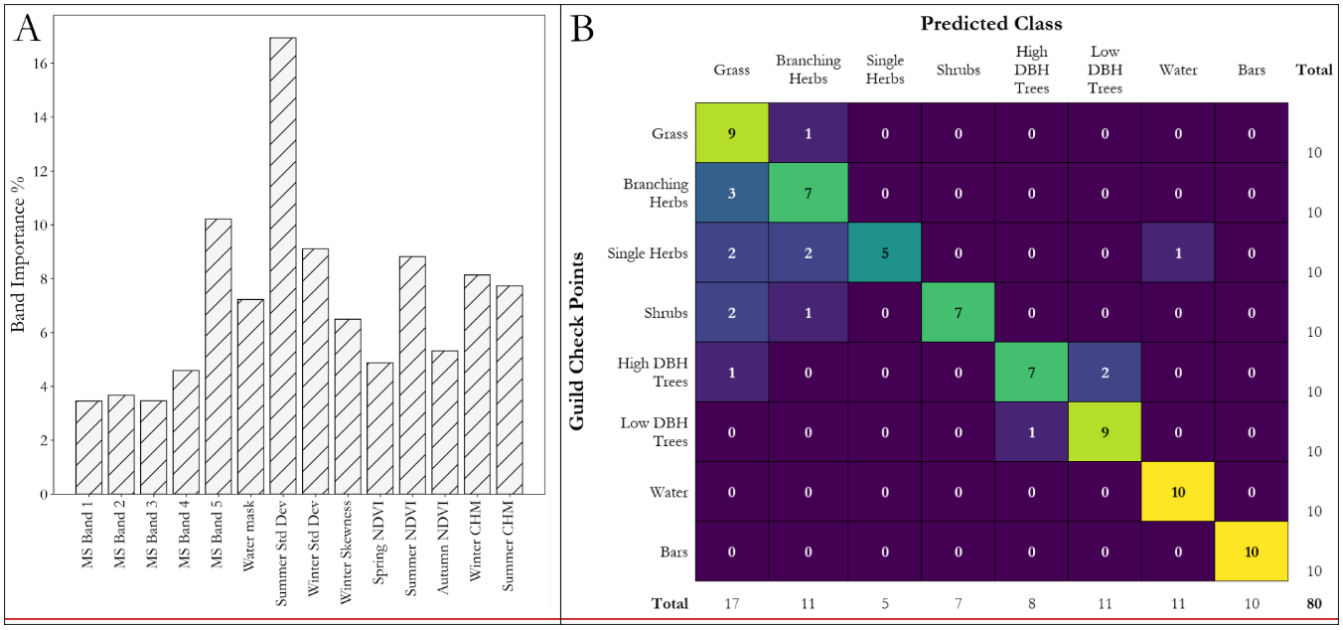

~~Figure 9~~

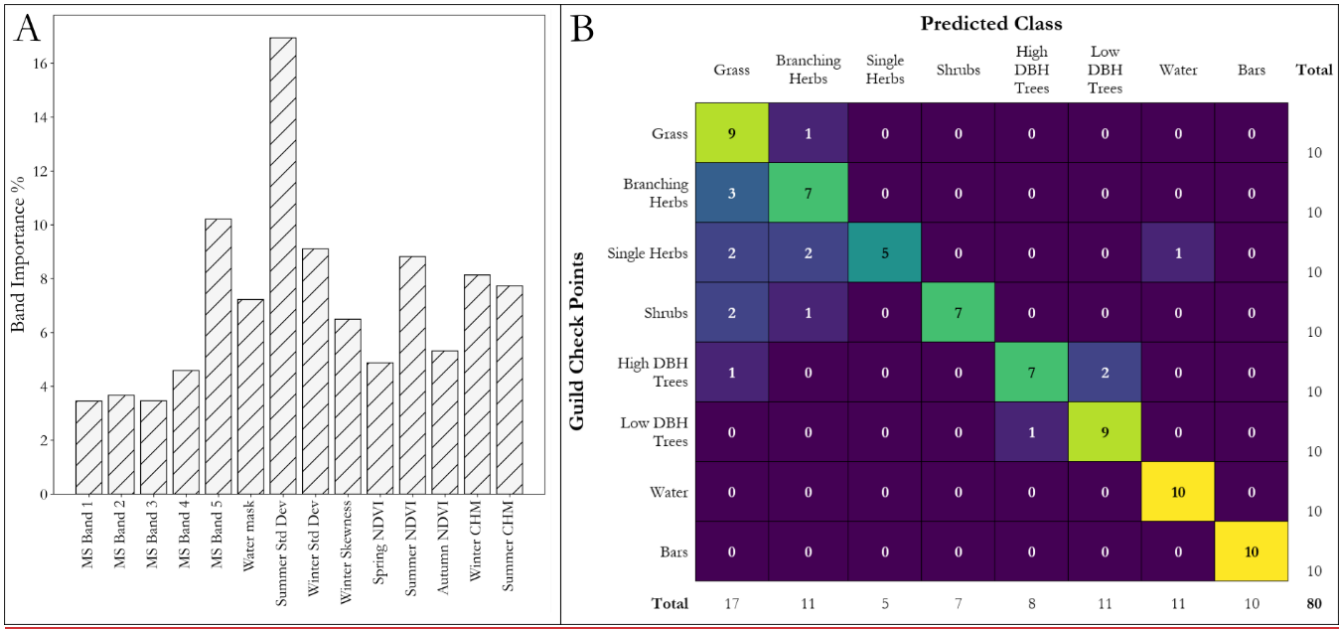

Figure 7 Individual band importance in the final classification (A) and confusion matrix (B) from the accuracy assessment. The band importance represents the contribution of an individual layer to the final classification. The confusion matrix demonstrates for which ~~guilds~~functional groups the classification struggled, showing an over-classification of grasses and the poor detection of single stem herbs. The overall classification accuracy was 80%.

Single branching herbs ~~however~~ were relatively poorly classified (50% accuracy), being misclassified as grass, branching herbs, and even water. However, their narrow structure and sparse spacing make them hard to identify from coarser imagery

~~and~~, as they return fewer laser scan points. This class also exhibited the greatest variation in values when using reach scale metrics to evaluate ~~guild~~functional group samples. Shrubs were predominantly misclassified as branching herbs and grass~~,~~; this may be due to the object segmentation not always isolating complete plants or including surrounding ground points which may have affected the classification. Low DBH trees with a top skew were classified well by the model, most likely due to their larger heights and winter skew, whereas higher DBH trees were misclassified as both low DBH trees and grass. The former likely due to the difficulty in separating out these two ~~guilds~~functional groups which have subtle differences in certain classification layers such as winter skew, and the latter from surrounding data being included in an object likely from shadowing continuing an object outside its true bounds. However, of all 20 tree check points, only one was incorrectly classified as a ~~guild~~functional group with clearly different traits, a High DBH Tree as Grass (see Figure ~~9~~7B).

4.3. Morphological Change

As ~~is~~ expected, the majority of morphological change occurs over winter months when there are high flows (Figure ~~10~~8). Conversely, over periods of lower flow during the summer both the extent and magnitude of change is reduced. Throughout the first winter period erosion occurs on the outer bank edges with fairly consistent planform evolution throughout the reach. Deposition is evident throughout the entire reach, however erosion is considerably more dominant than deposition, with ~~almost 14,000~~just under 3000 m^3 of net erosion. The second winter appears to have more localised effects on morphology, with clear channel reshaping through the upper half of the study area. ~~This has led to considerable~~ Overall, despite having similar levels of deposition ~~on~~across both ~~sides of~~ winters (~2000 m^3), the ~~channel~~increase in ~~areas of previously active~~ erosion ~~as well as localised erosional hot spots (~23,000 m^3~~ for the second year possibly due to an increased level of time at higher flows has led to a greater increase in net erosion (~5000 m^3). Both histograms of change within the winter seasons show a dominance in erosion overall. ~~This is in line with previous long-term analysis which shows this as an area of high mobility with previous channel reshaping occurring.~~ Over both winters, morphological change in the tree dominated downstream reach has undergone similar levels of change with areas of erosion and deposition influenced by the presence of large vegetation. Both summer periods have a greater degree of stability, with erosion and deposition taking place but in lower magnitudes. This is consistent throughout the reach with no hotspot areas of either deposition or erosion, with deposition showing to be more dominant overall.~~or erosion and deposition influenced by the~~

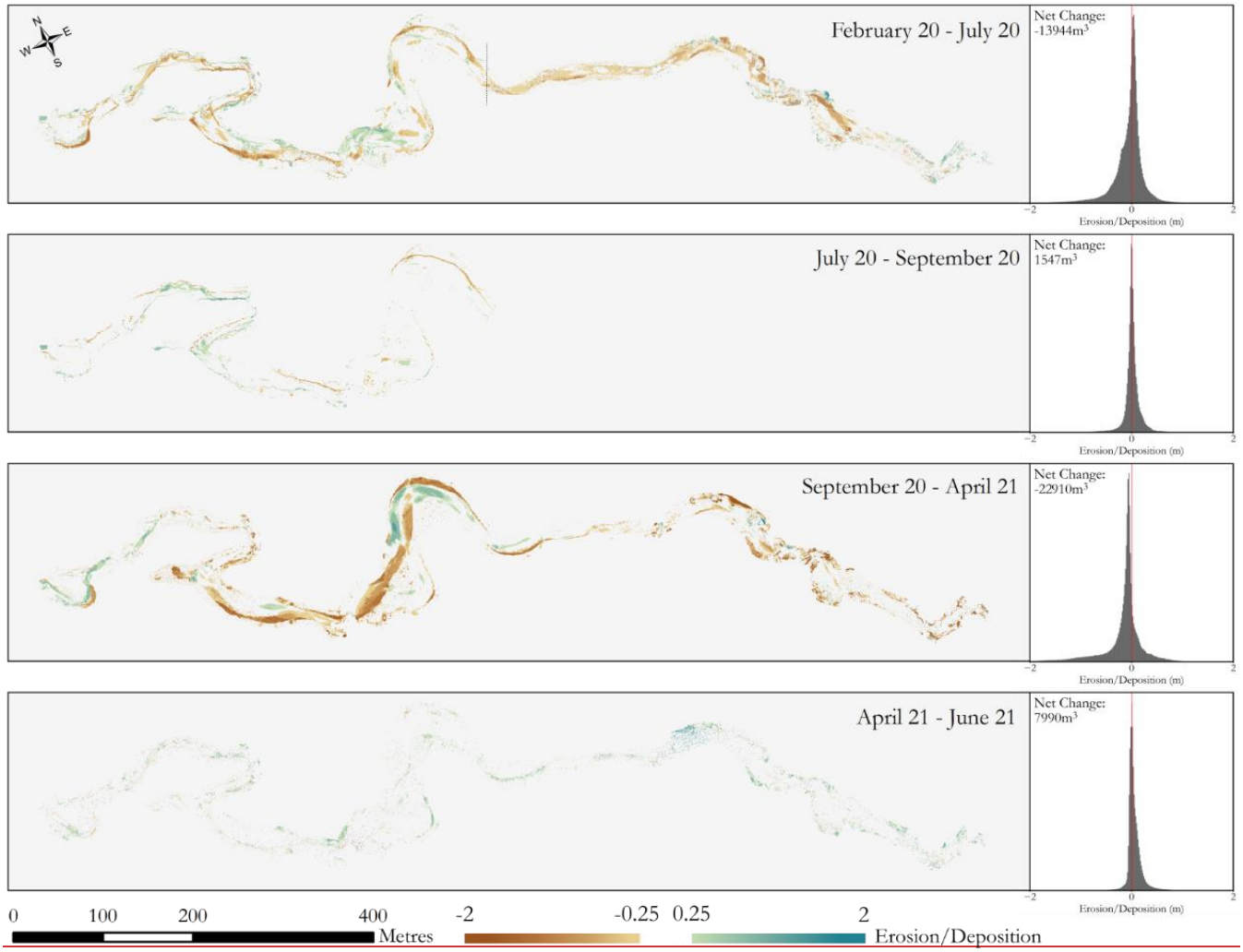
February 20 - July 20
Net Change:
-13944m³
July 20 - September 20
Net Change:
1547m³
September 20 - April 21
Net Change:
-22910m³
April 21 - June 21
Net Change:
7990m³
−2
0
2
Erosion/Deposition (m)
N
E
S
W
0
100
200
400
Metres
-2
-0.25
0.25
2
Erosion/Deposition

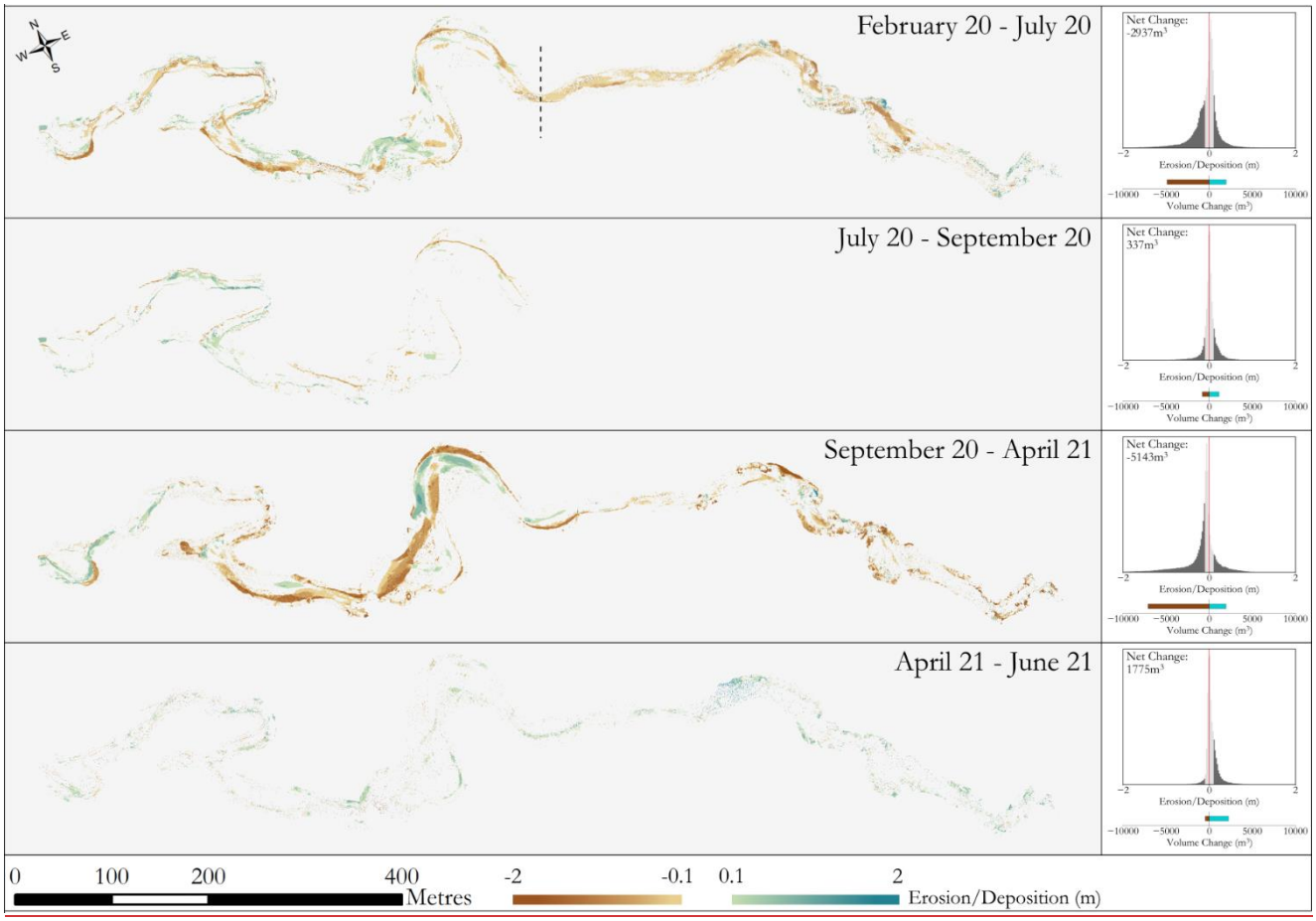

Figure ~~108~~. Morphological change throughout the monitoring period, showing the spatial variation in erosion and deposition as well as the net change in sediment. Note that February 20 – July 2020 is a composite DEM of difference consisting of comparisons between February and July to the left of the dashed line and February to September to the right of it. In July, only half of the survey area was captured. The stability of the reach over summer (July to September) justifies attributing change to the February – July result. ~~The histograms adjacent to each time period show the distribution of magnitude of change, and whether this tends to be favouring net erosion or deposition~~Change less than 0.1 m in elevation was not shown as this was deemed below the level of detection of the sensor (see Tomsett and Leyland (2021) for accuracy assessment details). The histograms adjacent to each time period show the distribution of magnitude of change, the volume of erosion and deposition over that time period, and states the net volume change across the corresponding time periods.

4.4. ~~presence of large vegetation.~~Eco-Geomorphic Interactions

A key benefit of being able to identify the location of different functionl groups, is the ability to decompose the overall distribution of morphological change into each functional group for each time period (Figure 9). When assessing the distirbutions of erosion and deposition between groups across the four time periods, each functional group follows the overall pattern presented in the general morphological analysis, whereby there is a clear dominance of erosion over deposition signals

in winter, and a balanced or deposition dominant signal in the summer periods. Unsurprisingly, there is a domanance in both winters of erosion in locations that are classed as water due to multiple areas experiencing movements of channel location in this time. In this case the presence of planform change was the prominent form of morphological change, accounting for a large proportion of the net volume shift, with only grass and high DBH trees seeing large volumes of net erosion at over 100 m^3. In fact, when compared to the changes in the summer, most of the functional groups saw similar magnitudes of change across the two time periods. Compared to winter 2021 however, the net change in volume for areas classified as water was similar, with the remainder of change happening throughout the remaining functional groups and on exposed bars. During this time, there was net deposition on channel bars, however there are large quantities of both erosion and depositon in this group, in line with the highly active nature of such features. Whilst across all functional groups there is an increase in the net erosion compared with the first winter period, this is exagerated amongst grasses and shrubs, accounting for 32% of net erosion. For both cases, these are likely to be the result of channel reactivation during overbank flow removing large quantities of floodplain sediment. Throughout all of the time periods, no group exhibits a consisitent pattern of erosion or deposition, changing based on season and year, making it difficult to identify any direct eco-geomorphic interactions at these scales. However all groups appear to undergo a dominnant erosion signal in the winter followed by an acretion signal in the summer, suggesting that vegetation that can recover or survive winter flows and act to trap sediment and stabilise the channel and adjacent floodplain during spring and summer.

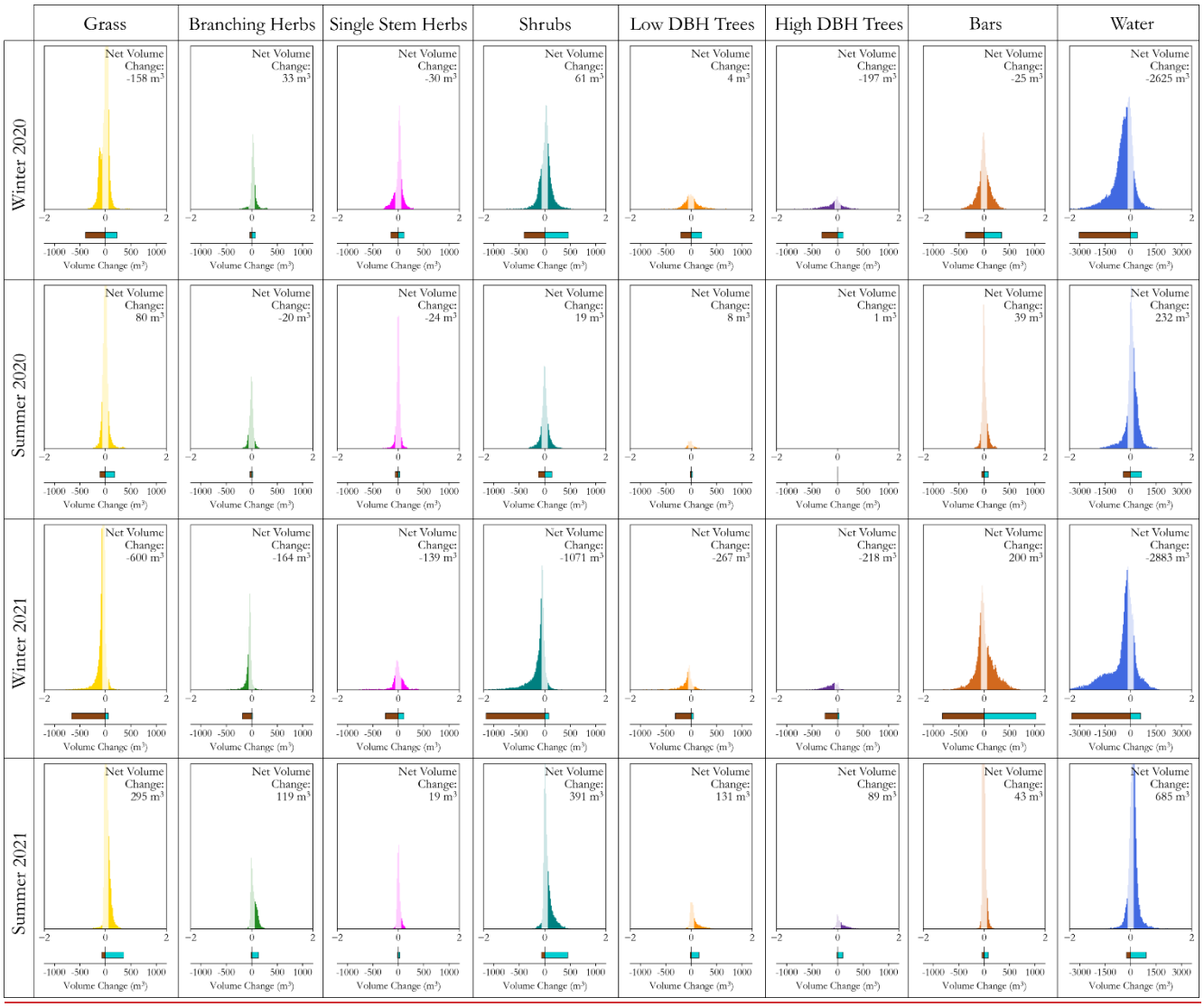

Figure 9. Histograms of morphological change for each classified functional group location throughout the reach for each of the time periods studied. Below each is the volume of erosion and deposition in m^3, as well as the net volume change. The transparent elements of the histogram show the changed that occurred below the minimum level of detection, and was not included in the eroison, deposition, and net volume change information. Note the change in X axis values for the erosion and depositon bars for the water class so as not to subdue the other groups due to the dispraportionate amount of change over both winters here.

Importantly, the above results show the spatial relationship between different functional groups and the geomorphic change that occurs at that location. Yet, the interaction each group has with flow is not accounted for, with different groups having a different proximity to the channel and areas of overbank flow. To assess the influence that each functional group is having on flow, the spatially varying drag calculated in section 3.4. was aggregated to identify how different functional groups interact with a simulated large flood across each time period. Table 3 documents the change in both the combined total area of each

functional group between each year, and the various excess drag exerted across the domain between summer and winter and between each year. Overall, it is clear that shrubs have the greatest influence on flow in terms of excess drag, due to their density and the uniformly structured vertical leaf profile. Low DBH trees also have relatively high excess drag across the reach, and when compared to the high DBH trees will exert a large influence on flow through the catchment. This is again most likely as a result of density and coverage, as the frontal area of the low DBH trees will be lower than those with a higher DBH. Yet the measured density of low DBH trees is an order of magnitude less and as such has less influence on overland flow. The excess drag created across the reach by single stemmed herbs is similar to that of high DBH trees, implying that proximity to the channel, vegetation coverage, depth of flow interaction, and seasonality, can all influence which functional groups play the biggest role across the domain.

The largest changes in excess drag between summer and winter occur within the herbacous and shrub groups, with single stemmed herbs showing the largest increase. As the majority of interactions between trees and flow throughout the year is with trunks rather than leaves, these experience the smallest difference in excess drag. The increases in excess drag may provide an explanantion of the deposition occuring in the summer months; and despite the lower flow depths occuring in the summer the increased foliage will help to trap any sediment during higher flow events.

Table 3. A comparison of total excess drag calculations for the functional groups across the study site, comparing changes between seasons and years, as well as assessing changes in group extent between years. Changes in seasonal drag are between the summer and the winter within a year, whereas the changes in annual drag are an average of the changes between winter 2020 and 2021, and summer 2020 and 2021. No excess drag was calculated for grass, water and bars, and so only comparisons in spatial extent are examined for these groups.

	2020				2022				
	Area (m2)	Excess Drag (N)		Seasonal Change in Drag	Area (m2)	Annual Change in Area	Drag (N)		Annual Change in Drag
		Winter	Summer				Winter	Summer	
Grass	49358	-	-	-	49671	1 %	-	-	-
Branching Herbs	2564	19	21	10 %	2784	9 %	22	24	12 %
Single Stemmed Herbs	3388	76	100	31 %	1680	-50 %	38	49	-49 %
Shrubs	20240	511	614	20 %	18780	-7 %	439	527	-14 %
High DBH Trees	8956	33	35	7 %	8744	-2 %	34	37	4 %
Low DBH Trees	5960	135	144	6 %	5732	-4 %	120	127	-12 %
Water	12360	-	-	-	11218	-9 %	-	-	-
Bars	4981	-	-	-	7872	58 %	-	-	-
Total	107807	775	914	18 %	106481	-1 %	652	765	-16 %

When comparing the annual changes, there are large shifts in both the excess drag components of individual groups and overall excess drag throughout the reach. Changes in excess drag can be attributed to total cover of each functional group, such as branching herbs where both area and drag increase by similar proportions, and the small decrease in High DBH trees is accompanied by a small increase in drag. Yet, for both low DBH trees and shurbs, the seperation between excess drag and coverage suggests that the distribution of each group is changing so that the interaction with flow is altered. The drop in both area and subsequent drag from single stemmed herbs at first seems to be related to the increase in area of chanel bars, suggesting a removal of such vegetation *in situ*. However, as Figure 10 shows, the change that is most prominent is from single stemmed herbs to water, whereby the channel has removed vegetation, and bars have formed in place of the old channel which are yet to be established with vegetation.

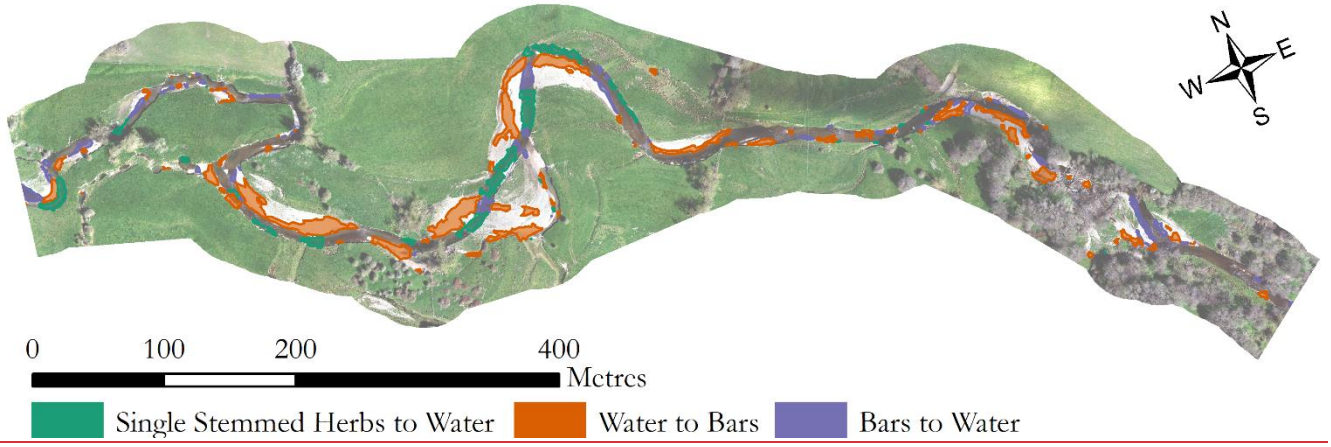

Figure 10. The three most common changes in functional groups and land cover across the study site, accounting for 45% of all change. Water to gravel bars was the most common change (28%), followed by single stemmed herbs to water (9%), and then gravel bars to water (8%).

~~Both summer periods have a greater degree of stability, with erosion and deposition taking place but in lower magnitudes. This is consistent throughout the reach with no hotspot areas of either deposition or erosion, with deposition showing to be more dominant overall.~~

5. DISCUSSION

~~5.1. Multi-Decadal Evolution~~

~~The multi-decadal evolution for this reach is complex and analysis of the formation of new channels implies that flood events might be a key control on the switching from one channel to another and the reoccupation of former channels. It is not possible to isolate a single variable that may cause such switches to take place, such as particular flow thresholds, baseline conditions, vegetation, or soil characteristics. However, it does appear that areas influenced by large vegetation experience less localised bank evolution, with the vegetation constraining the channel to some degree. This does not appear to stop large switches in channel position into or away from vegetated sections. This implies that vegetation is playing a role in the stabilisation of channels up to some, as yet unidentifiable, threshold. The reoccupation of former channels implies that vegetation plays a lesser role than topography in these conditions, suggesting that whilst vegetation can have controls on channel evolution, these eco-geomorphic feedbacks are locale and flow condition dependent. This supports the concept of vegetation acting as river system engineers and providing an influence on channel morphology (Gurnell, 2014) and that varying vegetation densities may be impacting the resistance to morphological evolution (Bertoldi et al., 2011). Therefore, at a decadal scale, although vegetation may not be the sole control on planform evolution, it is shown to be an important factor in this reach of the River Teme.~~

~~5.2.~~5.1. Trait Extraction and ~~Guild~~Functional Group Formation

Current measurements of plant functional traits are still predominantly ground based and therefore limited by on site access (Palmquist et al., 2019), requiring extensive sampling to extract enough data to create ~~guilds~~functional groups relevant to a particular study (e.g. Diehl et al., ~~2017~~2017a; Hortobágyi et al., 2017; Stromberg and Merritt, 2016). Remote sensing of these traits is therefore a potentially ~~novel~~useful way to collect data across large areas, depending on the vegetation size and methods of data collection. Although no ground truth data relating to traits was collected in the field, the assessment of variability in model construction and comparison to wider records based on dominant species suggests that the ~~final cylindrical models were of good fit for the point clouds collected.~~methods developed herein performed well at extracting physical attributes. This ~~suggests that~~highlights the ~~use~~potential of remote sensing to collect structural trait data ~~has an important role to play in~~for eco-geomorphic research moving forward, especially once trade-offs in terms of time and spatial extent are accounted for. For example, data from field surveys are generally limited to that site, and although the findings can be applied to locations elsewhere, this requires knowledge of the vegetation present at a site. If metrics can be extracted from remotely sensed data and be used to classify functional groups and over land cover, this represents an improvement in the applicability of traits-based research.

The use of pre-determined rather than site specific ~~guilds~~functional groups was a method employed by Butterfield et al. (2020) on the basis of ~~guilds~~those outlined in ~~Diehl et al. (2017).~~Diehl et al. (2017a). The sites used in both of these studies were similar, and the application to a temperate UK based site is challenging~~.~~ because of the complexity and similarities of some plants. However, the ~~comparatively smaller sample size used in this study, and the~~ lack of a comprehensive ~~guilds~~ list of functional groups for riparian vegetation~~,~~ made using predetermined ~~guilds described in Diehl et al. (2017) and O'hare et al. (2016)~~groups justified~~. The lack of suitable ultra-high resolution data reduced~~ in this case. When compared to previous studies, the reduction in the number of extracted herbaceous ~~guilds to~~ functional groups is due to the data resolution, whereby only two~~, on which most distinction~~ categories could be ~~observed. The variation in~~explicitly detected. For woody ~~vegetation created two guilds within this single previously outlined guild, as they were likely to~~ species, the method allowed for separation of two sub classes which have different impacts on flow, especially when used to determine excess drag. The methods used provided sensible separation of groups, each of which have a demonstrably different hydraulic ~~effect traits. This basis appears to have proved effective with differences in structural characteristics which are likely to impact flow and subsequent morphology noted between the guilds during PCA analysis. Predominantly single~~influence. Single stemmed herbs were taller~~, likely due to their improved structural standing,~~ and although the number of branches was similar to the branching herbaceous group, the number of branches per unit height was ~~different~~lower. A taller, stronger, and less branching herb is going to have a distinctly different impact than a shorter more flexible one (Nepf and Vivoni, 2000; Järvelä, 2004; Sand-Jensen, 2008)~~.~~ ~~Being~~, and being able to differentiate successfully between these two groups highlights the success of the survey and trait extraction methods~~.~~ developed herein. Likewise, the difference in flow conditions between low DBH trees, that are closely

packed, to less densely packed high DBH trees may show a resemblance to the influence found at smaller scales on plant density (Järvelä, ~~2002b~~2002a; Kim and Stoesser, 2011)~~.~~, with noticeable differences in estimated excess drag values. The relationship between DBH and vertical skew is not surprising; considering the higher plant spacing density, the competition for space is likely higher~~,~~ resulting in more mass higher up the tree profile. As plants cannot yet be easily differentiated by measuring their DBH, using vertical skew ~~gives~~provides promising results for upscaling to larger areas whereby ALS surveys may be able to differentiate between woody ~~guilds~~functional groups for better informed hydrological analysis~~.~~, with similar work being done using vertical distribution to classify forests already (Antonarakis et al., 2008; Michałowska and Rapiński, 2021).

~~However, UAV-LS has been shown to overestimate canopy reconstruction volume (Brede et al., 2019), which mirrors the over complexity demonstrated in Figure 2 (*QSM Cylinder Model)* with some awkwardly orientated cylinders. Extracting traits using remote sensing is novel and can outcompete~~UAV-LS has been shown to overestimate canopy reconstruction volume (Brede et al., 2019; Dalla Corte et al., 2022), which mirrors the over complexity demonstrated in the QSM Cylinder Model (Figure 2) with some awkwardly orientated cylinders. Extracting traits using remote sensing is novel and can improve on ground-based methods for coverage but is not yet likely to match the accuracy and interpretive ability of ~~in-field measurements. Moreover, use of TLS is highly localised with a limit to the survey extent that can be captured~~manual in-field measurements undertaken by an individual, as shown in estimations of forestry structure for height, DBH, and volume (Dalla Corte et al., 2022). Moreover, the use of TLS for analysing herbaceous functional groups is highly localised (Lague, 2020), meaning only a small number of samples can be analysed which may not reflect the full variation in vegetation morphology ~~from differing hydrological and environmental conditions. The UAV-LS data, although covering more ground, does take significant levels of time to post-process and extract multiple individual vegetation models, although as the spatial extent of coverage increases, the time gains improve as the same vegetation models can be used to classify increasingly larger sites. Algorithms which can extract traits and classify large areas are likely to improve with the increasing availability of very high-grade commercial UAV-LS surveying equipment in much the same way that SfM methods developed, beginning to rival the resolution and accuracy of ground-based TLS.~~. Despite covering a relatively large area of the river reach (Figure 1) the UAV-LS data collected for this study took a significant amount of time to post-process, although as the spatial extent of coverage increases the time gains improve as the same vegetation models can be used to classify increasingly larger areas. Algorithms which can extract traits and classify large areas are likely to improve in much the same way that SfM methods developed, such as those presented by Burt et al. (2019) and Krisanski et al. (2021).

Currently, UAV remote sensing methods can only obtain above ground structural traits, and although these make up a significant component of ~~hydrologically~~hydraulically relevant traits, they do ~~eliminate~~ignore the ~~collection~~importance of traits such as root structure, strength, and plant flexibility. Both UAV-LS and TLS also struggle to capture the complex structures of shrubs, with TLS requiring ~~too~~ many scans to resolve the structure of enough samples and UAV-LS having too low point

density and canopy penetration for such complex branching. However, methods pioneered by Manners et al. (2013) ~~may help to overcome this by relating vertical profiles from TLS and ALS data to enable upscaling to larger extents.~~ relating vertical profiles from TLS and ALS data may help to overcome this by upscaling to larger extents. Similarly, more work is needed to overcome the difficulty in separating out species that appear similar structurally (and spectrally), such as woody saplings and herbaceous plants, but which may have very different hydraulic roughness measurements. At present, these two different vegetation types could easily be misclassified, and with the likely different interactions with flow and subsequent morphology, not being able to account for these with remote sensing is currently a limiting factor. Efforts to further investigate this, possibly using proximity measures to other functional groups, or probabilistic rather than categorical classification methods, may help to overcome this issue.

~~5.3.~~5.2. Reach Scale ~~Guild mapping~~Functional Group Mapping

The benefits of remote sensing of plant traits does not come from individual plant analysis but from upscaling ~~to larger extents.~~across space and time. Using the same datasets provides continuity between both the individual analysis and reach wide ~~guilds.~~functional groups. Finding common features of defined ~~guilds~~functional groups is more computationally effective than analysing individual plants throughout the reach at present. Using structural characteristics of the point cloud alongside spectral properties across time allows the ~~absolute and~~ temporal patterns ~~of each layer~~ to enhance ~~guild~~functional group classification. It is clear that ~~distinctive~~initial separation between ~~guild~~functional group types can ~~initially~~ be made based on canopy height~~, with this providing the clearest initial separation.~~. The need for seasonal data is emphasised ~~by the~~ across functional groups, whereby herbaceous ~~guilds, whereby height is a useful separator but has large variability, whereas~~groups benefit from having winter and spring NDVI values ~~are more effective~~to complement the difference in height, and tree groups require leaf-off vertical distribution to help with separation, supporting previous work emphasising the need for seasonal data to improve eco-geomorphic research (Bertoldi et al., 2011; Nallaperuma and Asaeda, 2020~~; Bertoldi et al., 2011~~). ~~Variations in NDVI were distinct between several guilds, both in absolute values and seasonal variation. Single~~. Overall, single stemmed herbs appear to be more seasonal, with lower winter values than ~~multi stemmed~~branching herbs, whereas the NDVI of shrubs ~~NDVI experience~~experiences a dip in spring surveys as a consequence of flowering affecting spectral properties. ~~When investigating differences in woody guilds, winter data collection is key, as in leaf-off conditions the full~~For tree ~~structure is captured in more detail and so differences in skew which are related to DBH are better captured. Later~~ functional groups, capturing data in the ~~year, these variables become more overlapped between guilds with~~winter has a greater ~~variation. Therefore,~~penetration and as such the timing of data collection will likely impact classification results, with some ~~guilds~~functional groups being better separated at different times of the year. For these methods to be applied elsewhere, it ~~therefore~~ follows that ~~a~~the seasonal monitoring approach used herein and in other studies (Van Iersel et al., 2018; Souza and Hooke, 2021) is likely required.

The use of random forest classification for this study site has been successful and ~~builds on~~adds to the growing body of ~~research for~~evidence supporting their use for application to high resolution classifications (Adelabu and Dube, 2015; Chan and Paelinckx, 2008; Adam and Mutanga, 2009). The ~~misclassifications~~misclassification statistics from the random forest classifier are in line with ~~misclassifications experienced~~those reported by Butterfield et al. (2020) when using multispectral imagery alone, with most misclassifications happening in ~~guilds adjacent and most similar to the true class. Woody guilds appear to be buffered by shrub guilds, potentially resulting from the image segmentation not delineating the vegetation edge successfully. These locations are likely to have lower relative heights and so be misclassified as shrubs, whereas a better image segmentation may avoid these issues.~~ functional groups which are adjacent and most similar to the true class. This is unsurprising when viewing the uncertainties in functional group properties (Figure 5), where there is evidence of overlap across multiple attributes for two different groups. Moreover, where there are transitions between functional groups with similar properties, or where the image segmentation has incorrectly defined 'similar' pixels, it is likely that misclassification may occur. Identifying ways to better segment regions of vegetation may help to improve the overall classification success. A related drawback is that the categorical output used in this method means that a segmented region must be allocated to one type of functional group and as such cannot distinguish between the presence of multiple groups. This is especially the case for woody regions, which will have a mixture of understory vegetation which is not currently detected and characterised, and is another area which may need further developmental work to improve vegetation characterisation.

~~The~~ Despite the above limitations, the resulting classification accuracy (Figure ~~8~~6 and Figure ~~9B~~7B) shows promise for linking local scale trait modelling to larger ~~guilds,~~ functional group mapping. The overall distribution of classes throughout the reach is as expected, with ~~good separation between broad guilds and promising initial results for separation between similar guilds. The presence of~~ herbaceous species ~~in~~dominating the active meandering section ~~is as expected,~~ as these are more adaptable to changing and flood conditions, whilst larger woody species are seen in more stable sections of the river ~~when compared to the historical change,~~ as these species require more stable hydraulic conditions (Kyle and Leishman, 2009; Stromberg and Merritt, 2016; Aguiar et al., 2018). The classification herein ~~advances~~takes a different approach to work by (Butterfield et al., 2020) who used imagery to classify species and subsequently assign ~~guilds~~vegetation groups, whereas ~~this~~ the remote sensing method ~~uses~~used here utilises the structural and spectral characteristics to designate the spatial distribution of ~~guilds~~functional groups, removing the species identification component. This is important as the same species may display varying traits-based on their proximity to the channel ~~(Hortobágyi et al., 2017)~~(Hortobágyi et al., 2017), and as such~~,~~ using the physical characteristics of plants can be seen as an advantage. ~~The use of image segmentation~~Species identification still plays an important role, and has been used in this study to ~~delineate similar areas also helps to reduce the salt~~both assess the reconstruction of vegetation and ~~pepper effect~~to inform the coefficient of ~~high resolution~~drag values used. However, as noted previously, obtaining secondary data ~~classifications~~on a range of plant traits that are relevant to the area of study can be challenging, and ~~so provides an effective method when looking at high resolution structural and spectral features of a reach.~~may limit the applicability of traits-based methods in the wider scientific community,

~~5.4.~~5.3. Eco-Geomorphic Change

Given the hydrology of the river, the majority of morphological change occurs over the winter months as expected. The temporal resolution of the surveys is not capable of ~~picking out~~detecting whether this is the result of a single flow event or continuously high flows~~, however it is clear that significant geomorphological re-profiling can occur within a single winter~~. There appears to be more localised evolution in the second winter of surveying whereas the first winter appears to show a more continual response throughout the reach. The singular lower peak in water levels for the second winter as opposed to several higher peaks in the first (see Figure ~~1~~1C) suggests that priming may be more important for large avulsions, whereby a ~~singular~~single flow event of lower magnitude can incite a greater resultant planform shift. The response in summer is much smaller both in terms of deposition and erosion, with little morphological change occurring ~~unsurprisingly.~~. What change does occur may be from reductions in bank support (via confining water pressure) from high flows leaving banks exposed to collapse (Zhao et al., 2020)~~. The largest areas of change appear to be within the reaches absent of large vegetation, with the stable patches aligning well with those identified in the decadal analysis.~~.

It is difficult to identify any definitive links between the morphological change and vegetation presence, due to the limited time of study and the variations in vegetation extent and proximity to the channel. Yet, by aggregating the change across these various functional groups it was possible to see some of the effects of different groups, with areas such as grass consistently contributing to areas of erosion during the winter months, and tree functional groups undergoing just as much morphological change as herbaceous functional groups despite their well-known stabilising effects (Gurnell, 2014; Hortobágyi et al., 2018). Importantly, it is clear that the use of temporal monitoring to identify patterns of change is a challenge due to the inherent variability between seasons, exemplified when looking at the excess drag provided by each functional group between years. Changes in the spatial distribution and extent of different functional groups can alter the overall hydraulic roughness across the floodplain, and in this case results in a drop in roughness from one season to the next. Moreover, being able to adjust these for both summer and winter periods gives a greater insight in to the fluctuations in the influence of vegetation across a domain, and should continue to be accounted for when investigating the influence of vegetation on flow both in field studies and modelling (Song et al., 2017; De Doncker et al., 2009; Champion and Tanner, 2000; Cotton et al., 2006).

Herein we linked the functional groups to morphological change and, in addition, estimated the excess drag across the domain created by each functional group. Investigating the morphological change compared to depth dependent drag is challenging however, as it is spatially and temporally varying with different river stage. Yet, for the reference flood event used to predict flow depths, the morphological change experienced over that time period can be compared to each functional groups excess drag, and the impact this had on subsequent morphology assessed.

Figure ~~It is difficult to extract any definitive link between the types of morphological change occurring and the underlying vegetation. It is clear from the historical analysis that although vegetation plays a role in morphological evolution, it is not the sole driver of change. There are also a number of unique features in the reach which are hard to categorise or group, morphologically speaking, with different vegetation patterns, hydraulic conditions, and pre-existing morphology adding complexity. However, by grouping guilds based on their potential ability to influence vegetation, and categorising erosion and deposition into bands of morphological change in either direction, it is possible to visualise the links between vegetation and morphological change.~~

~~Figure 11 shows a bivariate classification of vegetation stability and morphological evolution. Grasses and herbaceous guilds are grouped along with bars as having the least morphological stability, followed by shrubs, and then woody guilds. Morphological evolution was split into 0 to 1 m of change, 1 to 2 m of change, and greater than 2m of change, which were chosen to represent the majority of change values. It is clear that most of the reach is shown in the lighter colour tones indicating low magnitudes of morphological change. However, areas with higher morphological change begin to become more apparent for areas of little vegetative stability, for example on the outer meander banks in several places. Darker oranges and purples~~

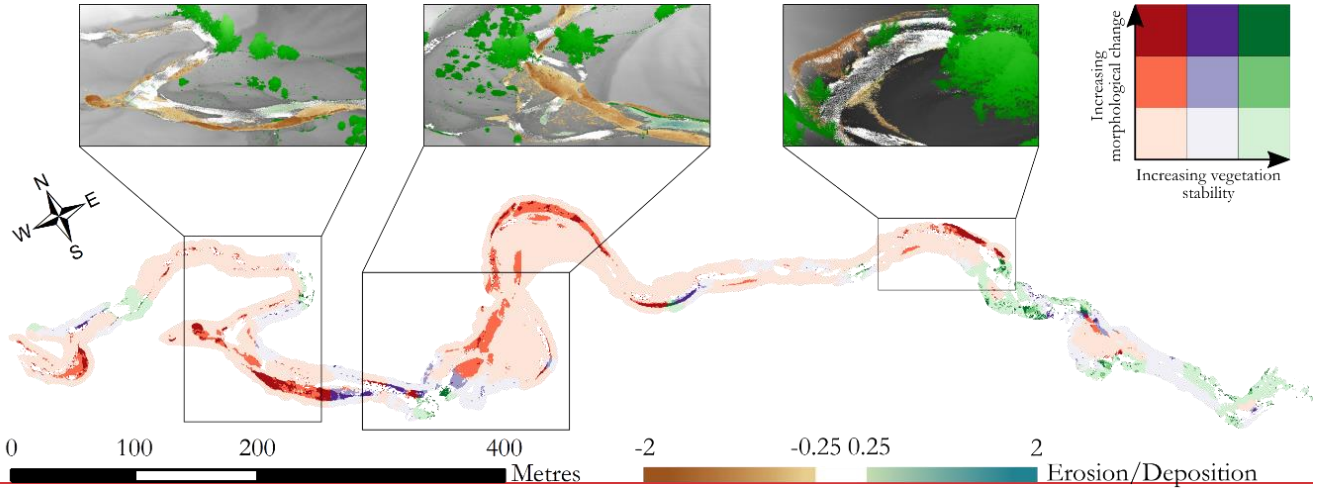

~~Figure 11 Bivariate classification of eco-geomorphic process-form interactions, with examples highlighting the stabilising effect of vegetation. The bivariate colour scheme shows the impact of the likely increase in stability from vegetation (red to green) and the increasing magnitudes of geomorphic change (light to dark shades). This allows the presence and potential influence of vegetation to be mapped together. Vegetation stability was classed by grouping grasses and herbs, shrubs and bushes, and different woody tree guilds. Morphological change was split into 0-1 m, 1-2 m, and greater than 2 m of change, regardless of whether this was erosion or deposition. Insets show patterns of erosion and deposition against the presence and absence of larger vegetation across various sections of the reach.~~

~~are dominant in comparison to the areas of dark green. Although compared to the overall areas of each vegetation stability class you would expect fewer dark green regions, there is clear evidence of light green patches where dark green patches may be expected had the vegetations stabilising effect not been present.~~

~~Some of these sections are highlighted in the panels of Figure 11 identifying regions where erosion may be expected but is not present. The left-hand panel shows a double meander bend, the first which has a heavily vegetated bank and the second which has little established vegetation. The total change in these two sections is dominated by erosion in the second meander bend which has a similar curvature to the first. The second bend does contain a knickpoint caused by overland flow which is not present in the first bend, yet the bend exit also shows far less erosion. Therefore, it is suggested that this dense patch of vegetation is having some stabilising effect, with soil cohesion increased, and flow velocities reduced. The central panel is just downstream and is constricted in planform by established vegetation, which despite substantial reworking across the survey period has remained relatively stable and exhibits deposition close to the vegetation on the left-hand bank. Subsequently, not only is the vegetation acting to stabilise banks, but likely slow the flow to encourage deposition in this area. Finally, the right-hand panel at the entrance to the region dominated by woody guilds is characterised by a large cut bank several metres in height that is progressively eroding, with the bulk of this erosion occurring just before entry into this woody guild dominated section. The vegetation on the outer bank is likely to play a stabilising role on the bank, until undercutting and removal of these trees occurs. There is evidence of such undercutting in action (Figure 12), suggesting that vegetation provides additional stability only as far as a given threshold, as was suggested in relation to the long-term decadal analysis.~~11 illustrates the changing excess drag provided by each functional group at different reference flow depths, and the equivalent morphological change experienced at these locations for the winter of 2021/22. All functional groups exhibit an increase in erosion with greater flow depths, implying that any variation in erosion patterns seen across the range of flow depths may be in part due to the function of the vegetation. For both herbaceous functional groups, the influence of the plant form on flow increases up until their maximum heights, and for both of these groups the level of erosion reduces up until below this maximum height, until above this height levels of erosion increase. Clearly, at greater flow depths the shear stress on the bed will increase (e.g. Biron et al., 2004; Phillips, 2015) and as such induce greater levels of erosion. Nevertheless, as this trend is not linear in nature with increasing depth, it suggests that herbaceous functional groups are having an impact on flow and subsequent morphological change within the reach over this time period. The remaining three functional groups all see consistently increasing levels of excess drag across flow depths as the plant heights exceed the maximum depth. Shrub frontal area increases more quickly with flow depth as the branching network becomes more complex with a greater presence of foliage. The difference in excess drag experienced by the low and high DBH groups is predominantly the result of differences in plant density. Shrubs show the most consistent morphological stability, most likely due to their ability to reduce flow speeds, and the root structures of larger vegetation providing greater soil cohesion. Both sets of tree groups follow a similar pattern, appearing to accelerate erosion at low flow depths, before showing a stabilising effect at greater depth, some of which may be in part due to the poor ability to classify understory vegetation, missing some of the variability in these areas.

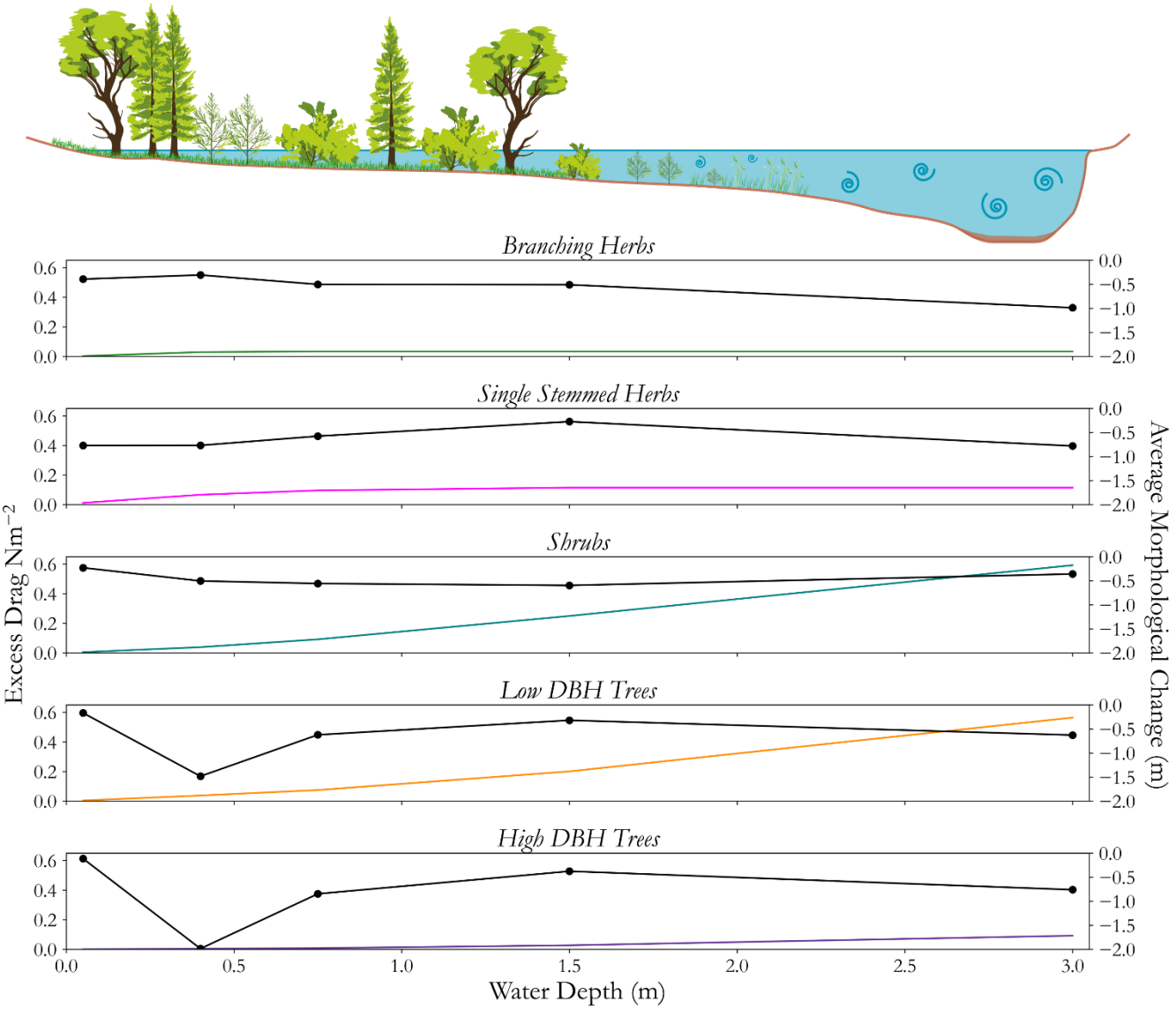

Figure 11. A comparison of how for each separate functional group, the excess drag (coloured lines, no dots) and morphological response (black line, dotted), changes with flow depth. The diagram at the top helps to illustrate how for different groups, different flow depths result in different proportions of the plant interacting with flow.

This begins to raise questions around the coupled nature of flow and vegetation, and at what point does one begin to dominate in dictating geomorphic evolution. The exploratory analysis undertaken here begins to disentangle this by using structural data across the domain to determine the vegetation influence at flow depths seen in the field, whilst also assessing real changes in morphology. Although the drag calculations are averaged for the entire functional group, and the morphological signal used is an average, this provides a new avenue of research which could relate an individual plants influence on various flood stages and the subsequent morphological response of the channel.

6. Remote Sensing of Plant Functional Traits: What Next?

One of the key benefits of using remote sensing is the ability to quickly capture datasets over scales not possible with ground-based surveying. It is clear from the analysis herein that although the collection of data is fairly straightforward, the subsequent post processing time has to be taken into account~~. Yet once~~ when considering routine application of a traits-based approach. Once data has been processed, and the seasonality of the data acquired through spectral and structural characteristics, the success of the classification suggests that ~~guilds can be classified for other sites that contain similar guilds, such as most temperate UK rivers which display these prominent guild types (O'hare et al., 2016), in much the same way as other research has used previous guild classes for similar environmental conditions~~functional groups can be classified for other sites that contain similar vegetation in much the same way as other research has used previous classes for similar environmental conditions before (e.g. Butterfield et al., 2020). It also allows ~~guild analysis for~~for functional groups to be mapped in regions that are more remote and less accessible to more traditional ~~surveys.~~survey techniques. This improves the applicability and usability of ~~traits~~trait based methods when compared to more traditional taxonomic vegetation discretisation approaches.

Combining vegetation structural and spectral data provides the opportunity to upscale to datasets collected via other platforms, with high resolution satellite imagery and ALS datasets offering the potential to improve the impact of such classification methods. ~~This also allows the direct measurement of trait variability rather than investigating species variability and subsequently linking these to traits. The use of purely species data may remove some of the nuance in their traits, based on location, and so limit the applicability to fluvial research.~~ Currently, the main difficulty with traits-based analysis is ~~getting~~collecting adequate data over large enough areas~~, this~~. The methodology developed here provides a potential starting point from which a set of tools to classify different ~~hydrologically~~hydraulically relevant ~~guilds~~functional groups across larger areas can be ~~based~~developed. This may overcome some of the scale issues in linking ~~guilds~~vegetation functional groups to geomorphic change ~~which are currently known.~~, whereby not enough data to link directions of change with different functional groups has previously been collected. Currently, most large-scale studies link platform evolution to vegetation presence~~,~~ and small studies are too localised to be applicable across ~~wider areas.~~reach scales and beyond. This research~~, although not large enough~~ which begins to ~~be able to link guilds statistically to~~explore the links between different functional groups and morphological evolution~~,~~ demonstrates that by upscaling to combine enough hydraulic and morphological conditions ~~may allow this to~~ further eco-geomorphic insights may be possible.

~~It is important to understand how the role of guilds may change. Figure 12 shows a pre and post image of the channel in this section, suggesting large scale mobilisation of large wood. Being able to identify these changes is key, because~~Whilst the analysis undertaken in this study is capable of assessing seasonal and annual changes in vegetation functional groups, one aspect that is not taken into account within those groups is the longer term life cycle of vegetation. During a complete growth life cycle, the functional role ~~large~~ vegetation plays ~~in~~within the river ~~corridor~~system changes ~~depending on its life stage. Our~~

~~data suggests that~~ . For example, the role that large trees ~~helps to stabilise the channel, likely through increases in soil cohesion and slowing flows during the flood stage. However, once a tree is undermined by erosion and collapses to form large woody debris, it provides an increase in in~~ play when they are uprooted changes significantly, from a stabilising feature for riverbanks, to one that potentially increases channel roughness and turbulence, ~~diverts~~dramatically alters flow~~,~~ directions and leads to ~~knock on~~subsequent morphological impacts (Jeffries et al., 2003; Sear et al., 2010). ~~It is therefore important~~Therefore, when classifying regions into functional groups, it may be necessary to consider that ~~guilds and their influence are not stationary, but that they are~~ these are dynamic ~~through time both in terms of seasonality and life cycles. This must be considered when looking at the implications of guild dispersal and modelling, as the impact of changing from one state to another needs to be accounted for. Although the temporal evolution of guilds was not~~

classes

~~**Figure 12 The impact of undercutting within a heavily wooded reach, highlighting how vegetation and river flow interactions change through a plant's life cycle. The fallen trees create key members**~~ **which** ~~**form debris dams, leading to**~~vary through timescales **greater** ~~**flow diversions, localised flooding and scour points, changing the role of vegetation from one of offering stability to inducing erosion.**~~

~~investigated, this presents itself as~~ than the period of repeat survey capture. How we begin to monitor and detect these shifts in groups is an area ~~of~~for future ~~work, and~~research, especially in terms of characterising the ~~possibility to investigate traits-based methods to classify~~impacts of large woody debris ~~based on~~ , which greatly contributes to the ~~surrounding vegetation structures~~dynamics of fluvial systems.

~~The~~ One of the challenges of traits-based approaches is the ability to collect widespread data as outlined previously. The classification inputs used herein predominantly focussed on structural and spectral characteristics of the vegetation~~; however~~ , and as a result require advanced data collection techniques. However, it ~~is~~has been widely shown that traits vary dependent on their underlying hydraulic and environmental conditions~~.~~ (e.g. Göthe et al., 2017; Corenblit et al., 2015). It is therefore not inconceivable that such metrics may be used in the future, ~~such as~~for example to show inundation frequency or extent, alongside species identification from imagery or the field (Butterfield et al., 2020) to determine the likely composition of traits

~~in these regions.~~. This may ~~take~~result in a more holistic approach and in cases where less structural data is present, allow for a more robust classification of ~~guilds~~functional groups.

~~There are however several limitations to the methods.~~Alternative approaches will also be necessary when the limit of trait detection is reached from remote sesning techniques. Variations in traits which are undetectable from TLS or UAV-LS methods will limit the ability to detect features for certain types of ~~guild~~functional groups, such as those too small to resolve ~~including different grasses~~ or those with too complex ~~structures~~a structure, such as ~~branching~~for grasses and shrubs. Both of these are prominent features of UK river corridors and so their ommision from ~~the~~current analysis is a limitation. ~~However, they~~The current methods can still ~~be mapped~~map their extents but would require in field trait collection or ~~species identification for~~ the use of trait databases ~~(~~, e.g. the TRY database (Kattge et al., 2020)~~). The remote sensing equipment used for this research is not cheap (see Tomsett and Leyland, 2021, noting that our custom system is considerably more economical than commercial off the shelf packages) and requires a degree of expertise in processing and manipulating the data. However, commercial improvements are seeing more easy to deploy,~~ whose limitations have already been discussed. Yet species identification can be achieved with platforms cheaper~~, sensor systems~~ than those used in this study and supplemented with in field data assuming access to the site is safe, providing opportunity for wider implementation.

A key discussion point tends to revolve around how much data is required? Within this study, the repeat surveying was used to better group and map the extents of different vegetation, yet it is not always possible to collect such quantities of data. The analysis above would suggest that the seasonality of data collection plays a critical role, with tree species being ~~brought to the market, likely to have a positive impact on eco-geomorphic research~~better seperated in ~~terms~~the winter, due to the leaf off conditions providing better conditions for identifying overall structure, whilst summer surveys better capture the extent of ~~allowing broad uptake of the methods developed herein for applied monitoring and river corridor management~~different herbaceous groups. As a result, it is unlikely that a singular time frame is best for capturing such variety and in order for traits-based approaches to become common using remote sensing, further work to indeitfy optimal timings for data collection needs to be undertaken.

7. Conclusion

~~We~~In this study, we have presented a novel method for collecting and extracting vegetation functional trait data that is relevant to eco-~~geomprohic~~geomorphic research. Herein we used~~-~~ UAV-LS and UAV-MS datasets to advance our ability to collect high resolution 4D datasets, improving the spatial and temporal resolution of riparian vegetation monitoring and geomorphic change detection~~, allowing~~. This has allowed us to gain an insight into how ~~ripairan~~the inlfuence of riparian vegetation ~~evolves~~chnages through time and to better discretise the spatial variation of vegetation in ~~a manner that is applicable and~~to functional groups which are scaleable ~~over large river reaches~~. As such, we have been able to provide insight in to how traits-

based frameworks for vegetation analysis can be linked to trends and patterns in morpholoigical evolution at scales that were previously not attainable. Throughout the study reach, shifts in planform were the dominant forcing of changes in group presence, with no group displaying consistent directions of change in erosion or deposition, with most eroson being seasonally driven across both winters. The shrub group was identified as being the greatest comntributer to reach excess drag, whereas single stemmed herbs saw the greatest change in interannual coverage and thus contirbution to total excess drag. When relating morphological change to each functional group and flow depth, although all vegetation groups saw an increase in erosion with greater flow depths, the variation in rates of erosion demonstarted some of the depth dependent interactions with vegetaion, and how they may limit or accelerate morphological change. We have also outlined the limits for current trait extraction from remote sensing techniques. UAV-LS can characterise larger vegetation structures and be used to upscale local TLS models, but even TLS is limited in its ability to characterise the spatial complexity of some vegetation traits at the resolution required to ~~link~~extract traits which can be linked with geomorphic change. This builds on current research which has analysed ecogeomorphic interactions on small river sections, or used species based imagery classification to ~~determine large~~investigate geomoprhic variations. The use of remote sensing allows data to be captured, analysed, related to broader dataset statistics, and upscaled to include larger reaches. Simultanously, the same data allows for the collection of topographic responses to flow events which can be linked to the variation in vegetation. This analysis uses seasonality to improve the classification of ~~guilds~~functional groups via chages in structural and spectral properties, advancing current methods available to the ecogeomrophology community. The trait data can then be used to infer changes in excess drag across the reach, and also be linked to specific flow events ot investigate how vegetation type and interaction with differening flows effects geomorphic response. Despite some noted limitations, this research represents an important step towards better discretisation of traits across greater scales and ~~the~~ furthers the possibility of implementing widespread traits-based research.

Future research is needed to investigate the limits of various remote sensing methods in relation to their ability to be used for traits extarction and thereby improve understanding of a systems ecogeomorphic evolution~~. Of particular note is the currently untapped resource that exists in relation to coarse scale global coverage of land cover from which vegeation traits could be extracted using methods such as those presented herein to link the scales of analysis.~~, with a focus on high resolution land cover data, remote sensing imagery, and ALS. Likewise, a need to advance the relationship between vegetation, morphology, and flow interaction is required, accounting for the spatial variations in flow depths and therefore identification of which elements of individual plants are interacting with the flow. This is especially important when examining the variation within different functional groups and across different hydrological regimes. These methods offer a bridge across sclaes, within which to consider the ways in which riparian vegetation within the river corridor is mapped, evaluated, and modelled through time, with implications for establishing new insights into the functioning of eco-geomorphic systems~~ across scales ranging from river sections to intercontinental basins~~.

Data Availability

The raw data ~~used~~collected and analysed in this analysis is available at https://zenodo.org/record/5529739#.YbDLBtDP1PY

Author Contributions

Study conceptualisation was done by C.T. and J.L. Data collection was undertaken by C.T. and J.L. Processing and data analysis was performed by C.T., with supervision from J.L. Original draft preparation by C.T. with reviewing and editing by C.T. and J.L. All authors have read and agreed to the published version of the manuscript.

Competing Interests

The authors declare that they have no conflict of interest.

Acknowledgements

This research was funded by the Natural Environment Research Council (NERC), grant number 1937474 via PhD studentship support to CT as part of the Next Generation Unmanned System Science (NEXUSS) Centre for Doctoral Training, hosted at University of Southampton. We thank the editors and two anonymous reviewers for thorough comments and suggestions which significantly improved the focus and narrative of the paper.

8. References

Abelleira Martínez, O. J., Fremier, A. K., Günter, S., Ramos Bendaña, Z., Vierling, L., Galbraith, S. M., Bosque-Pérez, N. A., and Ordoñez, J. C.: Scaling up functional traits for ecosystem services with remote sensing: concepts and methods, Ecol. Evol., 6, 4359-4371, https://doi.org/10.1002/ece3.2201, 2016.

Abernethy, B. and Rutherfurd, I. D.: The distribution and strength of riparian tree roots in relation to riverbank reinforcement, Hydrol. Process., 15, 63-79, https://doi.org/10.1002/hyp.152, 2001.

Adam, E. and Mutanga, O.: Spectral discrimination of papyrus vegetation (Cyperus papyrus L.) in swamp wetlands using field spectrometry, ISPRS Journal of Photogrammetry and Remote Sensing, 64, 612-620, https://doi.org/10.1016/j.isprsjprs.2009.04.004, 2009.

Adelabu, S. and Dube, T.: Employing ground and satellite-based QuickBird data and random forest to discriminate five tree species in a Southern African Woodland, Geocarto International, 30, 457-471, 10.1080/10106049.2014.885589, 2015.

Aguiar, F. C., Segurado, P., Martins, M. J., Bejarano, M. D., Nilsson, C., Portela, M. M., and Merritt, D. M.: The abundance and distribution of guilds of riparian woody plants change in response to land use and flow regulation, J. Appl. Ecol., 55, 2227-2240, 10.1111/1365-2664.13110, 2018.

Aguirre-Gutiérrez, J., Rifai, S., Shenkin, A., Oliveras, I., Bentley, L. P., Svátek, M., ~~Girardin, C. A. J., Both, S., Riutta, T., Berenguer, E., Kissling, W. D., Bauman, D., Raab, N., Moore, S., Farfan-Rios, W., Figueiredo, A. E. S., Reis, S. M., Ndong, J. E., Ondo, F. E., N'Ssi Bengone, N., Mihindou, V., Moraes de Seixas, M. M., Adu-Bredu, S., Abernethy, K., Asner, G. P., Barlow, J., Burslem, D. F. R. P., Coomes, D. A., Cernusak, L. A., Dargie, G. C., Enquist, B. J., Ewers, R. M., Ferreira, J., Jeffery, K. J., Joly, C. A., Lewis, S. L., Marimon Junior, B. H., Martin, R. E., Morandi, P. S., Phillips, O. L., Quesada, C. A., Salinas, N., Schwantes Marimon, B., Silman, M., Teh, Y. A., White, L. J. T., and. . .~~ Malhi, Y.: Pantropical modelling of canopy functional traits using Sentinel-2 remote sensing data, Remote Sens. Environ., 252, 112122, https://doi.org/10.1016/j.rse.2020.112122, 2021.

Al-Ali, Z. M., Abdullah, M. M., Asadalla, N. B., and Gholoum, M.: A comparative study of remote sensing classification methods for monitoring and assessing desert vegetation using a UAV-based multispectral sensor, Environ. Monit. Assess., 192, 389, 10.1007/s10661-020-08330-1, 2020.

Alaibakhsh, M., Emelyanova, I., Barron, O., Sims, N., Khiadani, M., and Mohyeddin, A.: Delineation of riparian vegetation from Landsat multi-temporal imagery using PCA, Hydrol. Process., 31, 800-810, https://doi.org/10.1002/hyp.11054, 2017.

~~APX 15 UAV Datasheet: https://www.applanix.com/downloads/products/specs/APX15_DS_NEW_0408_YW.pdf, last access: 25/01/2018.~~

~~Armanini, A., Righetti, M., and Grisenti, P.: Direct measurement of vegetation resistance in prototype scale, Journal of Hydraulic Research, 43, 481-487, 10.1080/00221680509500146, 2005.~~

Anderson, K. E., Glenn, N. F., Spaete, L. P., Shinneman, D. J., Pilliod, D. S., Arkle, R. S., Mcilroy, S. K., and Derryberry, D. R.: Estimating vegetation biomass and cover across large plots in shrub and grass dominated drylands using terrestrial lidar and machine learning, Ecol. Indic., 84, 793-802, https://doi.org/10.1016/j.ecolind.2017.09.034, 2018.

Antonarakis, A. S., Richards, K. S., and Brasington, J.: Object-based land cover classification using airborne LiDAR, Remote Sens. Environ., 112, 2988-2998, https://doi.org/10.1016/j.rse.2008.02.004, 2008.

Baattrup-Pedersen, A., Larsen, S. E., and Riis, T.: Long-term effects of stream management on plant communities in two Danish lowland streams, Hydrobiologia, 481, 33-45, 10.1023/a:1021296519187, 2002.

Baattrup-Pedersen, A., Göthe, E., Riis, T., and ~~O'Hare~~O'hare, M. T.: Functional trait composition of aquatic plants can serve to disentangle multiple interacting stressors in lowland streams, Science of The Total Environment, 543, 230-238, https://doi.org/10.1016/j.scitotenv.2015.11.027, 2016.

Baattrup-Pedersen, A., Gothe, E., Larsen, S. E., ~~O'Hare~~O'hare, M., Birk, S., Riis, T., and Friberg, N.: Plant trait characteristics vary with size and eutrophication in European lowland streams, J. Appl. Ecol., 52, 1617-1628, 10.1111/1365-2664.12509, 2015.

Baattrup-Pedersen, A., Garssen, A., Gothe, E., Hoffmann, C. C., Oddershede, A., Riis, T., ~~van~~Van Bodegom, P. M., Larsen, S. E., and Soons, M.: Structural and functional responses of plant communities to climate change-mediated alterations in the hydrology of riparian areas in temperate Europe, Ecol. Evol., 8, 4120-4135, 10.1002/ece3.3973, 2018.

Bankhead, N. L., Thomas, R. E., and Simon, A.: A combined field, laboratory and numerical study of the forces applied to, and the potential for removal of, bar top vegetation in a braided river, Earth Surf. Process. Landf., 42, 439-459, https://doi.org/10.1002/esp.3997, 2017.

Bertoldi, W., Drake, N. A., and Gurnell, A. M.: Interactions between river flows and colonizing vegetation on a braided river: exploring spatial and temporal dynamics in riparian vegetation cover using satellite data, Earth Surf. Process. Landf., 36, 1474-1486, https://doi.org/10.1002/esp.2166, 2011.

Bertoldi, W., Welber, M., Gurnell, A. M., Mao, L., Comiti, F., and Tal, M.: Physical modelling of the combined effect of vegetation and wood on river morphology, Geomorphology, 246, 178-187, https://doi.org/10.1016/j.geomorph.2015.05.038, 2015.

Biron, P. M., Robson, C., Lapointe, M. F., and Gaskin, S. J.: Comparing different methods of bed shear stress estimates in simple and complex flow fields, Earth Surf. Process. Landf., 29, 1403-1415, https://doi.org/10.1002/esp.1111, 2004.

Blondel, J.: Guilds or functional groups: does it matter?, Oikos, 100, 223-231, https://doi.org/10.1034/j.1600-0706.2003.12152.x, 2003.

Blöschl, G., Ardoin-Bardin, S., Bonell, M., Dorninger, M., Goodrich, D., Gutknecht, D., ~~Matamoros, D., Merz, B., Shand, P., and. . .~~ Szolgay, J.: At what scales do climate variability and land cover change impact on flooding and low flows?, Hydrol. Process., 21, 1241-1247, https://doi.org/10.1002/hyp.6669, 2007.

~~Boothroyd, R., Hardy, R., Warburton, J., and Marjoribanks, T.: Modeling complex flow structures and drag around a submerged plant of varied posture, Water Resources Research, 53, 2877-2901, 10.1002/2016wr020186, 2017.~~

~~Box, E.: Macroclimate and Plant Forms: An Introduction to Predictive Modeling in Phytogeography, 1, Springer Netherlands, 10.1007/978-94-009-8680-0, 1981.~~

~~Box, E. O.: Plant functional types and climate at the global scale, Journal of Vegetation Science, 7, 309-320, 1996.~~

Brasington, J., Vericat, D., and Rychkov, I.: Modeling river bed morphology, roughness, and surface sedimentology using high resolution terrestrial laser scanning, Water Resources Research, 48, 18, 10.1029/2012wr012223, 2012.

Brede, B., Calders, K., Lau, A., Raumonen, P., Bartholomeus, H. M., Herold, M., and Kooistra, L.: Non-destructive tree volume estimation through quantitative structure modelling: Comparing UAV laser scanning with terrestrial LIDAR, Remote Sens. Environ., 233, 111355, https://doi.org/10.1016/j.rse.2019.111355, 2019.

Brodu, N. and Lague, D.: 3D terrestrial lidar data classification of complex natural scenes using a multi-scale dimensionality criterion: Applications in geomorphology, ISPRS Journal of Photogrammetry and Remote Sensing, 68, 121-134, https://doi.org/10.1016/j.isprsjprs.2012.01.006, 2012.

Burgess, P., Graves, A., De Jalón, S. G., Palma, J., Dupraz, C., and Van Noordwijk, M.: Modelling agroforestry systems, in: Agroforestry for sustainable agriculture, Burleigh Dodds Science Publishing, 209-238, 2019.

Burt, A., Disney, M., and Calders, K.: Extracting individual trees from lidar point clouds using treeseg, Methods in Ecology and Evolution, 10, 438-445, 2019.

Butterfield, B. J., Grams, P. E., Durning, L. E., Hazel, J., Palmquist, E. C., Ralston, B. E., and Sankey, J. B.: Associations between riparian plant morphological guilds and fluvial sediment dynamics along the regulated Colorado River in Grand Canyon, River Research and Applications, 36, 410-421, https://doi.org/10.1002/rra.3589, 2020.

Bywater-Reyes, S., Wilcox, A., and Diehl, R.: Multiscale influence of woody riparian vegetation on fluvial topography quantified with ground-based and airborne lidar, J. Geophys. Res.-Earth Surf., 122, 1218-1235, 10.1002/2016jf004058, 2017.

Caponi, F., Vetsch, D. F., and Siviglia, A.: A model study of the combined effect of above and below ground plant traits on the ecomorphodynamics of gravel bars, Scientific Reports, 10, 17062, 10.1038/s41598-020-74106-9, 2020.

Champion, P. D. and Tanner, C. C.: Seasonality of macrophytes and interaction with flow in a New Zealand lowland stream, Hydrobiologia, 441, 1-12, 10.1023/a:1017517303221, 2000.

Chan, J. C.-W. and Paelinckx, D.: Evaluation of Random Forest and Adaboost tree-based ensemble classification and spectral band selection for ecotope mapping using airborne hyperspectral imagery, Remote Sens. Environ., 112, 2999-3011, https://doi.org/10.1016/j.rse.2008.02.011, 2008.

Chen, W., Xiang, H., and Moriya, K.: Individual Tree Position Extraction and Structural Parameter Retrieval Based on Airborne LiDAR Data: Performance Evaluation and Comparison of Four Algorithms, Remote Sensing, 12, 571, 2020.

Colbert, K. C., Larsen, D. R., and Lootens, J. R.: Height-Diameter Equations for Thirteen Midwestern Bottomland Hardwood Species, Northern Journal of Applied Forestry, 19, 171-176, 10.1093/njaf/19.4.171, 2002.

Corenblit, D., Baas, A., Balke, T., Bouma, T., Fromard, F., Garófano-Gómez, V., ~~González, E., Gurnell, A. M., Hortobágyi, B., Julien, F., Kim, D., Lambs, L., Stallins, J. A., Steiger, J., Tabacchi, E., and. . .~~ Walcker, R.: Engineer pioneer plants respond to and affect geomorphic constraints similarly along water–terrestrial interfaces world-wide, Global Ecology and Biogeography, 24, 1363-1376, 10.1111/geb.12373, 2015.

Cotton, J. A., Wharton, G., Bass, J. A. B., Heppell, C. M., and Wotton, R. S.: The effects of seasonal changes to in-stream vegetation cover on patterns of flow and accumulation of sediment, Geomorphology, 77, 320-334, https://doi.org/10.1016/j.geomorph.2006.01.010, 2006.

Coulthard, T. J.: Effects of vegetation on braided stream pattern and dynamics, Water Resources Research, 41, https://doi.org/10.1029/2004WR003201, 2005.

Crosato, A. and Saleh, M. S.: Numerical study on the effects of floodplain vegetation on river planform style, Earth Surf. Process. Landf., 36, 711-720, https://doi.org/10.1002/esp.2088, 2011.

Dalla Corte, A. P., De Vasconcellos, B. N., Rex, F. E., Sanquetta, C. R., Mohan, M., Silva, C. A., . . . Broadbent, E. N.: Applying High-Resolution UAV-LiDAR and Quantitative Structure Modelling for Estimating Tree Attributes in a Crop-Livestock-Forest System, Land, 11, 507, 2022.

De Baets, S., Poesen, J., Knapen, A., Barberá, G. G., and Navarro, J.: Root characteristics of representative Mediterranean plant species and their erosion-reducing potential during concentrated runoff, Plant and Soil, 294, 169-183, 2007.

De Bello, F., Lepš, J., and Sebastià, M. T.: Variations in species and functional plant diversity along climatic and grazing gradients, Ecography, 29, 801-810, 2006.

De Doncker, L., Troch, P., Verhoeven, R., Bal, K., Desmet, N., and Meire, P.: Relation between resistance characteristics due to aquatic weed growth and the hydraulic capacity of the river Aa, River Research and Applications, 25, 1287-1303, https://doi.org/10.1002/rra.1240, 2009.

Deltares: Delft3D-FLOW User Manual, 2021.

Diehl, R. M., Merritt, D. M., Wilcox, A. C., and Scott, M. L.: Applying Functional Traits to Ecogeomorphic Processes in Riparian Ecosystems, Bioscience, 67, 729-743, 10.1093/biosci/bix080, ~~2017~~2017a.

Diehl, R. M., Wilcox, A. C., Merritt, D. M., Perkins, D. W., and Scott, J. A.: Development of an eco-geomorphic modeling framework to evaluate riparian ecosystem response to flow-regime changes, Ecological Engineering, 123, 112-126, https://doi.org/10.1016/j.ecoleng.2018.08.024, 2018.

~~Dixon, S. J., Sambrook Smith, G. H., Best, J. L., Nicholas, A. P., Bull, J. M., Vardy, M. E., Sarker, M. H., and Goodbred, S.: The planform mobility of river channel confluences: Insights from analysis of remotely sensed imagery, Earth Science Reviews, 176, 1-18, https://doi.org/10.1016/j.earscirev.2017.09.009, 2018.~~

Diehl, R. M., Wilcox, A. C., Stella, J. C., Kui, L., Sklar, L. S., and Lightbody, A.: Fluvial sediment supply and pioneer woody seedlings as a control on bar-surface topography, Earth Surf. Process. Landf., 42, 724-734, https://doi.org/10.1002/esp.4017, 2017b.

Douss, R. and Farah, I. R.: Extraction of individual trees based on Canopy Height Model to monitor the state of the forest, Trees, Forests and People, 8, 100257, https://doi.org/10.1016/j.tfp.2022.100257, 2022.

Duro, D. C., Franklin, S. E., and Dube, M. G.: A comparison of pixel-based and object-based image analysis with selected machine learning algorithms for the classification of agricultural landscapes using SPOT-5 HRG imagery, Remote Sens. Environ., 118, 259-272, 10.1016/j.rse.2011.11.020, 2012.

~~EMLID: RTK GNSS modules for UAV mapping, 2021.~~

Engindeniz, S. and Olgun, A.: Determination of land and tree values of hybrid poplar plantations: A case study for Turkey, Southern African Forestry Journal, 197, 31-38, 10.1080/20702620.2003.10431719, 2003.

ESRI: Imagery [Basemap], Maxar Imagery (28/09/2014), 2021.

Fang, R. and Strimbu, B. M.: Comparison of Mature Douglas-Firs' Crown Structures Developed with Two Quantitative Structural Models Using TLS Point Clouds for Neighboring Trees in a Natural Regime Stand, Remote Sensing, 11, 1661, 2019.

Felzenszwalb, P. F. and Huttenlocher, D. P.: Efficient Graph-Based Image Segmentation, International Journal of Computer Vision, 59, 167-181, 10.1023/B:VISI.0000022288.19776.77, 2004.

Follett, E. and Nepf, H.: Sediment patterns near a model patch of reedy emergent vegetation, Geomorphology, 179, 141–151, 10.1016/j.geomorph.2012.08.006, 2012.

Fox, G. A., Wilson, G. V., Simon, A., Langendoen, E. J., Akay, O., and Fuchs, J. W.: Measuring streambank erosion due to ground water seepage: correlation to bank pore water pressure, precipitation and stream stage, Earth Surf. Process. Landf., 32, 1558-1573, 2007.

Francalanci, S., Paris, E., and Solari, L.: On the vulnerability of woody riparian vegetation during flood events, Environmental Fluid Mechanics, 20, 635-661, 10.1007/s10652-019-09726-5, 2020.

Garnier, E., Lavorel, S., Ansquer, P., Castro, H., Cruz, P., Dolezal, J., ~~Eriksson, O., Fortunel, C., Freitas, H., Golodets, C., Grigulis, K., Jouany, C., Kazakou, E., Kigel, J., Kleyer, M., Lehsten, V., Lepš, J., Meier, T., Pakeman, R., Papadimitriou, M., Papanastasis, V. P., Quested, H., Quétier, F., Robson, M., Roumet, C., Rusch, G., Skarpe, C., Sternberg, M., Theau, J. P., Thébault, A., Vile, D., and. . .~~ Zarovali, M. P.: Assessing the Effects of Land-use Change on Plant Traits, Communities and Ecosystem Functioning in Grasslands: A Standardized Methodology and Lessons from an Application to 11 European Sites, Annals of Botany, 99, 967-985, 10.1093/aob/mcl215, 2006.

Gilvear, D., Tyler, A., and Davids, C.: Detection of estuarine and tidal river hydromorphology using hyper-spectral and LiDAR data: Forth estuary, Scotland, Estuar. Coast. Shelf Sci., 61, 379-392, 10.1016/j.ecss.2004.06.007, 2004.

Google Earth Pro: River Teme, 52°21'28.96"N, 3° 4'12.82"W, elevation 180 m., 2021.

Göthe, E., Timmermann, A., Januschke, K., and Baattrup-Pedersen, A.: Structural and functional responses of floodplain vegetation to stream ecosystem restoration, Hydrobiologia, 769, 79-92, 10.1007/s10750-015-2401-3, 2016.

Göthe, E., Baattrup-Pedersen, A., Wiberg-Larsen, P., Graeber, D., Kristensen, E. A., and Friberg, N.: Environmental and spatial controls of taxonomic versus trait composition of stream biota, Freshwater Biology, 62, 397-413, 10.1111/fwb.12875, 2017.

Gupta, N., Atkinson, P. M., and Carling, P. A.: Decadal length changes in the fluvial planform of the River Ganga: bringing a mega-river to life with Landsat archives, Remote Sensing Letters, 4, 1-9, 10.1080/2150704X.2012.682658, 2013.

Gurnell, A.: Plants as river system engineers, Earth Surf. Process. Landf., 39, 4-25, 2014.

Hackenberg, J., Spiecker, H., Calders, K., Disney, M., and Raumonen, P.: SimpleTree —An Efficient Open Source Tool to Build Tree Models from TLS Clouds, Forests, 6, 4245-4294, 2015.

Harvey, J. and Gooseff, M.: River corridor science: Hydrologic exchange and ecological consequences from bedforms to basins, Water Resources Research, 51, 6893-6922, doi:10.1002/2015WR017617, 2015.

Henshaw, A. J., Gurnell, A. M., Bertoldi, W., and Drake, N. A.: An assessment of the degree to which Landsat TM data can support the assessment of fluvial dynamics, as revealed by changes in vegetation extent and channel position, along a large river, Geomorphology, 202, 74-85, 10.1016/j.geomorph.2013.01.011, 2013.

Himmelstoss, E. A., Farris, A. S., Henderson, R. E., Kratzmann, M. G., Ergul, A., Zhang, O., Zichichi, J. L., and Thieler, E. R.: Digital Shoreline Analysis System (version 5.0), 2018.

Hortobágyi, B., Corenblit, D., Steiger, J., and Peiry, J.-L.: Niche construction within riparian corridors. Part I: Exploring biogeomorphic feedback windows of three pioneer riparian species (Allier River, France), Geomorphology, 305, 94-111, https://doi.org/10.1016/j.geomorph.2017.08.048, 2018.

Hortobágyi, B., Corenblit, D., Ding, Z., Lambs, L., and Steiger, J.: Above-and belowground responses of Populus nigra L. to mechanical stress observed on the Allier River, France, Géomorphologie: relief, processus, environnement, 23, 219-231, 2017.

Houborg, R., Fisher, J. B., and Skidmore, A. K.: Advances in remote sensing of vegetation function and traits, International Journal of Applied Earth Observation and Geoinformation, 43, 1-6, https://doi.org/10.1016/j.jag.2015.06.001, 2015.

Huang, H. Q. and Nanson, G. C.: The influence of bank strength on channel geometry: an integrated analysis of some observations, Earth Surf. Process. Landf., 23, 865-876, https://doi.org/10.1002/(SICI)1096-9837(199810)23:10<865::AID-ESP903>3.0.CO;2-3, 1998.

Hughes, A. O.: Riparian management and stream bank erosion in New Zealand, New Zealand Journal of Marine and Freshwater Research, 50, 277-290, 10.1080/00288330.2015.1116449, 2016.

Hupp, C. R. and Osterkamp, W.: Riparian vegetation and fluvial geomorphic processes, Geomorphology, 14, 277-295, 1996.

Jalonen, J., Järvelä, J., and Aberle, J.: Leaf area index as vegetation density measure for hydraulic analyses, Journal of Hydraulic Engineering, 139, 461-469, 2012.

James, C. S., Goldbeck, U. K., Patini, A., and Jordanova, A. A.: Influence of foliage on flow resistance of emergent vegetation, Journal of Hydraulic Research, 46, 536-542, 10.3826/jhr.2008.3177, 2008.

Järvelä, J.: Determination of flow resistance of vegetated channel banks and floodplains, River Flow 2002, 311-318, 2002a.

Järvelä, J.: Flow resistance of flexible and stiff vegetation: a flume study with natural plants, Journal of Hydrology, 269, 44-54, https://doi.org/10.1016/S0022-1694(02)00193-2, 2002b2002a.

Järvelä, J.: Determination of flow resistance of vegetated channel banks and floodplains, River Flow 2002, 311-318, 2002b.

Järvelä, J.: Determination of flow resistance caused by non-submerged woody vegetation, Int. J. River Basin Manag., 2, 61-70, 10.1080/15715124.2004.9635222, 2004.

Jeffries, R., Darby, S. E., and Sear, D. A.: The influence of vegetation and organic debris on flood-plain sediment dynamics: case study of a low-order stream in the New Forest, England, Geomorphology, 51, 61-80, https://doi.org/10.1016/S0169-555X(02)00325-2, 2003.

Julian, J. P. and Torres, R.: Hydraulic erosion of cohesive riverbanks, Geomorphology, 76, 193-206, https://doi.org/10.1016/j.geomorph.2005.11.003, 2006.

Jurekova, Z., Baranec, T., Paganová, V., Kotrla, M., and Elias, P.: Comparison of the ecological characteristic the willow-poplar floodplain forest fragments on the stands with different height of groundwater level, ECOLOGY-BRATISLAVA-, 27, 31, 2008.

Kang, R. S.: GEOMORPHIC EFFECTS OF MOSSES IN A LOW-ORDER STREAM IN FAIRFAX COUNTY, VIRGINIA, Phys. Geogr., 33, 360-382, 10.2747/0272-3646.33.4.360, 2012.

Kattge, J., Diaz, S., Lavorel, S., Prentice, I. C., Leadley, P., Bönisch, G., Garnier, E., Westoby, M., Reich, P. B., and . . ., Wright, I. J.: TRY–a global database of plant traits, Global change biology, 17, 2905-2935, 2011.

Kattge, J. and Bönisch, G. and Díaz, S. and Lavorel, S. and Prentice, I. C. and Leadley, P., and Tautenhahn, S. and Werner, G. D. A. and Aakala, T. and Abedi, M. and Acosta, A. T. R. and Adamidis, G. C. and Adamson, K. and Aiba, M. and Albert, C. H. and Alcántara, J. M. and Alcázar C, C. and Aleixo, I. and Ali, H. and Amiaud, B. and Ammer, C. and Amoroso, M. M. and Anand, M. and Anderson, C. and Anten, N. and Antos, J. and Apgaua, D. M. G. and Ashman, T.-L. and Asmara, D. H. and Asner, G. P. and Aspinwall, M. and Atkin, O. and Aubin, I. and Baastrup-Spohr, L. and Bahalkeh, K. and Bahn, M. and Baker, T. and Baker, W. J. and Bakker, J. P. and Baldocchi, D. and Baltzer, J. and Banerjee, A. and Baranger, A. and Barlow, J. and Barneche, D. R. and Baruch, Z. and Bastianelli, D. and Battles, J. and Bauerle, W. and Bauters, M. and Bazzato, E. and Beckmann, M. and Beeckman, H. and Beierkuhnlein, C. and Bekker, R. and Belfry, G. and Belluau, M. and Beloiu, M. and Benavides, R. and Benomar, L. and Berdugo-Lattke, M. L. and Berenguer, E. and Bergamin, R. and Bergmann, J. and Bergmann Carlucci, M. and Berner, L. and Bernhardt-Römermann, M. and Bigler, C. and Bjorkman, A. D. and Blackman, C. and Blanco, C. and Blonder, B. and Blumenthal, D. and Bocanegra González, K. T. and Boeckx, P. and Bohlman, S. and Böhning-Gaese, K. and Boisvert-Marsh, L. and Bond, W. and Bond-Lamberty, B. and Boom, A. and Boonman, C. C. F. and Bordin, K. and Boughton, E. H. and Boukili, V. and Bowman, D. M. J. S. and Bravo, S. and Brendel, M. R. and Broadley, M. R. and Brown, K. A. and Bruelheide, H. and Brumnich, F. and Bruun, H. H. and Bruy, D. and Buchanan, S. W. and Bucher, S. F. and Buchmann, N. and Buitenwerf, R. and Bunker, D. E. and Bürger, J. and Burrascano, S. and Burslem, D. F. R. P. and Butterfield, B. J. and Byun, C. and Marques, M. and Scalon, M. C. and Caccianiga, M. and Cadotte, M. and Cailleret, M. and Camac, J. and Camarero, J. J. and Campany, C. and Campetella, G. and Campos, J. A. and Cano-Arboleda, L. and Canullo, R. and Carbognani, M. and Carvalho, F. and Casanoves, F. and Castagneyrol, B. and Catford, J. A. and Cavender-Bares, J. and Cerabolini, B. E. L. and Cervellini, M. and Chacón-Madrigal, E. and Chapin, K. and Chapin, F. S. and Chelli, S. and Chen, S. C. and Chen, A. and Cherubini, P. and Chianucci, F. and Choat, B. and Chung, K. S. and Chytrý, M. and Ciccarelli, D. and Coll, L. and Collins, C. G. and Conti, L. and Coomes, D. and Cornelissen, J. H. C. and Cornwell, W. K. and Corona, P. and Coyea, M. and Craine, J. and Craven, D. and Cromsigt, J. P. G. M. and Csecserits, A. and Cufar, K. and Cuntz, M. and da Silva, A. C. and Dahlin, K. M. and Dainese, M. and Dalke, I. and Dalle Fratte, M. and Dang-Le, A. T. and Danihelka, J. and Dannoura, M. and Dawson, S. and de Beer, A. J. and De Frutos, A. and De Long, J. R. and Dechant, B. and Delagrange, S. and Delpierre, N. and Derroire, G. and Dias, A. S. and Diaz-Toribio, M. H. and Dimitrakopoulos, P. G. and Dobrowolski, M. and Doktor, D. and Dřevojan, P. and Dong, N. and Dransfield, J. and Dressler, S. and Duarte, L. and Ducouret, E. and Dullinger,

S. and Durka, W. and Duursma, R. and Dymova, O. and E-Vojtkó, A. and Eckstein, R. L. and Ejtehadi, H. and Elser, J. and Emilio, T. and Engemann, K. and Erfanian, M. B. and Erfmeier, A. and Esquivel-Muelbert, A. and Esser, G. and Estiarte, M. and Domingues, T. F. and Fagan, W. F. and Fagúndez, J. and Falster, D. S. and Fan, Y. and Fang, J. and Farris, E. and Fazlioglu, F. and Feng, Y. and Fernandez-Mendez, F. and Ferrara, C. and Ferreira, J. and Fidelis, A. and Finegan, B. and Firn, J. and Flowers, T. J. and Flynn, D. F. B. and Fontana, V. and Forey, E. and Forgiarini, C. and François, L. and Frangipani, M. and Frank, D. and Frenette-Dussault, C. and Freschet, G. T. and Fry, E. L. and Fyllas, N. M. and Mazzochini, G. G. and Gachet, S. and Gallagher, R. and Ganade, G. and Ganga, F. and García-Palacios, P. and Gargaglione, V. and Garnier, E. and Garrido, J. L. and de Gasper, A. L. and Gea-Izquierdo, G. and Gibson, D. and Gillison, A. N. and Giroldo, A. and Glasenhardt, M. C. and Gleason, S. and Gliesch, M. and Goldberg, E. and Göldel, B. and Gonzalez-Akre, E. and Gonzalez-Andujar, J. L. and González-Melo, A. and González-Robles, A. and Graae, B. J. and Granda, E. and Graves, S. and Green, W. A. and Gregor, T. and Gross, N. and Guerin, G. R. and Günther, A. and Gutiérrez, A. G. and Haddock, L. and Haines, A. and Hall, J. and Hambuckers, A. and Han, W. and Harrison, S. P. and Hattingh, W. and Hawes, J. E. and He, T. and He, P. and Heberling, J. M. and Helm, A. and Hempel, S. and Hentschel, J. and Hérault, B. and Hereş, A.-M. and Herz, K. and Heuertz, M. and Hickler, T. and Hietz, P. and Higuchi, P. and Hipp, A. L. and Hirons, A. and Hock, M. and Hogan, J. A. and Holl, K. and Honnay, O. and Hornstein, D. and Hou, E. and Hough-Snee, N. and Hovstad, K. A. and Ichie, T. and Igić, B. and Illa, E. and Isaac, M. and Ishihara, M. and Ivanov, L. and Ivanova, L. and Iversen, C. M. and Izquierdo, J. and Jackson, R. B. and Jackson, B. and Jactel, H. and Jagodzinski, A. M. and Jandt, U. and Jansen, S. and Jenkins, T. and Jentsch, A. and Jespersen, J. R. P. and Jiang, G. F. and Johansen, J. L. and Johnson, D. and Jokela, E. J. and Joly, C. A. and Jordan, G. J. and Joseph, G. S. and Junaedi, D. and Junker, R. R. and Justes, E. and Kabzems, R. and Kane, J. and Kaplan, Z. and Kattenborn, T. and Kavelenova, L. and Kearsley, E. and Kempel, A. and Kenzo, T. and Kerkhoff, A. and Khalil, M. I. and Kinlock, N. L. and Kissling, W. D. and Kitajima, K. and Kitzberger, T. and Kjøller, R. and Klein, T. and Kleyer, M. and Klimešová, J. and Klipel, J. and Kloeppel, B. and Klotz, S. and Knops, J. M. H. and Kohyama, T. and Koike, F. and Kollmann, J. and Komac, B. and Komatsu, K. and König, C. and Kraft, N. J. B. and Kramer, K. and Kreft, H. and Kühn, I. and Kumarathunge, D. and Kuppler, J. and Kurokawa, H. and Kurosawa, Y. and Kuyah, S. and Laclau, J. P. and Lafleur, B. and Lallai, E. and Lamb, E. and Lamprecht, A. and Larkin, D. J. and Laughlin, D. and Le Bagousse-Pinguet, Y. and le Maire, G. and le Roux, P. C. and le Roux, E. and Lee, T. and Lens, F. and Lewis, S. L. and Lhotsky, B. and Li, Y. and Li, X. and Lichstein, J. W. and Liebergesell, M. and Lim, J. Y. and Lin, Y.-S. and Linares, J. C. and Liu, C. and Liu, D. and Liu, U. and Livingstone, S. and Llusià, J. and Lohbeck, M. and López-García, Á. and Lopez-Gonzalez, G. and Lososová, Z. and Louault, F. and Lukács, B. A. and Lukeš, P. and Luo, Y. and Lussu, M. and Ma, S. and Maciel-Rabelo-Pereira, C. and Mack, M. and Maire, V. and Mäkelä, A. and Mäkinen, H. and Malhado, A. C. M. and Mallik, A. and Manning, P. and Manzoni, S. and Marchetti, Z. and Marchino, L. and Marcilio-Silva, V. and Marcon, E. and Marignani, M. and Markesteijn, L. and Martin, A. and Martínez-Garza, C. and Martínez-Vilalta, J. and Mašková, T. and Mason, K. and Mason, N. and Massad, T. J. and Masse, J. and Mayrose, I. and McCarthy, J. and McCormack, M. L. and McCulloh, K. and McFadden, I. R. and McGill, B. J. and McPartland, M. Y. and Medeiros, J. S. and Medlyn, B. and Meerts, P. and Mehrabi, Z. and Meir, P. and Melo, F. P. L. and Mencuccini, M. and Meredieu, C. and Messier, J. and Mészáros, I. and Metsaranta, J. and Michaletz, S. T. and Michelaki, C. and Migalina, S. and Milla, R. and Miller, J. E. D. and Minden, V. and Ming, R. and Mokany, K. and Moles, A. T. and Molnár V, A. and Molofsky, J. and Molz, M. and Montgomery, R. A. and Monty, A. and Moravcová, L. and Moreno-Martínez, A. and Moretti, M. and Mori, A. S. and Mori, S. and Morris, D. and Morrison, J. and Mucina, L. and Mueller, S. and Muir, C. D. and Müller, S. C. and Munoz, F. and Myers-Smith, I. H. and Myster, R. W. and Nagano, M. and Naidu, S. and Narayanan, A. and Natesan, B. and Negoita, L. and Nelson, A. S. and Neuschulz, E. L. and Ni, J. and Niedrist, G. and Nieto, J. and Niinemets, Ü. and Nolan, R. and Nottebrock, H. and Nouvellon, Y. and Novakovskiy, A. and Network, T. N. and Nystuen, K. O. and O'Grady, A. and O'Hara, K. and O'Reilly-Nugent, A. and Oakley, S. and Oberhuber, W. and Ohtsuka, T. and Oliveira, R. and Öllerer, K. and Olson, M. E. and Onipchenko, V. and Onoda, Y. and Onstein, R. E. and Ordonez, J. C. and Osada, N. and Ostonen, I. and Ottaviani, G. and Otto, S. and Overbeck, G. E. and Ozinga, W. A. and Pahl, A. T. and Paine, C. E. T. and Pakeman, R. J. and Papageorgiou, A. C. and Parfionova, E. and Pärtel, M. and Patacca, M. and Paula, S. and Paule, J. and Pauli, H. and Pausas, J. G. and Peco, B. and Penuelas, J. and Perea, A. and Peri, P. L. and Petisco-Souza, A. C. and Petraglia, A. and Petritan, A. M. and Phillips, O. L. and Pierce, S. and Pillar, V. D. and Pisek, J. and Pomogaybin, A. and Poorter, H. and Portsmuth, A. and Poschlod, P. and Potvin, C. and Pounds, D. and Powell, A. S. and Power, S. A. and Prinzing, A. and Puglielli, G. and Pyšek, P. and Raevel, V. and Rammig, A. and Ransijn, J. and Ray, C. A. and Reich, P. B. and Reichstein, M. and Reid, D. E. B. and Réjou-Méchain, M. and de Dios, V. R. and Ribeiro, S. and Richardson, S. and Riibak, K. and Rillig, M. C. and Riviera, F. and Robert, E. M. R. and Roberts, S. and

Robroek, B. and Roddy, A. and Rodrigues, A. V. and Rogers, A. and Rollinson, E. and Rolo, V. and Römermann, C. and Ronzhina, D. and Roscher, C. and Rosell, J. A. and Rosenfield, M. F. and Rossi, C. and Roy, D. B. and Royer-Tardif, S. and Rüger, N. and Ruiz-Peinado, R. and Rumpf, S. B. and Rusch, G. M. and Ryo, M. and Sack, L. and Saldaña, A. and Salgado-Negret, B. and Salguero-Gomez, R. and Santa-Regina, I. and Santacruz-García, A. C. and Santos, J. and Sardans, J. and Schamp, B. and Scherer-Lorenzen, M. and Schleuning, M. and Schmid, B. and Schmidt, M. and Schmitt, S. and Schneider, J. V. and Schowanek, S. D. and Schrader, J. and Schrodt, F. and Schuldt, B. and Schurr, F. and Selaya Garvizu, G. and Semchenko, M. and Seymour, C. and Sfair, J. C. and Sharpe, J. M. and Sheppard, C. S. and Sheremetiev, S. and Shiodera, S. and Shipley, B. and Shovon, T. A. and Siebenkäs, A. and Sierra, C. and Silva, V. and Silva, M. and Sitzia, T. and Sjöman, H. and Slot, M. and Smith, N. G. and Sodhi, D. and Soltis, P. and Soltis, D. and Somers, B. and Sonnier, G. and Sørensen, M. V. and Sosinski Jr, E. E. and Soudzilovskaia, N. A. and Souza, A. F. and Spasojevic, M. and Sperandii, M. G. and Stan, A. B. and Stegen, J. and Steinbauer, K. and Stephan, J. G. and Sterck, F. and Stojanovic, D. B. and Strydom, T. and Suarez, M. L. and Svenning, J. C. and Svitková, I. and Svitok, M. and Svoboda, M. and Swaine, E. and Swenson, N. and Tabarelli, M. and Takagi, K. and Tappeiner, U. and Tarifa, R. and Tauugourdeau, S. and Tavsanoglu, C. and te Beest, M. and Tedersoo, L. and Thiffault, N. and Thom, D. and Thomas, E. and Thompson, K. and Thornton, P. E. and Thuiller, W. and Tichý, L. and Tissue, D. and Tjoelker, M. G. and Tng, D. Y. P. and Tobias, J. and Török, P. and Tarin, T. and Torres-Ruiz, J. M. and Tóthmérész, B. and Treurnicht, M. and Trivellone, V. and Trolliet, F. and Trotsiuk, V. and Tsakalos, J. L. and Tsiripidis, I. and Tysklind, N. and Umehara, T. and Usoltsev, V. and Vadeboncoeur, M. and Vaezi, J. and Valladares, F. and Vamosi, J. and van Bodegom, P. M. and van Breugel, M. and Van Cleemput, E. and van de Weg, M. and van der Merwe, S. and van der Plas, F. and van der Sande, M. T. and van Kleunen, M. and Van Meerbeek, K. and Vanderwel, M. and Vanselow, K. A. and Vårhammar, A. and Varone, L. and Vasquez Valderrama, M. Y. and Vassilev, K. and Vellend, M. and Veneklaas, E. J. and Verbeeck, H. and Verheyen, K. and Vibrans, A. and Vieira, I. and Villacís, J. and Violle, C. and Vivek, P. and Wagner, K. and Waldram, M. and Waldron, A. and Walker, A. P. and Waller, M. and Walther, G. and Wang, H. and Wang, F. and Wang, W. and Watkins, H. and Watkins, J. and Weber, U. and Weedon, J. T. and Wei, L. and Weigelt, P. and Weiher, E. and Wells, A. W. and Wellstein, C. and Wenk, E. and Westoby, M. and Westwood, A. and White, P. J. and Whitten, M. and Williams, M. and Winkler, D. E. and Winter, K. and Womack, C. and Wright, I. J. and Wright, S. J. and Wright, J. and Pinho, B. X. and Ximenes, F. and Yamada, T. and Yamaji, K. and Yanai, R. and Yankov, N. and Yguel, B. and Zanini, K. J. and Zanne, A. E. and Zelený, D. and Zhao, Y. P. and Zheng, J. and Zheng, J. and Ziemińska, K. and Zirbel, C. R. and Zizka, G. and Zo-Bi, I. C. and Zotz, G. and., . . . Wirth, C.: TRY plant trait database – enhanced coverage and open access, Global Change Biology, 26, 119-188, https://doi.org/10.1111/gcb.14904, 2020.

Kim, S. J. and Stoesser, T.: Closure modeling and direct simulation of vegetation drag in flow through emergent vegetation, Water Resources Research, 47, https://doi.org/10.1029/2011WR010561, 2011.

Krisanski, S., Taskhiri, M. S., Gonzalez Aracil, S., Herries, D., Muneri, A., Gurung, M. B., Montgomery, J., and Turner, P.: Forest Structural Complexity Tool—An Open Source, Fully-Automated Tool for Measuring Forest Point Clouds, Remote Sensing, 13, 4677, 2021.

Kyle, G. and Leishman, M. R.: Plant functional trait variation in relation to riparian geomorphology: The importance of disturbance, Austral Ecology, 34, 793-804, 10.1111/j.1442-9993.2009.01988.x, 2009.

Lague, D.: Chapter 8 - Terrestrial laser scanner applied to fluvial geomorphology, in: Developments in Earth Surface Processes, edited by: Tarolli, P., and Mudd, S. M., Elsevier, Amsterdam, The Netherlands, 231-254, https://doi.org/10.1016/B978-0-444-64177-9.00008-4, 2020.

Lague, D., Brodu, N., and Leroux, J.: Accurate 3D comparison of complex topography with terrestrial laser scanner: Application to the Rangitikei canyon (NZ), ISPRS journal of photogrammetry and remote sensing, 82, 10-26, 2013.

Lane, S. N.: Natural flood management, Wiley Interdiscip. Rev.-Water, 4, 14, 10.1002/wat2.1211, 2017.

Lawson, J. R., Fryirs, K. A., Lenz, T., and Leishman, M. R.: Heterogeneous flows foster heterogeneous assemblages: relationships between functional diversity and hydrological heterogeneity in riparian plant communities, Freshwater Biology, 60, 2208-2225, 10.1111/fwb.12649, 2015.

Leyland, J., Hackney, C. R., Darby, S. E., Parsons, D. R., Best, J. L., Nicholas, A. P., Aalto, R., and Lague, D.: Extreme flood-driven fluvial bank erosion and sediment loads: direct process measurements using integrated Mobile Laser Scanning (MLS) and hydro-acoustic techniques, Earth Surf. Process. Landf., 42, 334-346, 10.1002/esp.4078, 2017.

Lightbody, A. F. and Nepf, H. M.: Prediction of near-field shear dispersion in an emergent canopy with heterogeneous morphology, Environmental Fluid Mechanics, 6, 477-488, 10.1007/s10652-006-9002-7, 2006.

Lukacs, B. A., E-Vojtko, A., Eros, T., Molnar, V. A., Szabo, S., and Gotzenberger, L.: Carbon forms, nutrients and water velocity filter hydrophyte and riverbank species differently: A trait-based study, Journal of Vegetation Science, 30, 471-484, 10.1111/jvs.12738, 2019.

Lytle, D. A., Merritt, D. M., Tonkin, J. D., Olden, J. D., and Reynolds, L. V.: Linking river flow regimes to riparian plant guilds: a community-wide modeling approach, Ecological applications, 27, 1338-1350, 2017.

Manners, R., Schmidt, J., and Wheaton, J. M.: Multiscalar model for the determination of spatially explicit riparian vegetation roughness, J. Geophys. Res.-Earth Surf., 118, 65-83, 10.1029/2011jf002188, 2013.

Manners, R. B., Wilcox, A. C., Kui, L., Lightbody, A. F., Stella, J. C., and Sklar, L. S.: When do plants modify fluvial processes? Plant-hydraulic interactions under variable flow and sediment supply rates, Journal of Geophysical Research: Earth Surface, 120, 325-345, https://doi.org/10.1002/2014JF003265, 2015.

McCoyMccoy-Sulentic, M. E., Kolb, T. E., Merritt, D. M., Palmquist, E., Ralston, B. E., Sarr, D. A., and Shafroth, P. B.: Changes in Community-Level Riparian Plant Traits over Inundation Gradients, Colorado River, Grand Canyon, Wetlands, 37, 635-646, 10.1007/s13157-017-0895-3, 2017.

McGillMcgill, B. J., Enquist, B. J., Weiher, E., and Westoby, M.: Rebuilding community ecology from functional traits, Trends in ecology & evolution, 21, 178-185, 2006.

RedEdge-MX: https://micasense.com/rededge-mx/, last access: 17/11/2021.

Michałowska, M. and Rapiński, J.: A Review of Tree Species Classification Based on Airborne LiDAR Data and Applied Classifiers, Remote Sensing, 13, 353, 2021.

Millar, R. G. and Quick, M. C.: Stable Width and Depth of Gravel-Bed Rivers with Cohesive Banks, Journal of Hydraulic Engineering, 124, 1005-1013, doi:10.1061/(ASCE)0733-9429(1998)124:10(1005), 1998.

Myint, S. W., Gober, P., Brazel, A., Grossman-Clarke, S., and Weng, Q.: Per-pixel vs. object-based classification of urban land cover extraction using high spatial resolution imagery, Remote Sens. Environ., 115, 1145-1161, https://doi.org/10.1016/j.rse.2010.12.017, 2011.

Naiman, R. J., Decamps, H., and Pollock, M.: THE ROLE OF RIPARIAN CORRIDORS IN MAINTAINING REGIONAL BIODIVERSITY, Ecological Applications, 3, 209-212, 10.2307/1941822, 1993.

Naiman, R. J., Bechtold, J. S., Drake, D. C., Latterell, J. J., O'keefe, T. C., and Balian, E. V.: Origins, patterns, and importance of heterogeneity in riparian systems, in: Ecosystem function in heterogeneous landscapes, Springer, 279-309, 2005.

Nallaperuma, B. and Asaeda, T.: The long-term legacy of riparian vegetation in a hydrogeomorphologically remodelled fluvial setting, River Research and Applications, 36, 1690-1700, https://doi.org/10.1002/rra.3665, 2020.

Nepf, H. M. and Vivoni, E. R.: Flow structure in depth-limited, vegetated flow, Journal of Geophysical Research: Oceans, 105, 28547-28557, https://doi.org/10.1029/2000JC900145, 2000.

~~O'hare~~O'Hare, J., ~~O'hare~~O'Hare, M., Gurnell, A., Dunbar, M., Scarlett, P., and Laize, C.: Physical constraints on the distribution of macrophytes linked with flow and sediment dynamics in British rivers, River Research and Applications, 27, 671-683, 2011.

O'Hare, M., Mountford, J., Maroto, J., and Gunn, I.: Plant traits relevant to fluvial geomorphology and hydrological interactions, River Research and Applications, 32, 179-189, 2016.

O'Briain, R., Shephard, S., and Coghlan, B.: Pioneer macrophyte species engineer fine-scale physical heterogeneity in a shallow lowland river, Ecological Engineering, 102, 451-458, https://doi.org/10.1016/j.ecoleng.2017.02.047, 2017.

Oorschot, M. V., Kleinhans, M., Geerling, G., and Middelkoop, H.: Distinct patterns of interaction between vegetation and morphodynamics, Earth Surf. Process. Landf., 41, 791-808, https://doi.org/10.1002/esp.3864, 2016.

Palmer, M. A., Lettenmaier, D. P., Poff, N. L., Postel, S. L., Richter, B., and Warner, R.: Climate change and river ecosystems: protection and adaptation options, Environmental management, 44, 1053-1068, 2009.

Palmquist, E. C., Sterner, S. A., and Ralston, B. E.: A comparison of riparian vegetation sampling methods along a large, regulated river, River Research and Applications, 35, 759-767, 10.1002/rra.3440, 2019.

Phillips, J. D.: Hydrologic and geomorphic flow thresholds in the Lower Brazos River, Texas, USA, Hydrological Sciences Journal, 60, 1631-1648, 10.1080/02626667.2014.943670, 2015.

Quétier, F., Lavorel, S., Thuiller, W., and Davies, I.: Plant-trait-based modeling assessment of ecosystem-service sensitivity to land-use change, Ecological Applications, 17, 2377-2386, 2007.

Raumonen, P., Kaasalainen, M., Åkerblom, M., Kaasalainen, S., Kaartinen, H., Vastaranta, M., Holopainen, M., Disney, M., and Lewis, P.: Fast Automatic Precision Tree Models from Terrestrial Laser Scanner Data, Remote Sensing, 5, 491-520, 2013.

~~Reich, P. B., Wright, I. J., and Lusk, C. H.: Predicting leaf physiology from simple plant and climate attributes: a global GLOPNET analysis, Ecological Applications, 17, 1982-1988, 2007.~~

Rivaes, R. P., Rodriguez-Gonzalez, P. M., Ferreira, M. T., Pinheiro, A. N., Politti, E., Egger, G., Garcia-Arias, A., and Frances, F.: Modeling the Evolution of Riparian Woodlands Facing Climate Change in Three European Rivers with Contrasting Flow Regimes, Plos One, 9, 14, 10.1371/journal.pone.0110200, 2014.

Roussel, J.-R., Auty, D., Coops, N. C., Tompalski, P., Goodbody, T. R. H., Meador, A. S., Bourdon, J.-F., ~~de~~De Boissieu, F., and Achim, A.: lidR: An R package for analysis of Airborne Laser Scanning (ALS) data, Remote Sens. Environ., 251, 112061, https://doi.org/10.1016/j.rse.2020.112061, 2020.

Sand-Jensen, K.: Drag and reconfiguration of freshwater macrophytes, Freshwater Biology, 48, 271-283, https://doi.org/10.1046/j.1365-2427.2003.00998.x, 2003.

Sand-Jensen, K.: Drag forces on common plant species in temperate streams: consequences of morphology, velocity and biomass, Hydrobiologia, 610, 307-319, 2008.

Sand-Jensen, K. and Pedersen, O.: Velocity gradients and turbulence around macrophyte stands in streams, Freshwater Biology, 42, 315-328, 1999.

Savage, V. M., Webb, C. T., and Norberg, J.: A general multi-trait-based framework for studying the effects of biodiversity on ecosystem functioning, Journal of theoretical biology, 247, 213-229, 2007.

Schuster, C., Förster, M., and Kleinschmit, B.: Testing the red edge channel for improving land-use classifications based on high-resolution multi-spectral satellite data, Int. J. Remote Sens., 33, 5583-5599, 10.1080/01431161.2012.666812, 2012.

Sear, D. A., Millington, C. E., Kitts, D. R., and Jeffries, R.: Logjam controls on channel:floodplain interactions in wooded catchments and their role in the formation of multi-channel patterns, Geomorphology, 116, 305-319, https://doi.org/10.1016/j.geomorph.2009.11.022, 2010.

Sharpe, R. and James, C.: Deposition of sediment from suspension in emergent vegetation, Water Sa, 32, 211-218, 2006.

Simon, A., Curini, A., Darby, S. E., and Langendoen, E. J.: Bank and near-bank processes in an incised channel, Geomorphology, 35, 193-217, 2000.

Song, S., Schmalz, B., Xu, Y. P., and Fohrer, N.: Seasonality of Roughness - the Indicator of Annual River Flow Resistance Condition in a Lowland Catchment, Water Resources Management, 31, 3299-3312, 10.1007/s11269-017-1656-z, 2017.

Southall, E., Dale, M. P., and Kent, M.: Floristic variation and willow carr development within a southwest England wetland, Appl. Veg. Sci., 6, 63-72, https://doi.org/10.1111/j.1654-109X.2003.tb00565.x, 2003.

Souza, J. and Hooke, J.: Influence of seasonal vegetation dynamics on hydrological connectivity in tropical drylands, Hydrol. Process., 35, e14427, https://doi.org/10.1002/hyp.14427, 2021.

Stromberg, J. C. and Merritt, D. M.: Riparian plant guilds of ephemeral, intermittent and perennial rivers, Freshwater Biology, 61, 1259-1275, 10.1111/fwb.12686, 2016.

Sweeney, B. W., Bott, T. L., Jackson, J. K., Kaplan, L. A., Newbold, J. D., Standley, L. J., Hession, W. C., and Horwitz, R. J.: Riparian deforestation, stream narrowing, and loss of stream ecosystem services, Proc. Natl. Acad. Sci. U. S. A., 101, 14132-14137, 10.1073/pnas.0405895101, 2004.

Tabacchi, E., González, E., Corenblit, D., Garófano-Gómez, V., Planty-Tabacchi, A.-M., and Steiger, J.: Species composition and plant traits: Characterization of the biogeomorphological succession within contrasting river corridors, River Research and Applications, 35, 1228-1240, 10.1002/rra.3511, 2019.

Thoms, M. C. and Parsons, M.: Eco-geomorphology: an interdisciplinary approach to river science, International Association of Hydrological Sciences, Publication, 276, 113-119p, 2002.

Tomsett, C. and Leyland, J.: Remote sensing of river corridors: A review of current trends and future directions, River Research and Applications, 35, 779-803, 10.1002/rra.3479, 2019.

Tomsett, C. and Leyland, J.: Development and Testing of a UAV Laser Scanner and Multispectral Camera System for Eco-Geomorphic Applications, Sensors, 21, 7719, 2021.

~~UNISDR~~Unisdr and ~~CRED~~Cred: The Human Cost of Weather Related Disasters: 1995-2015, United Nations Office for Disaster Risk Reduction, 2015.

~~Van Bodegom, P., Douma, J., Witte, J., Ordonez, J., Bartholomeus, R., and Aerts, R.: Going beyond limitations of plant functional types when predicting global ecosystem–atmosphere fluxes: exploring the merits of traits-based approaches, Global Ecology and Biogeography, 21, 625-636, 2012.~~

Valbuena, R., O'connor, B., Zellweger, F., Simonson, W., Vihervaara, P., Maltamo, M., . . . Coops, N. C.: Standardizing Ecosystem Morphological Traits from 3D Information Sources, Trends in Ecology & Evolution, 35, 656-667, https://doi.org/10.1016/j.tree.2020.03.006, 2020.

Van Dijk, W. M., Teske, R., Van De Lageweg, W. I., and Kleinhans, M. G.: Effects of vegetation distribution on experimental river channel dynamics, Water Resources Research, 49, 7558-7574, https://doi.org/10.1002/2013WR013574, 2013.

Van Iersel, W., Straatsma, M., Addink, E., and Middelkoop, H.: Monitoring height and greenness of non-woody floodplain vegetation with UAV time series, ISPRS Journal of Photogrammetry and Remote Sensing, 141, 112-123, https://doi.org/10.1016/j.isprsjprs.2018.04.011, 2018.

Van Leeuwen, B. H.: The consequences of predation in the population biology of the monocarpic species Cirsium palustre and Cirsium vulgare, Oecologia, 58, 178-187, 10.1007/BF00399214, 1983.

Vasilopoulos, G.: Characterising the structure and fluvial drag of emergent vegetation, Geography and the Environment, Univeristy of Southampton, 2017.

~~VLP-16 User manual: https://velodynelidar.com/wp-content/uploads/2019/12/63-9243-Rev-E-VLP-16-User-Manual.pdf, last access: 17/11/2021.~~

Violle, C., Navas, M. L., Vile, D., Kazakou, E., Fortunel, C., Hummel, I., and Garnier, E.: Let the concept of trait be functional!, Oikos, 116, 882-892, 2007.

Wang, D., Wan, B., Qiu, P., Su, Y., Guo, Q., and Wu, X.: Artificial Mangrove Species Mapping Using Pléiades-1: An Evaluation of Pixel-Based and Object-Based Classifications with Selected Machine Learning Algorithms, Remote Sensing, 10, 294, 2018.

Whittaker, P., Wilson, C., Aberle, J., Rauch, H. P., and Xavier, P.: A drag force model to incorporate the reconfiguration of full-scale riparian trees under hydrodynamic loading, Journal of Hydraulic Research, 51, 569-580, 10.1080/00221686.2013.822936, 2013.

Wiel, M. J. V. D. and Darby, S. E.: A new model to analyse the impact of woody riparian vegetation on the geotechnical stability of riverbanks, Earth Surf. Process. Landf., 32, 2185-2198, https://doi.org/10.1002/esp.1522, 2007.

Wilkinson, M. E., Addy, S., Quinn, P. F., and Stutter, M.: Natural flood management: small-scale progress and larger-scale challenges, Scott. Geogr. J., 135, 23-32, 10.1080/14702541.2019.1610571, 2019.

Wilson, C., Bateman, A., Bates, P., and Stoesser, T.: Open Channel Flow through Different Forms of Submerged Flexible Vegetation, Journal of Hydraulic Engineering, 129, 10.1061/(ASCE)0733-9429(2003)129:11(847), 2003.

Wilson, C. A. M. E., Yagci, O., Rauch, H. P., and Olsen, N. R. B.: 3D numerical modelling of a willow vegetated river/floodplain system, Journal of Hydrology, 327, 13-21, https://doi.org/10.1016/j.jhydrol.2005.11.027, 2006.

~~Wright, I. J., Reich, P. B., Cornelissen, J. H., Falster, D. S., Garnier, E., Hikosaka, K., Lamont, B. B., Lee, W., Oleksyn, J., and Osada, N.: Assessing the generality of global leaf trait relationships, New phytologist, 166, 485-496, 2005.~~

~~Yao, Z. Y., Xiao, J. H., Ta, W. Q., and Jia, X. P.: Planform channel dynamics along the Ningxia-Inner Mongolia reaches of the Yellow River from 1958 to 2008: analysis using Landsat images and topographic maps, Environ. Earth Sci., 70, 97-106, 10.1007/s12665-012-2106-0, 2013.~~

Zhang, Y., Tian, Y., Ding, S., Lv, Y., Samjhana, W., and Fang, S.: Growth, Carbon Storage, and Optimal Rotation in Poplar Plantations: A Case Study on Clone and Planting Spacing Effects, Forests, 11, 842, 2020.

Zhao, K., Gong, Z., Zhang, K., Wang, K., Jin, C., Zhou, Z., Xu, F., and Coco, G.: Laboratory Experiments of Bank Collapse: The Role of Bank Height and Near-Bank Water Depth, Journal of Geophysical Research: Earth Surface, 125, e2019JF005281, https://doi.org/10.1029/2019JF005281, 2020.

Zhao, X., Su, Y., Hu, T., Cao, M., Liu, X., Yang, Q., Guan, H., Liu, L., and Guo, Q.: Analysis of UAV lidar information loss and its influence on the estimation accuracy of structural and functional traits in a meadow steppe, Ecol. Indic., 135, 108515, https://doi.org/10.1016/j.ecolind.2021.108515, 2022.

Zhong, L., Cheng, L., Xu, H., Wu, Y., Chen, Y., and Li, M.: Segmentation of Individual Trees From TLS and MLS Data, IEEE J. Sel. Top. Appl. Earth Observ. Remote Sens., 10, 1-14, 10.1109/JSTARS.2016.2565519, 2016.